Norwegian University of Life Sciences
Faculty of Veterinary Medicine and Biosciences
Department of Chemistry, Biotechnology and
Food Science

Master Thesis 2016
60 credits

Gut microbiota and tumorigenesis in A/J Min mice.

Line Skute Bråten

Acknowledgements

This thesis was performed at the Norwegian University of Life Science (Institute of Chemistry, Biotechnology and Food Science), with Professor Knut Rudi as supervisor and Professor Jan Erik Paulsen as secondary supervisor.

First, I want to thank Jan Erik Paulsen and Knut Rudi for giving me the opportunity to work with both microbiota and cancer in this project. Thanks to Marianne Sødring and Christina Steppeler for sampling cecum from mice for my project.

I also want to thank Jane Ludvigsen for analysing my 16S sequencing results in QIIME and answering questions while I was doing my lab work.
I also need to give a special thanks to Jon Fredrik Hanssen and Kari Olsen for helping me with all the challenges that occurred during the Gas chromatography analysis.
Furthermore, I want to thank Lars Gustav Snipen who helped me and answered all my questions while I was working with statistics in R studio. Thank you for answering emails at all times of day and all days of the week.

Also, thanks to all the people in the Microbial diversity group for always being nice and welcoming and for making it fun to be in and "around" the lab.

Finally, a special thanks to my friends and family who have always been supportive no matter what. I appreciate you a lot!

Ås, March 2016
Line S. Bråten

Sammendrag

Tykktarmskreft er en av de vanligste formene for kreft i verden. Et viktig verktøy for kreftforskning er musemodeller og det har vist seg at den nylig utviklede A/J Min/+ musen utvikler et stort antall lesjoner i tykktarm, noe som tilsvarer tykktarmkreft observert hos mennesker. Utviklingen av sekvenseringsmetoder og annen teknologi har gitt mer innsikt i rollen til mikrobiota i utviklingen av tarmkreft, men lite undersøkelser har blitt gjort i forhold til å se på ko-variasjonen mellom alder, svulstutvikling og mikrobiota. Målet med denne oppgaven var derfor å undersøke den mikrobielle sammensetningen i cecum fra A/J Min/+ mus og se hvordan sammensetningen varierer med utviklingen av svulster og alder. Variasjonen av smørsyre i cecum ble også undersøkt.

Vi observerte at diversiteten i mikrobiotaen stabiliserer ser med alder, dette gir en indikasjon på at mikrobiotaen hos mus, som hos mennesker, utvikler seg til å likne en «voksen» mikrobiota. Våre resultater viste også at det er bakterier som er assosiert med både alders- og svulstutvikling. Vi fant et stort antall grupper av bakterier som korrelerte med utviklingen av svulster alene, dette kan tyde på at kreftutviklingen hadde større innflytelse på sammensetningen av bakterier enn alder i denne studien. Vi fant ingen signifikant korrelasjon mellom smørsyre og alder eller smørsyre og svulstutvikling, så fra vårt ståsted ser det ikke ut som smørsyre har en stor innvirkning på utviklingen av svulster. Forståelsen av hvordan mikrobiota påvirker sykdom eller hvordan verts-genotype og sykdom påvirker mikrobiota er fortsatt ikke fullstendig, men denne studien kan bidra med innsikt som er viktig å ta med i videre analyser av interaksjonen mellom vert og mikrobiota.

Abstract

Colorectal cancer is one of the most common cancer type worldwide. Mouse models are important tools in cancer research and the recently developed A/J Min+ mouse model has shown to develop a great amount of lesions in colon, which resembles human CRC where the colon is heavily involved in tumor formation. Advances in sequencing and computational technology have facilitated determination of the role of the intestinal microbiota in CRC however little research have been done investigating the co-variation between age, tumor progression and microbiota. Therefore, this study aimed to investigate the microbial composition in cecum from A/J Min/+ mice and how the composition varies with tumor progression and age. Variations in levels of butyrate from luminal microbiota was also investigated. Our results indicated that the compositional diversity of the mouse microbiota stabilizes and that the mouse microbiota, as in humans evolves towards an "adult-microbiota". Our results also suggest that there are bacteria associated with both age and tumor progression. We found groups of bacteria that correlated with tumor progression alone, which indicates that tumor progression likely had a stronger impact on the microbial composition than age in this study. We could not find any significant correlation between butyrate and either age or tumor progression, so from our point of view it does not seem like butyrate have a great impact on tumor progression in these samples. The understanding of how the microbiota affects disease or how host genotype and disease affect microbiota is still not complete. However, this study provides some insight to consider in further analysis of host-microbial interactions.

Abbreviations

Abbreviation	Meaning
ACF	Aberrant crypt foci
APC	adenomatous polyposis coli
bp	base pair
CK1	Casein kinase 1
CRC	colorectal cancer
DC	Destruction complex
ddNTP	dideoxy nucleotide triphosphate
DNA	Deoxyribonucleic acid
dsDNA	double stranded DNA
Dvl	Dishevelled
ENU	Ethylnitrosourea
FAP	familial adenomatous polyposis
FDR	False discovery rate
FID	Flame ionization detector
Fz	Frizzled membrane protein
GC	Gas Chromatography
GI	Gastrointestinal
GI	Gastro intestinal
GSK3	Glycogen synthase kinase 3
HDAC	Histone deacetylate
HMP	Human microbiome project
HNPCC	Hereditary nonpolyposis colorectal cancer
LOH	Loss of heterozygosity
LPR	Lipoprotein receptor
MetaHIT	Metagenomics of the human intestinal tract

Min	Multiple intestinal neoplasia
mM	Milli molar
NGS	Next generation sequencing
nM	Nano molar
OTU	Operational taxonomic unit
PBS	phosphate buffer solution
PC	Principial component
PCA	Principial component analysis
PCR	Polymerase chain reaction
PEG	Polyethylene glycol
pM	Pico molar
PP2A	Protein phosphatase 2A
QIIME	Quantitative insights into microbial ecology
qPCR	quantitative polymerase chain reaction
RNA	Ribonucleic acid
rRNA	ribosomal ribonucleic acid
S.T.A.R	Stool transport and recovery
SCFA	Short-chained fatty acid
ssDNA	single stranded DNA
TAE	Tris-acetate EDTA
Tris	Tris(hydroxymethyl)aminomethane
UV	Ultra-Violette
V	Volt
µL	Micro litre

Table of content

1. Introduction

The gut microbiota has important metabolic, trophic and protective functions for its host (Guarner, 2006). Recent studies have begun to examine differences in gut bacteria profiles in patients with and without disease, and also how the microbiota can affect inflammation and cancer in the gastrointestinal tract (Baxter et al., 2014a).

Mouse models are important tools in both mechanistic studies and drug development in colon cancer (CRC) research. Advances in sequencing and computational technology have facilitated determination of the role of the intestinal microbiota in CRC. Microbiota in mouse models have been investigated before, most studies have focused on the microbiota in early life and colonization, but there has been little research on how the composition of microbiota varies with age and tumor progression in colon cancer.

1.1 Colorectal cancer

CRC is the third most common cancer in men and the second most common cancer in women worldwide. In 2012 there were almost 1.4 million new cases and approximately 700.000 deaths reported (Ferlay et al., 2013). In Norway there were 4166 new cases with CRC in 2014, 2157 men and 2009 women (Norway, 2015).

CRC arises through a series of characterized histopathological changes in the colon and several different signalling pathways play an important role in the development of CRC (Roy and Majumdar, 2012). The rapid renewal of the epithelium also increases the risk of mutations that can lead to the development of tumors.

There are two main types of CRC, the inherited and the sporadic type. Hereditary nonpolyposis colorectal cancer (HNPCC) accounts for 3-4% of CRC cases and familial adenomatous polyposis (FAP) causes approximately <1%. Inactivation of adenomatous polyposis coli *(APC)* is viewed as an early event in both sporadic tumors and other types of CRC. Approximately 60% of patients with CRC have a mutation in *APC* and inactivation of this tumor suppressor gene is also thought to be a critical event in 80% of all sporadic tumors. Even though *APC* inactivation is an important event it may take years for cancer to fully develop (Rustgi, 2007, Song et al., 2014, Najdi et al., 2011, Srivastava et al., 2001).

1.1.1 Intestinal morphology

The mucosal surface in mammalian intestine is lined by an absorptive and secretory single-celled layer called epithelium. In the small intestine this layer projects into the lumen to form a finger-like structure called villi, this is a specialised structure for absorption of nutrients and is only found in the small intestine. The villus structure increases the surface of the absorptive cells, providing an extremely efficient absorption of nutrients. This epithelial layer also penetrates into the underlying tissue, forming tubular glands called crypts (Clevers, 2013). (Figure 1)

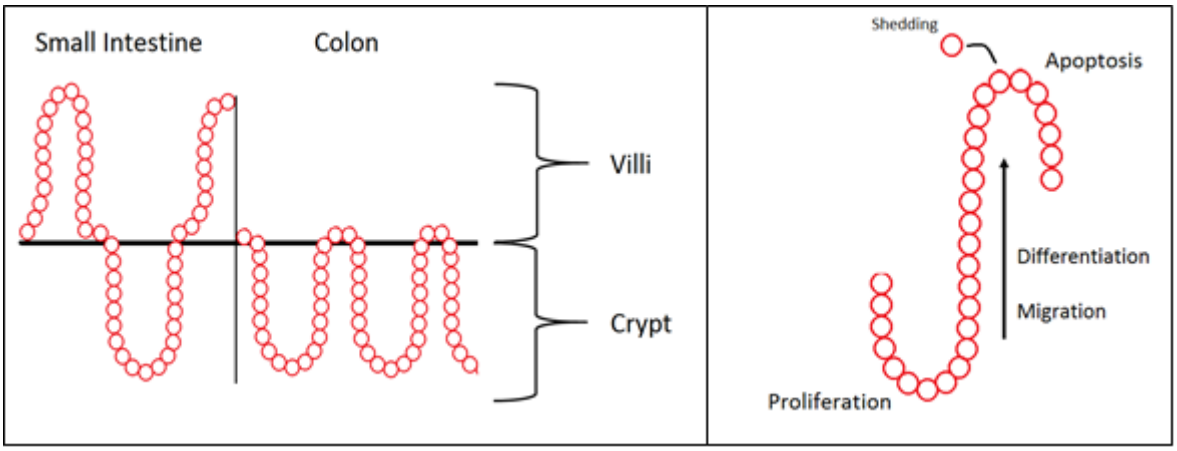

Figure 1: Illustration of villi and crypt structure of the small intestine and colon, villi projecting into the intestinal lumen and crypts penetrating the underlying tissue. (Left) Direction of migration and differentiation in crypts from proliferation centre in the bottom of the crypts. (Right) (Bråten, this thesis)

The crypt is the main centre for renewal of tissue in the intestine, often called the proliferation unit. The colon of a normal adult contains about 10^7 crypts, and each crypt contains thousands of cells. The proliferation of cells in the crypt is tightly controlled by Wnt ligands; a gradient of these ligands along the crypt axis causes a differential distribution of proliferative and differential cells (Roy and Majumdar, 2012, Song et al., 2014).

The Wnt signal contributes to the proliferation of the epithelial stem cell or progenitor cells, these stem cells reside near the bottom of the crypts and here the Wnt signal is turned on. Control of proliferation is important in order to maintain the rate of tissue renewal, under production of cells may lead to loss of tissue or atrophy while over production of cells may result in tumor production (Holmberg et al., 2006, Krausova and Korinek, 2014).

1.1.2 *APC* and intestinal carcinogenesis

The *APC* gene encodes a multifunctional protein that controls several processes in the cell. APC is a large multidomain protein and its gene consists of 8535 bp encoding 2843 amino acids (Senda et al., 2007, Fearnhead et al., 2001). *APC* is located on chromosome 5q21 and early studies of FAP syndrome found *APC* to be the responsible gene for the disease (Nishisho et al., 1991, Kinzler et al., 1991, Miyaki et al., 1994).

The majority of FAP patients harbours a germline mutation in *APC* that can lead to a truncated protein product. Tumorigenesis driven by *APC* seems to also be dependent on other events in order to achieve inactivation of both *APC* alleles, this is called loss of heterozygosity (LOH)(Miyaki et al., 1994, Fearnhead et al., 2001). Most sporadic tumors of CRC (~80%) develops as a response to a somatic mutation in *APC* (Fearnhead et al., 2001).

Germline and somatic mutations of *APC* are spread between many codons and will affect the gene product in different ways depending on the location and type of mutation (Fearnhead et al., 2001). FAP-patiens are more likely to develop CRC because they are born with *APC* +/- and have only one intact allele. These patients only need a "one-hit scenario" in order to develop LOH and are therefore more sensitive to factors that will damage *APC* and induce CRC. The "one-hit scenario" is an event that will lead to a mutation in the functional allele of the gene, which results in LOH. This can in turn lead to the loss off a function that has tumor-suppressive effect. An important role in *APC*'s tumor suppressive effect is the regulation of β-catenin in the Wnt signalling pathway (Morin et al., 1997, Korinek et al., 1997, Gregorieff and Clevers, 2005, Senda et al., 2007).

1.1.3 The Wnt/β-catenin signalling pathway

The Wnt/β-catenin signalling pathway is important in the control of several processes in the cell; proliferation, stem cell self-renewal, migration of cells along crypt axis and specification of cell fate. The Wnt/β-catenin signalling pathway is activated by binding of a Wnt protein (Wnt signal) to a surface receptor at the plasma membrane, which initiates a cascade of signalling(Najdi et al., 2011).

β-catenin is a protein shown to interact with transcription factors in the nucleus, this interaction can lead to transcriptional activation (Gregorieff and Clevers, 2005, Cadigan and Liu, 2006, Kimelman and Xu, 2006). In absence of Wnt signal a destruction complex DC contributes to

keeping the cytosolic and nuclear levels of β-catenin low, by binding of β-catenin and marking it for degradation. DC is a large complex of proteins and the core complex are axin, APC, Glycogen synthase kinase 3 (GSK3), casein kinase 1 (CK1), protein phospatase 2A (PP2A) and β-catenin. More proteins are also associated with this complex; SCF ubiquitin ligase complex and its β-TRCP1 component, and finally the E2-ligase-binding protein (Kimelman and Xu, 2006, Krausova and Korinek, 2014).

In the presence of a Wnt signal DC is "turned off" and β-catenin can accumulate in the cell and eventually translocate into the nucleus and turn on the transcription of Wnt target genes. (Figure 2a) The Wnt ligand binds to a transmembrane protein called Frizzled (Fz) and its co-receptor, low-density lipoprotein receptor related protein 6 (LRP6) or LRP5 (Cadigan and Liu, 2006). Together the Wnt-Fz-LRP6 complex recruits the scaffolding protein Dishevelled (Dvl) (MacDonald et al., 2009). This leads to an inhibition of DC and β-catenin will not be marked for degradation. As a result, β-catenin will accumulate in the cell and translocate into the nucleus to form a complex with transcription factors that in turn will initiate the transcription of Wnt target genes. (Figure 2b)

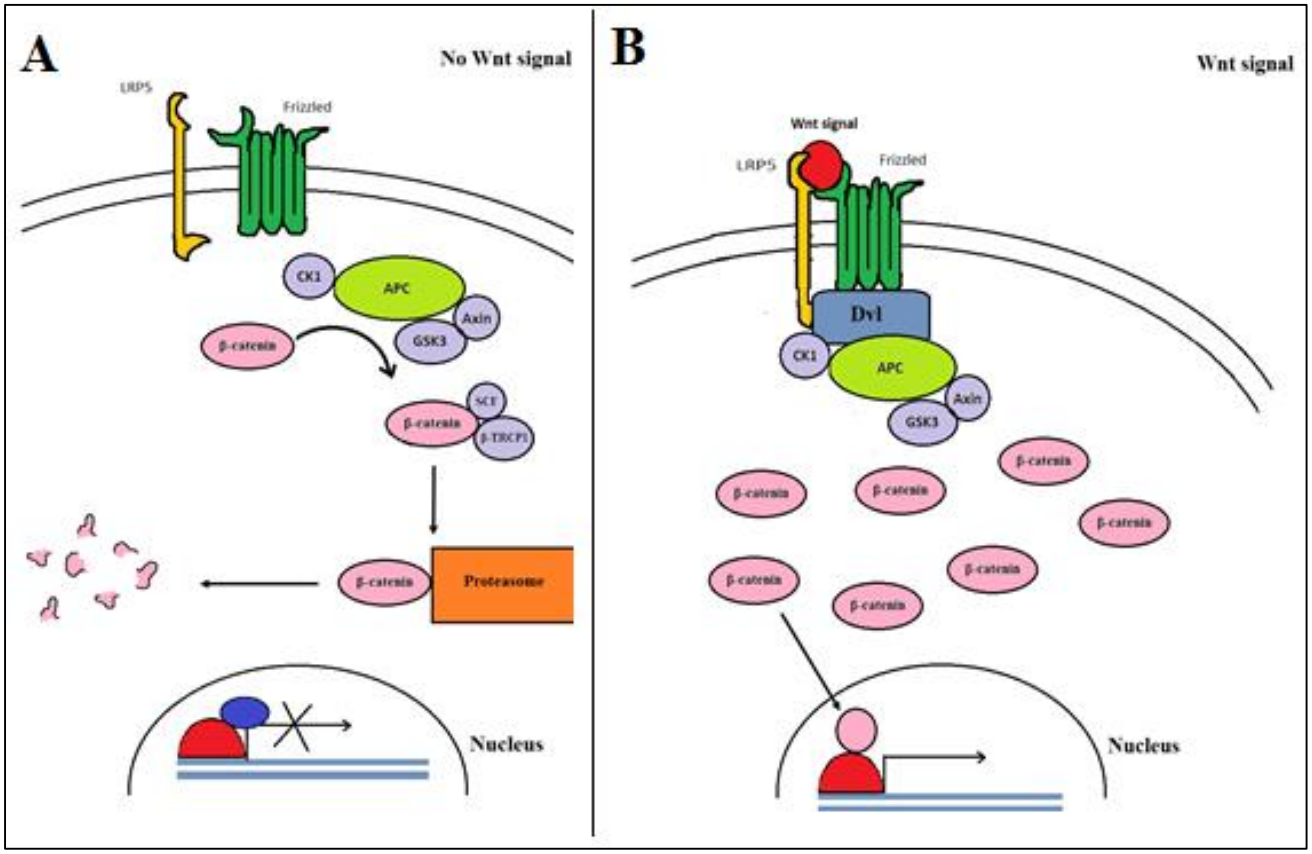

Figure 2: A) In the absence of wnt signal DC will mark β-catenin for degradation by the proteasome. B) Wnt signal will turn off the DC and β-catenin will accumulate and translocate into the nucleus and turn on Wnt target genes. The image was inspired by: "Wnt signaling: complexity at the surface" (Cadigan and Liu, 2006).

A mutation in *APC* is prevalent in colorectal cancer, this will affect the Wnt signalling pathway and lead to accumulation of β-catenin. This accumulated β-catenin will in turn lead to increased transcriptional activation and cell proliferation, as it would when a Wnt signal is present (Senda et al., 2007, Bienz and Hamada, 2004).

1.1.4 The A/J Min/+ mouse model for CRC

Mice with mutations in *APC* and in genes that interact or modify *APC* are important models in the studies of FAP. The most frequently used murine model for FAP is the multiple intestinal neoplasia (Min) mouse. The Min/+ mouse contains only one functional allele of *APC* (Su et al., 1992), and the specific Min-mutation was first identified in a colony of mice following random ethylnitrosourea (ENU)-induced mutagenesis (Moser et al., 1990). The induced mutation of the Min/+ mouse is analogous to the mutation in human *APC*, and resembles the event of germline mutations of *APC* in patients with FAP syndrome where a point mutation at codon 850 leads to truncation of the polypeptide (Moser et al., 1990, Moser et al., 1995).

The primary phenotype of the Min/+ mouse develops multiple adenomas in the small intestines, and only a few adenomas in the colon. Research of the Min/+ mouse mutation indicated that somatic events also is necessary in order for tumor formation. The intestinal sensitivity to tumor formation is age specific in these mice and the tumors showed loss of the wild-type allele (Moser et al., 1995, Moser et al., 1990). These murine models for FAP have been test systems for the development of dysplastic crypts and for development and growth of adenomas (Paulsen, 2000).

In human CRC colon is heavily involved in tumor formation. Min/+ mice develop a greater amount of lesions in the small intestine. A different mouse strain called A/J Min/+ mouse has later proved to develop a greater amount of lesions in the colon, which resembles human CRC more closely (Sodring et al., 2015a).

1.1.5 Tumor progression in the A/J Min/+ mouse

The A/J Min/+ mouse is a backcross with C57BL6/J Min and A/J +/+ females (Sodring et al., 2015a). The first step in colon carcinogenesis in this model is the appearance of preneoplastic lesions. In the Min mouse or patients with FAP syndrome tumor initiation occur when the *APC* in stem cells are fully inactivated (*APC* -/-) and the stem cell loses its full-length APC protein. This event gives rise to a lineage of dysplastic cells and the crypt will be filled with cells of low differentiation, high duplication rate, unstable mitosis and downregulated apoptosis (Paulsen, 2000).

Polyp precursors or preneoplastic lesions, also known as aberrant crypt foci (ACF) have been described in carcinogen-treated mice. These lesions were identified by a characteristic morphology of thickened epithelial lining, irregular lumens, enlarged crypts, increased pericryptal space and elevation from the mucosa. (Srivastava et al., 2001, Bird and Good, 2000) Another type of ACF, later called flat ACF, have also been described in the colon of both C57BL/6 Min/+ mice and rats. The flat ACF differ from the original ACF by their flat structure and they were only visible by staining with methylene blue and transillumination (Paulsen et al., 2000).

Research has shown that flat ACF are early stages of colon carcinogenesis and that they will develop into tumors and progress further to carcinomas in the A/J Min/+ mouse (Sodring et al., 2015a, Paulsen et al., 2000). The colonic environment seems to play an important role in the development of cancer and it is influenced by lifestyle and changes in the microbiome.

1.2 Gut Microbiota

Billions of bacteria populate the mammalian intestinal tract and this diverse microbial ecosystem is called the microbial flora or the gut microbiota. The gut microbiota is a complex community involving interactions between host cells and hundreds of bacterial species. This bacterial community have a profound effect on the human health and some of its biological effects include; development of the host immune system, intestinal epithelial integrity, energy source, vitamin biosynthesis, preventing pathogen colonization and processing drug metabolites (Dave et al., 2012).

Most of the microorganisms associated with the microbiota are non-pathogenic and live in a symbiotic relationship with their host, a commensalistic or a mutualistic relationship that is either beneficial or leaves the host unaffected (Collins et al., 2012). However; studies have suggested that the gut microbiota can affect CRC together with genetic mutations, diet and inflammatory processes (Irrazabal et al., 2014, Akin and Tozun, 2014).

Large-scale projects such as The US Human microbiome Project (HMP) (2014) and the European Metagenomics of the Human Intestinal Tract (MetaHIT) (Qin et al., 2010) have made progress towards characterizing the baseline microbiome and microbiota in humans. These projects have laid a foundation for the identification of differences in the microbiota that are associated with various diseases, inflammation and cancer.

1.2.1 Colonization of the gut

The colonization of microbiota in infants and early life may play an important role in the composition of the adult microbiota, and it can influence the risk of other diseases later in life (Zeng et al., 2013). After birth a baby is rapidly colonized and the colonization is influenced on several factors including the delivery mode, antibiotic treatment, feeding patterns and the environment (Palmer et al., 2007).

The first microbes an infant encounter are from vaginal mucosa, skin, hair, food or other nonsterile objects it comes in contact with after birth. Infants who are born naturally will have a microflora that resembles the mothers in the earliest parts of life, and babies that are delivered by caesarean section might have microbiota characteristics that resemble skin microbes (Clemente et al., 2012, Zeng et al., 2013, Dave et al., 2012). During the first 1-2 years of life the microbiota

evolves towards a relatively stable and adult like microbiota (Dave et al., 2012, Palmer et al., 2007).

The human gut microbiota consists of bacteria from different bacterial phyla, seven phyla accounts for the vast majority of detected species. These seven phyla include the Gram-positive Firmicutes, Gram-negative Bacteroidetes, Actinobacteria, Cyanobacteria, Fusobacteria, Proteobacteria, and Verrucomicrobia. Firmicutes and Bacteroidetes being the most abundant of the different phyla (Sankar et al., 2015).

Facultative anaerobes such as *Enterobacteria* and *Enterococci* are the first colonizers. These bacteria gradually create a more anaerobic environment allowing anaerobes such as *Bacteroides, Bifidobacteria* and *Lactobacilli* to colonize (Palmer et al., 2007, Tojo et al., 2014). The composition of intestinal bacteria is relatively stable throughout adult life, but the specific strain composition can vary from person to person (Lozupone et al., 2012).

1.2.2 Mucosal adherent bacteria

The commensal bacteria in the gastrointestinal tract can be divided in to compartments within the large bowel, the luminal compartment and the mucosa-adherent compartment. Mucosa-adherent bacteria is a designation for bacteria associated with the mucus layer. The mucus layer consists of mucin glycoprotein sheets that are secreted by goblet cells in the epithelium. The inner mucus layer is tightly packed with glycoproteins while the outer layer is looser and can contain bacteria (Li et al., 2015).

The two compartments of microbiota are influenced by different environmental factors and compositional differences between the mucosal layer and the luminal content of the microbiota have been found (Li et al., 2015). While the fecal/luminal microbiota is influenced by diet, the mucosal associated bacteria can be influenced by surface-associated factors and changes in the mucosal layer or the epithelium. Microbiota in these two compartments may relate differently to the growth of colorectal adenomas (Shen et al., 2010).

A research by Son *et al.* have shown that a mutation in *APC* and alterations in the colonic epithelial cells may alter colonic-microbial interactions prior to polyposis (Son et al., 2015a). Different colonization patterns between non-malignant mucosa and tumor tissue indicates that tumors forms a niche for specific bacteria (Marchesi et al., 2011), and in this study by Marchesi *et*

al. some potentially pathogenic bacteria were underrepresented in tumor tissue. Based on this they suggested that commensal-like bacteria with probiotic properties found in the tumor microenvironment have a competitive advantage and may even replace other pathogenic bacteria upon CRC progression (Marchesi et al., 2011).

1.2.3 Microbiota function and SCFA

The gut microbiota breaks down food into useable nutrients and provides energy for the host through fermentation of non-digestible dietary components. The end products of anaerobic bacterial fermentation are short-chain fatty acids (SCFA) and these products interact both with the intestinal microbiota and the host cells. The most abundant of these SCFAs are acetate, propionate and butyrate. These metabolites play an important role as nutrients for the colon epithelium and are important factors for colonic health. The level of these SCFAs in colon depends on diet, site of fermentation and microbial composition (Cummings et al., 1987, Vinolo et al., 2011).

The SCFAs have been shown to contribute as modulators of intracellular and colonic pH, cell volume and other functions associated with transport and vesicular endothelial cells. SCFAs also protect the intestinal epithelium from infection, regulate proliferation, differentiation of cells and gene expression. The production of SCFAs has also been connected to an anti-carcinogenic and anti-inflammatory potential in the intestinal tract (Aoyama et al., 2010, Donohoe et al., 2012).

1.2.3.1 Butyrate

Butyrate has received the most attention out of the SCFAs and is thought to have tumor-suppressive properties in colorectal cancer (Donohoe et al., 2014). Butyrate has energetic and epigenetic functions in colonocytes in addition to play an important role as an apoptosis activator (Kolar et al., 2007, Donohoe et al., 2012). The effect of dietary fibres and butyrate have been discussed to be both protective and non-protective in inflammation and colorectal cancer (Alberts et al., 2000, Park et al., 2005, Peters et al., 2003, Vinolo et al., 2011, Hester et al., 2015).

Glucose is the favoured energy source in cancerous cells due to the a metabolic shift called the Warburg effect (Donohoe et al., 2012), as a result unmetabolized butyrate will accumulate in the cell and enter the nucleus. In the nucleus butyrate functions as a histone deacetylase (HDAC) inhibitor, which can epigenetically regulate gene expression, inhibit cell proliferation and induce apoptosis (Bultman, 2014, Donohoe et al., 2014). The HDAC effect of butyrate might play an important role in the activation of apoptosis and increase of histone acetylation and altering of the

position and/or the conformation of nucleosomes in the cell which gives butyrate a potential tumor-protective effect (Waldecker et al., 2008, Cress and Seto, 2000).

1.2.4 Microbiota and disease

External factors as diet, medicine, stress and geographical location are factors that can affect the microbiota and lead to a misbalance in the composition (dysbiosis). A disturbance in the composition or metabolism of the colon microbiota might shift the homeostatic environment and lead to inflammation, dysplasia and cancer (Irrazabal et al., 2014, Zhu et al., 2011, Hester et al., 2015). Many studies have also targeted bacterial metabolites and toxins to investigate how they affect the host in both health and disease (Machiels et al., 2014, Remely et al., 2014).
Some bacterial species and/or dysbiosis have been suspected to be causing infections and alterations in the gut, and this kind of changes are associated with various diseases including irritable bowel syndrome, inflammation, ulcerative colitis, polyposis and CRC (Sankar et al., 2015, Machiels et al., 2014). Components of the microbiota are linked to numerous physiological functions known to promote diseases.

In humans there are several examples of bacterial species linked with disease, some of these are; *Roseburia* and *Faecalibacterium prausnitzii* who have been connected with type 2- diabetes (Karlsson et al., 2013), *F. prausnitzii* is also connected to anti-inflammatory activity (Furet et al., 2010). *Helicobacter pylori* who colonize gastric epithelium and are connected to gastric cancer (Abreu and Peek, 2014).

Studies of microbiota in germ-free animals are probably the strongest argument for the involvement of microbiota in disease, in these types of studies you can see how microbiota alters the nature of a disease when it is introduced to germ-free animals living in a “germ-free” environment. A study that transplanted microbiota from CRC patients and healthy humans to germ-free mouse found that the baseline microbiota determines the susceptibility to colonic tumorigenesis (Baxter et al., 2014b).

1.2.5 Mouse as a model for human microbiota

Mouse models are frequently used as models for human microbiota. Due to our advanced knowledge of the mouse genome and the availability of many different genetically modified strains, murine models can be beneficial in functional studies of disease. High reproductive rates and short life cycle are additional advantages of the mouse model. Experimental manipulation of

the mouse genetics also allows research on host-microbiota interactions (Nguyen et al., 2015). Both the human and mouse gastrointestinal (GI) tract are put together by organs that have a similar anatomy, however there are some differences between the two. (Figure 3)

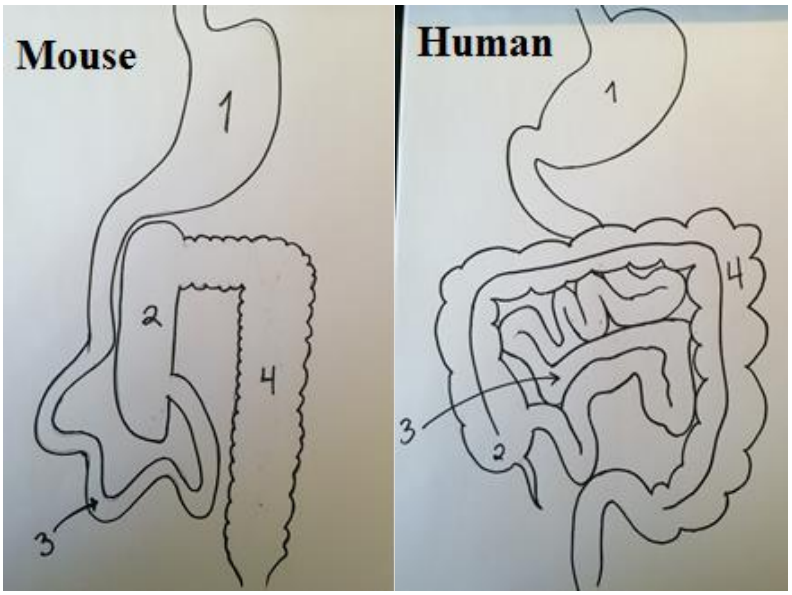

Figure 3: Differences between human and mouse GI tract. **1)** Stomach **2)** Cecum **3)** Small intestine **4)** Colon. Main sections are numbered in this photo, different sections of human colon (ascending, transverse and descending colon) and other compartments absent in mouse GI were not numbered. The image was inspired from "How informative is the mouse for human gut microbiota research?" by Nguyen TLA, Vieira-Silva S, Liston A, Raes J 2015. (Nguyen et al., 2015)

A human being is presented to a lot of different variables and environmental conditions as an outbred population and unfortunately studies on microbiota rely on experiments of inbred mice living in controlled, homogenous environments where they often get the same diet, and have a similar genetic background. As a result, these kind of controlled environments lead to little variation in the microbiota between species. However, mouse studies also allow for better-controlled observations in e.g. functional studies (Ericsson et al., 2015).

Many bacteria found in mice represent bacterial genras not detected in humans, similarities between human and mouse gut microbiota has still been suggested (Ley et al., 2005). Host-microbial co-evolution between different mammalian species may have arisen due to both anatomical divergences and differences in diet (Nguyen et al., 2015).

1.3 16S as a genetic marker

Sequencing of the 16S rRNA gene amplicon is an established approach for identification of bacteria in samples from sites with high bacterial density and is also a widely used technique for phylogenetic reconstruction, based on reference sequences and other bioinformatic analyses. Some advantages with 16S is the distribution in all bacterial species, size (~1500bp) and stability over time (Sankar et al., 2015).

The 16S rRNA gene consists of nine hypervariable regions flanked by more conserved regions. The ribosomal subunits have a highly conserved secondary structure and these structural features can be used in positional homology in multiple sequence alignments and other phylogenetic analysis. The V3 and V4 hypervariable regions or 16S rRNA gene provides information for taxonomic classification of microbial communities (Fadrosh et al., 2014, Yarza et al., 2014, 2014).

The variable regions of the 16S gene enable comparison of both distant and closely related microorganisms and comparative analysis of sequences of thousands of organisms has demonstrated sequences that are specific for a phylogenetically defined group of organisms (Willey et al., 2012).

1.4 Operational Taxonomic units

An operational taxonomic unit (OTU) is used as a definition of a species or group of species, and is often used when only DNA sequences are available. OTU is most commonly used as a microbial diversity unit and as a taxonomic level of sampling. Groups of sequences are separated from other sequences by hierarchical clustering techniques, using strict sequence identity thresholds and without phylogenetic inferences. A reference data base is used to assign taxonomy to the different groups of sequences (Yarza et al., 2014).

1.5 Sequencing

DNA sequencing is a process where you can determine the exact order of nucleotides in a genome or a DNA molecule. Sequencing can be used to determine the sequence of genes, full chromosomes, large genetic regions or entire genomes of humans, animals, plants, bacteria and archaea.

1.5.1 First generation sequencing

In the 1970s Maxam and gilbert and Sanger and his colleagues developed methods to sequence DNA (Sanger et al., 1977, Maxam and Gilbert, 1977). These sequencing methods were based on chain termination and fragmentation techniques. Sanger sequencing has been an important method for the sequencing technology for over 3 decades, and this method relies on incorporating random chain terminators on a single stranded template by use of DNA polymerase (Hall, 2007, Sanger et al., 1977).

The classical sequencing methods such as Sanger sequencing and the Maxam and Gilbert method both have limitations. The main limitation is low throughput because of the template preparation and the enzymatic reaction required in Sanger sequencing (Morey et al., 2013). When The Human Genome Project started, a project that had a goal to sequence all of a human genome, it was clear that they would need faster and cheaper technology with higher throughput (van Dijk et al., 2014).

Over the last couple of decades sequencing methods have greatly improved and now billions of reads can be carried out in parallel and large numbers of sequences can be obtain in a short time. The decrease in both time and cost required for DNA sequencing have helped accelerate biological and medical research. The development of high-throughput sequencing has also improved researcher's ability to investigate complex bacterial communities and bacterial systems.

1.5.2 Next generation sequencing

Next-generation sequencing (NGS) or high-throughput sequencing is a term used to collectively describe a number of different technologies such as; Illumina (solexa) sequencing, Roche 454 sequencing, Iron torrent (proton /PGM sequencing) and SOLiD sequencing. NGS is based on the concept where DNA-polymerase catalyses the incorporation of fluorescently labeled deoxyribonucleotide triphospates (dNTPs) into a DNA template strand. This is done by sequential cycles of DNA synthesis.

The main difference between NGS and classical sequencing is that instead of sequencing a single DNA fragment NGS will use millions of fragments in a massive parallel process (Morey et al., 2013). The NGS methods also rely on the preparation of NGS libraries, which means that bacterial cloning is not required. The sequencing output is directly detected and the base interrogation is performed cyclically and in parallel, which means that there is no need for electrophoresis before the sequencing reaction (van Dijk et al., 2014).

1.5.3 Illumina sequencing

Illumina is a “sequencing by synthesis” technology, which is one of the most successful next generation sequencing platform worldwide (van Dijk et al., 2014). Illumina sequencing consists of different steps; library preparation, cluster generation/bridge amplification, sequencing and data analysis.

The sequencing library is prepared in different ways depending on what you are investigation. In genome sequencing a sequencing library is prepared by random fragmentation of the DNA/cDNA sample followed by 5’ and 3’ adapter ligation. In 16S rRNA sequencing an amplicon enrichment of the selected fragment is done. Adapters that contain additional motifs such as binding site for the sequencing primer and complementary regions to the oligos on the flowcell lawn are ligated to the fragment before cluster generation/bridge amplification.

In the first step of bridge amplification, the sequencing library (with complementary adapter ends) is loaded to the flowcell. The flowcell consists of a surface with a “lawn” of surface-bound oligos and individual molecules in the library bind to their complementary oligos as they “flow” across the surface of the cell. Each fragment is then amplified into distinct, clonal clusters trough bridge amplification. When the cluster generation is complete, the templates are ready for the sequencing step. (Fig.4)

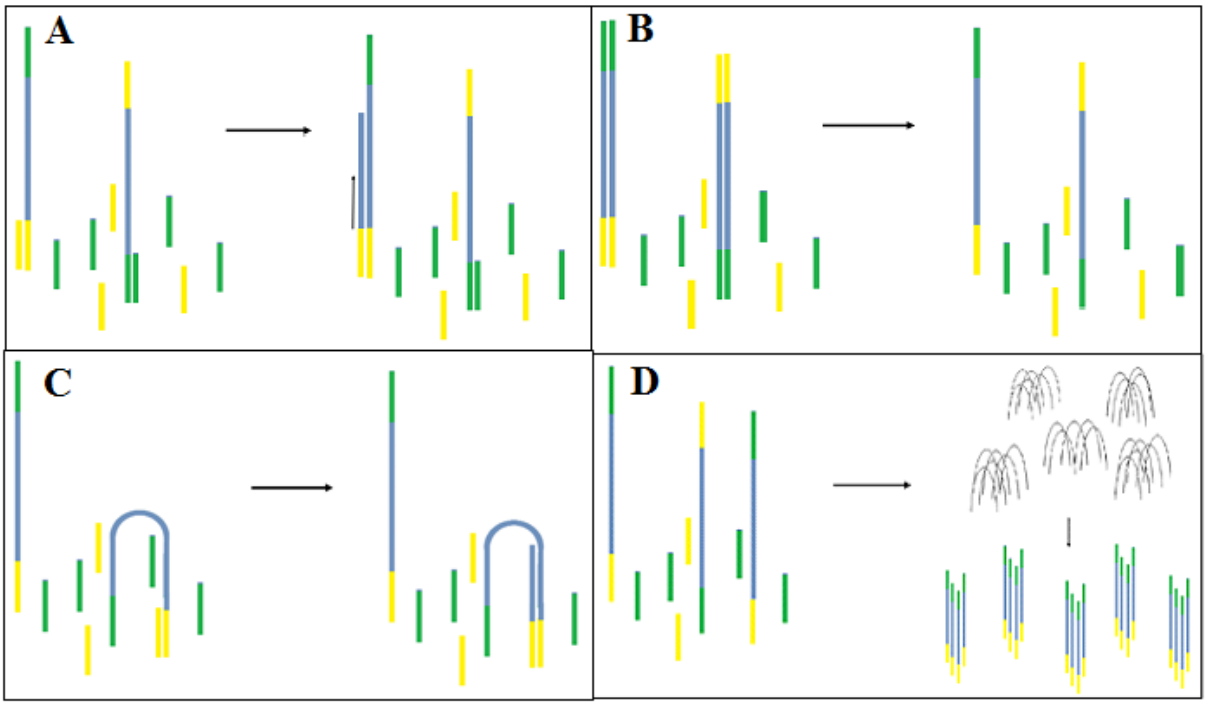

Figure 4: A) Oligo's on the DNA strand binds to Complementary oligo's on the flow cell lawn. Polymerase creates a complementary strand to the hybridized fragment. **B)** The double stranded molecule is denaturised and the original template is washed away. **C)** In the clonal amplification the strand bends and hybridizes to another oligo on the flow cell. Polymerase creates a complementary strand, forming a double stranded bridge. **D)** The double stranded bridge is denatured resulting in two single stranded copies of the molecule. This is repeated over and over in different clusters. After the bridge amplification all the reverse strands are cleaved off, leaving only the forward strand on the flowcell lawn. (Bråten, this thesis)

Sequencing-by-synthesis consists of the polymerase-catalysed addition of reverse-terminator fluorescently labelled bases. The bases are added simultaneously to the reaction and compete to form a union with oligo-primed cluster fragments. When the base is added, it prevents addition of subsequent bases, meaning that only one base will be attached per cycle (Morey et al., 2013). After base incorporation there is an imaging step. Each flowcell lane is divided into panels for a given cluster density. This step is done to record cluster-specific fluorescence. Each image represents one panel and the emission from each cluster is recorded in the imaging step. (Fig. 6).

The emission wavelength and intensity are used to identify the incorporated base. After each imaging step, 3' blocking is chemically removed and the process is restarted, the cycle is repeated "n" times to create a read for "n" bases. During the data analysis the identified sequence reads are aligned to a reference genome or a reference database.

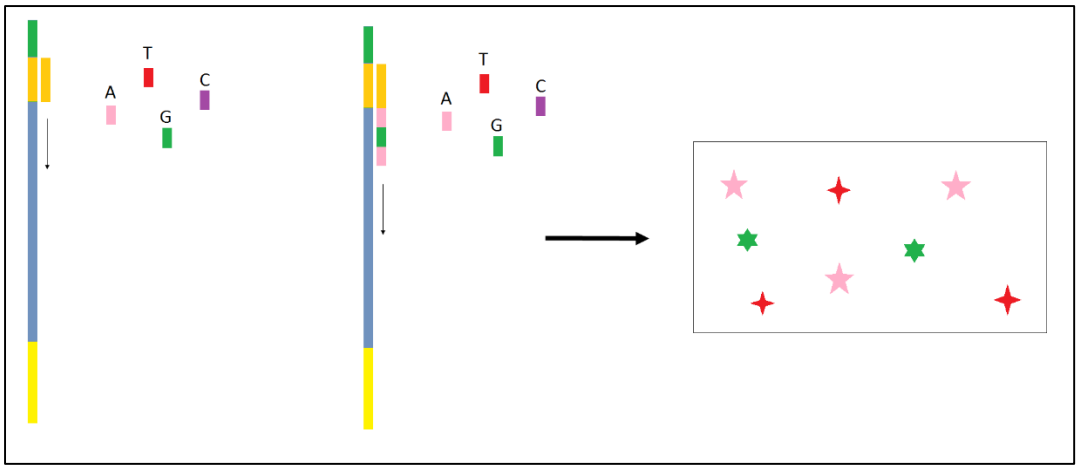

Figure 5: Extension of the sequencing primer by a fluorescently labelled dNTP results in emission of a specific wavelength for the base incorporated. An imaging step records cluster-specific fluorescence. (Bråten, this thesis)

1.5.4 Multiplex sequencing

Multiplex sequencing is a sequencing method where each sequence is given an individual "barcode" which allows you to sort the different sequences during data analysis. Barcodes can also be used to analyse a large number of sequences in a single run by pooling samples together. There are several benefits associated with multiplexing; you can achieve improved productivity and reduce reagent use because you only have one sample after pooling, accurate read lengths of unknown sequences can be maintained. Samples will be automatically identified by barcodes and by the use of data analysis software.

1.6 Aim of study

Mouse models are important tools in both mechanistic studies and drug development in colon cancer research. The A/J Min mice has shown to develop a great amount of lesions in the colon, which resembles human CRC where the colon is heavily involved in tumor formation. (Sodring et al., 2015a) Researchers have associated microbial composition with the susceptibility to colonic tumorigenesis (Marchesi et al., 2011, Baxter et al., 2014b), however little research has been done investigating the co-variation between age, tumor progression and microbiota.

The aim of this thesis was therefore to investigate the co-variation between age, tumor progression and microbiota in A/J Min mice. In achieving this we had following sub goals:

- **Investigate the microbial composition in both luminal and mucosa-adherent microbiota.**
- **Investigate the taxonomic composition in different age groups.**
- **Investigate the correlation of microbiota and tumor progression in colon and small intestine.**
- **Investigate the correlation between butyrate levels from the luminal microbiota and age.**
- **Investigate the correlation between butyrate levels from the luminal microbiota and tumor progression.**
- **Investigate the correlation between butyrate levels from luminal microbiota and the variation of bacterial composition.**

Methods used to investigate this included Illumina 16S rRNA gene sequencing and gas chromatography. 16S rRNA gene sequencing was used for the characterization of microbiota in cecum of A/J min mice and gas chromatography was used to investigate levels of butyrate in samples obtained from cecum content. Statistical analysis was performed to investigate the correlation between the different parameters.

2. Temporal flow of work

In order to get a better insight in how this project were executed it is important to give an overview of the temporal flow of work. The different tasks performed in the lab required different amounts of time, and a lot of time was spent trying to resolve challenges regarding the Gas Chromatograph (GC) used for SCFA analysis.

The project started in January 2015 and the first lab was the 16S gene analysis. This was done from January until May approximately. The SCFA analysis performed on GC started out in May 2015 and there were a lot of challenges to get this method to work.

Standard solutions of SCFA were first run to test the system and to see if any optimizing needed to be done to the method, or if any parts of the GC needed to be changed. This initial testing with standards showed that there was something not working as it should. We first tried to check if there were something "left" in the system from earlier analysation. The suspicion was due to poor documentation from previous analysis. Because of the poor documentation we had no chance of knowing if the system had been saturated from too concentrated samples or standards with too high concentrations. Several months of different washing procedures and "burning of" the column was tried. The standards still did not come out as it should and we could see indications of "carry over" from one sample to the next. Substantial testing was required to resolve this problem.

Water and formic acid were both tried out as washing solutions. The formic acid provided a problem because it both could saturate the system in high concentrations and it made the syringe sticky and slow. This again made errors in the injection and we could see from the chromatograms that the injection volume differed between injections. After this only water was used as wash solution, more washing with water and several water samples were included in the procedure after this.

Errors concerning the auto sampler were also quite frequent and this required a service from a service engineer. The engineer decided to change the autosampler. All samples that had been run before the autosampler was changed had to be tested again, this decision was made in order to minimize the systematic errors that might have occurred using two different autosamplers in the project.

Another challenge with this GC system was that the samples were stored over the oven and the heat from the oven made all the samples warm. It is hard to say if this would have had any effect on the samples, but because of this we only had 6-7 hours run at the time and with all the washing steps and blanks between each sample we were only able to run 5 samples a day. The analysis of SCFA was done by the end of November 2015.

3. Materials and methods

3.1 Project overview and sample information

Project overview are presented in figure 6.

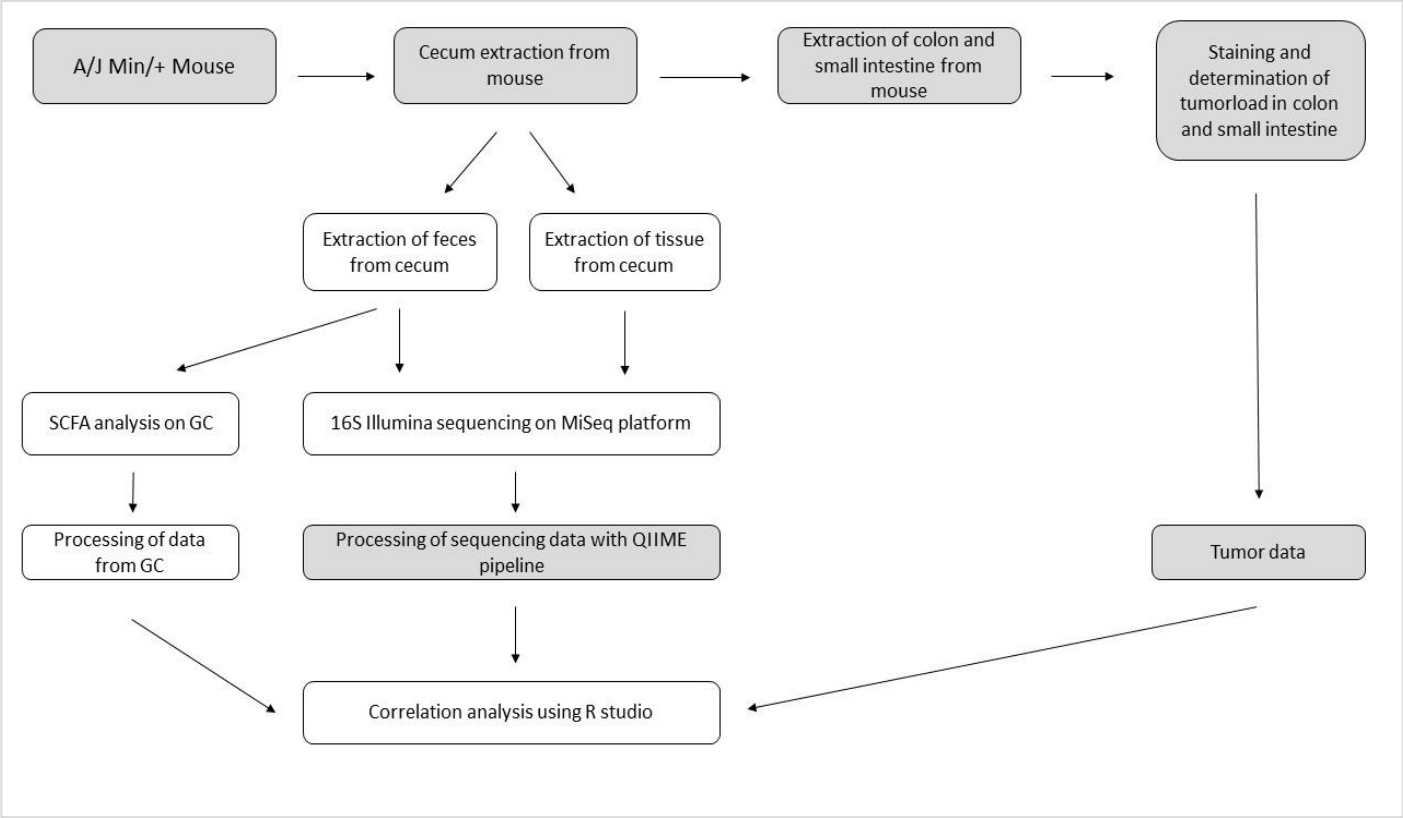

Figure 6: Project overview illustrating the work flow of this project. Tasks in grey area were performed before the start of this project or by an extern part of the project.

This research used a Min mouse strain, suited as a model for human CRC (Sodring et al., 2015a). The mouse strain called A/J Min/+ was established at the Norwegian Institute of Public Health. This strain is the result of a backcross with C57BL6/J Min and A/J for more than 12 generations. The strain was transferred to the Norwegian University of Life Sciences, Campus Adamstuen where it has been maintained for several generations. The A/J Min/+ has been maintained at Campus Adamstuen as an inbred colony for several years (Sodring et al., 2015b). Cecum from 68 mice from a previous study (Sodring et al., 2015a) and an ongoing study at the same institute were used in this project. Cecum was extracted and put in tubes at -20^{o}C before transfer to -80^{o}C for storage.

3.2 Sample preparation

Cecum was stored at -80°C and then at -20°C before defrosting and preparation.

Tubes for cecum content and tissue samples were filled with 250mg glass beads (Sigma-Aldrich, Germany) and 800µL and 500µL of the stool transport and recovery (S.T.A.R) buffer (Roche, Germany) respectively.

Defrosted cecum was cut in half and content from inside the cecum was transferred to the prepared tubes. The remaining tissue was washed with 1x PBS before they were transferred to tubes. All samples were kept at -20°C until further use. Material weights of each sample is presented in appendix A.

3.2.1 DNA extraction

DNA extraction was performed using the Mag™ Midi kit (LGC genomics, Germany) for DNA extraction. Before extraction a mechanical lysis of all samples were done using "MagNA lyser" (Roche, Germany). The lysis step was done twice at 6500rpm for 20 seconds, with one-minute rest on ice between runs.

The MagNa lyser automatically disrupts cells and other biological material, the 250mg glass beads (<106 µm) in the samples contributed to the mechanical crushing, during the mechanical lysis heat is developed. The rest on ice was done to prevent the sample temperature to get too high. The result of this lysis step is a supernatant that contains nucleic acids and this is suitable for DNA extraction and purification.

After the lysis step, tubes were centrifuged at 13000rpm for 5 minutes before automatic DNA extraction using the KingFisher flex robot (Thermo Scientific, USA) and the Mag™ Midi kit (LGC genomics, Germany).

In the KingFisher robot the first extraction step involves additional chemical lysis of the cells, here proteinase and lysis buffer is added to the sample before incubation at 55°C for 10 min. Proteinase removes proteins that could potentially inhibit the following PCR reaction. After lysis, the DNA binds to paramagnetic beads and the sample goes through three different washing steps, in order to remove contamination like salt and alcohol based buffer before elution of the DNA with the elution buffer. The elution buffer helps releasing the DNA from the magnetic beads. Extracted DNA was stored at -20°C until further processing.

3.3 Illumina library preparation

Regions of 16Sr RNA gene (V3 and V4 regions) was sequenced using Illumina sequencing on samples obtained from cecum content and cecum tissue. The V3 and V4 region was targeted in order to study bacterial composition. Several amplification steps were performed before sequencing library was ready for sequencing.

An overview of all primers used in the library preparation and their target regions are presented in appendix B. All primers were used with a final concentration of 0,2µM.

3.3.1 Targeting of 16SrRNA gene

An initial quantitative PCR (qPCR) was done to check the total amount of bacterial DNA in each sample, tissue samples would most likely contain less bacteria than samples from cecum content and the amount in both samples types was quantified to make sure there was enough DNA before we proceeded.

The qPCR was performed with 5x HOT FIREpol® EvaGreen qPCR mix (Solis BioDyne, Estonia) final concentration1x, Universal 16S rRNA gene foreward and revers primers (Nadkarni et al., 2002) (Life Technologies™, USA), 1 µL of DNA and the total reaction volume was 25µL.

Thermal condition was; initial denaturation at 95ºC for 15 minutes, denaturation at 95ºC for 30 seconds, annealing at 50ºC for 30 seconds and elongation at 72ºC for 45 seconds. 40 cycles were used with a final hold at 10ºC. All quantitative-PCR (qPCR) was performed on LightCycler 480 II (Roche, Germany). A selection of samples was checked on agarose gel, gel pictures are presented in appendix C.

Regions of 16Sr RNA gene (V3 and V4 regions) was amplified by using forward primer PRK341 and reverse PRK806 (Invitrogen ™, Thermo Fisher Scientific, USA) (Yu et al., 2005). The used reaction mix was: HotFirePol® DNA polymerase (SolisBioDyne, Estonia) at a final concentration of 1,25U, HotFirePol® buffer B2 1x, dNTPs with a concentration of 200µM (SolisBiodyne, Estonia), MgCl2 2,5mM,1 µL template DNA, the total reaction volume was 25µL. The amplification was performed on 2720 Thermal Cycler (Applied biosystems, USA), with an initial denaturation step at 95ºC for 15 minutes, 25 cycles of denaturation at 95ºC for 30 seconds,

annealing at 50ºC for 30 sec and elongation at 72ºC for 1 minutes and a final elongation step at 72ºC for 7 minutes before cooling at 4ºC ∞. Ampure purification was performed on the amplified PCR products.

3.3.2 Ampure purification

Ampure purification with AMPure® XP beads (Beckman Coulter, USA) was used for purification of PCR products. In Ampure purification the paramagnetic AMPure® XP beads (SPRI beads) bind the negatively charged DNA fragments in the sample. Each bead is made of polystyrene surrounded by a layer of magnetite, which is coated with carboxyl molecules. The paramagnetic beads become magnetic only in the presence of a magnetic field. The carboxyl molecules bind DNA in the presence of a "crowding agent", polyethylene glycol (PEG) and salt (NaCl). PEG causes the negatively-charged DNA to bind to the carboxyl groups on the bead surface. The reaction is dependent on the concentration of PEG and salt in the solution which makes the ratio of beads to DNA important.

The protocol includes two washing steps with freshly prepared 80% ethanol, in which contamination such as salt, polymerase, primer dimers and nucleotides is removed. This contributes to a purer yield of the DNA or PCR product. After the wash steps a mix of Tris and PCR grade water was added to elute the DNA.

The purification was performed on Biomek®3000 Laboratory Automation Workstation (Beckman Coulter, USA). With 0,6-1,0x concentration of beads.

3.3.3 Illumina-indexing PCR

PRK- primers with Illumina adapters (32 primers, 8 forward and 24 reverse primers) combined in a specific combination for each sample were used in a nested PCR. The 3' end of the modified primers contained the gene specific region, while the 5' ends contained a colony amplification region. The colony amplification region is specific for the attachment to complementary oligos on the flow cell used in the Illumina MiSeq platform. The colony amplification region also contains an Illumina sequencing region and a unique primer tag sequence. The unique combinations of primers in each sample and the primer tags makes it possible to distinguish the different 16S amplicons from the different samples.

The amplification of 16S rRNA gene with Illumina-indexed PRK primers was performed on 2720 Thermal Cycler (Applied Biosystems, USA) with the same thermal conditions and reaction mix described for PRK PCR in section 2.3.1 Targeting of 16S rRNA gene.

PCR products from the Illumina adapter PCR were diluted 1:200 and then quantified using qPCR. Quantification of the PCR products was done with Illumina colony forward and reverse primers and a specific TaqMan probe, a hydrolysis probe designed to increase the specificity of the qPCR reaction. HotfirePol probe qPCRmix (SolisBioDyne, Estonia) with a final concentration of 1x, 0,1µM TaqMan probe (Life Technologies™, USA) and 1µL template DNA was used as reaction mix. Thermal conditions for TaqMan qPCR was as follows; initial denaturation step at 95ºC for 15 minutes, following 40 cycles of denaturation at 95ºC for 30 seconds and elongation at 60ºC for 1 minute.

A standard curve was included in the analysis and the amount of DNA in each sample was calculated using the standard curve method, standard curve appendix D.

All samples were normalized and pooled together based on the calculated concentrations from the TaqMan quantification. Volumes needed from each sample was calculated to ensure equal concentration of DNA in the final pooled library sample. A lower and upper limit for volumes was set at 1µL and 10µL respectively. Ampure purification was performed on the pooled sample in order to remove potential primer dimers and excess nucleotides in the solution.

3.3.4 Quantification by the standard curve method

The standard curve method is a method used for calculating an unknown value from a standard curve made from multiple samples with known concentration. Use of a standard curve allows calculations of unknown concentrations to be determined for an unknown sample by interpolation on a graph. Standard curves and equations used are presented in appendix D.

3.3.5 Sequencing PCR

Concentration of the pooled library sample was quantified by using the PerfeCta® NGS Library Quantification kit for illumina® (Quanta Biosciences, USA). PerfeCta SYBR Green SuperMix at a final concentration of 2x, Illumina primer mix at a final concentration of 10µM each was used for the reaction cocktail. The final reaction volume was 20µL.

An Illumina standard curve including 5 standards of linear, dsDNA standard was included in the amplification and used for calculation of concentration using the standard curve method. Quantification was performed with 25 cycles of denaturation at 95ºC for 15 seconds, annealing at 60ºC for 20 sec and elongation at 72ºC for 45 seconds. Calculations was done as described in section 2.3.4 Standard curve method. The pooled library sample was then diluted with Tris pH8,5 until 4nM DNA concentration based on the results from the Perfecta quantification of the original pooled sample.

3.3.6 Library Denaturing and MiSeq sample loading

The library denaturation and the MiSeq sample loading was done as described in the "Library Denaturing and MiSeq Sample Loading" protocol following the manufacturer's instructions. A MiSeq reagent cartridge was prepared as described in the protocol before the library denaturation.

For the library denaturation, pooled DNA amplicon library and PhiX library were combined. PhiX and Amplicon library was combined to achieve a 15% spike-in control of PhiX in the sample before loading it into the MiSeq reagent cartridge. Spike in was used to provide a quality control for sequencing, clustering generation and also to act as a quality control for cross-talk Matrix Generation. In this case the spike in was used at a high concentration (15%) to create more diverse set of clusters. This can be beneficial for these types of samples where a significant number of reads have the same sequence.

The amplicon library was loaded on the flow cell in a concentration of 6pM, following the Illumina protocol for 16S rRNA sequencing and the manufacturer's instructions for loading the MiSeq® system (Illumina, USA).

3.4 Control of PCR quality

3.4.1 Gel electrophoresis

A selection of samples from the different PCR runs were checked on 1% agarose gel, prepared by dissolving 1g agarose (Sigma Aldrich, Germany) in 1x Tris-acetate EDTA (TAE) buffer. The different selection of samples was run in order to check the PCR quality and to make sure that the amplification had produced the right amplicons. A 100bp DNA ladder (Solis BioDyne, Estonia) was used as a size marker in all gels.

The agarose gel is a matrix with channels and pores that allows biomolecules to pass. When an electric field is applied to the gel by a power supply, the charged DNA molecules is attracted to the positive charged end of the gel system because of the negative charge on the phosphate backbone in the DNA molecules. The fragments migrate through the gel matrix and the DNA fragments are separated by length and charge while running through the matrix of agarose. The concentration of agarose in the gel determines the pore size of the gel, and thus the separation properties.

PeqGreen (Peqlab, Germany) added to the gel solution was used as staining method.
Gels were run with the Bio Rad power pac 300 at 80-90V and processed with Molecular Imager ®, Gel Doc™, XR imaging system. Quantity One 1-D analysis software v.4.6.7 (BioRad, USA) was used for visualization of the PCR products, by using UV light. Gel pictures are presented in appendix C.

3.4.2 Qubit quantification

DNA was quantified using Qubit® dsDNA High Sensitivity Assay Kit (Life Technologies, USA), an assay designed to calculate DNA concentrations. Quantification was performed using 2µL of DNA sample and 198µL working solution. The concentration was read using the Qubit® Fluorometer v1.0.

3.5 Analysis of butyric acid in cecum content

Quantification of butyric acid in cecum content was performed by Gas Chromatography. (Szczesniak et al., 2015)

Stock solutions of butyric acid were made from 10,831M butyric acid (Sigma Aldrich, Germany). Concentration of the stock solutions were 0,0025M, 0,00125M and 0,000625M butyric acid in 2,5% formic acid.

Samples were prepared by centrifugation of original samples stored in S.T.A.R buffer, at 13.000 rpm for 10 minutes after mechanical lysation. 300µl of the supernatant were transferred to centrifugal filter tubes, with modified Nylon 0,2µm (VWR, Norh America). The samples were centrifuged at 10.000 rpm for 5 minutes. The eluate from each sample was transferred to new Eppendorf tubes. 100µL of the eluate was transferred to GC vials with 300µL Fixed insert vial (Chromacol, Thermo Scientific) and diluted 1:1 with 5% formic acid, the vials were closed with aluminium caps with rubber/buty/TEF septa (VWR, North America) and placed in the refrigerator until further use.

SCFA was separated using “Auto system GC” (1994, Perkin Elmer USA) with FID detector, and the software was TotalChrom workstation, version 6.2.1 (Perkin Elmer, USA).
Helium (AGA, Norway) was used as a carrier gas at a constant flow rate 20ml/min. Stabilwax®-DA (30m x 0,5mm x 0,25µm) column (Restek, USA) was used for the separation of components. Detector temperature 230^{o}C, injector temperature 210^{o}C, the injection volume was 0,5µL with a 20:1 split ratio. Temperature program is presented in figure 7.

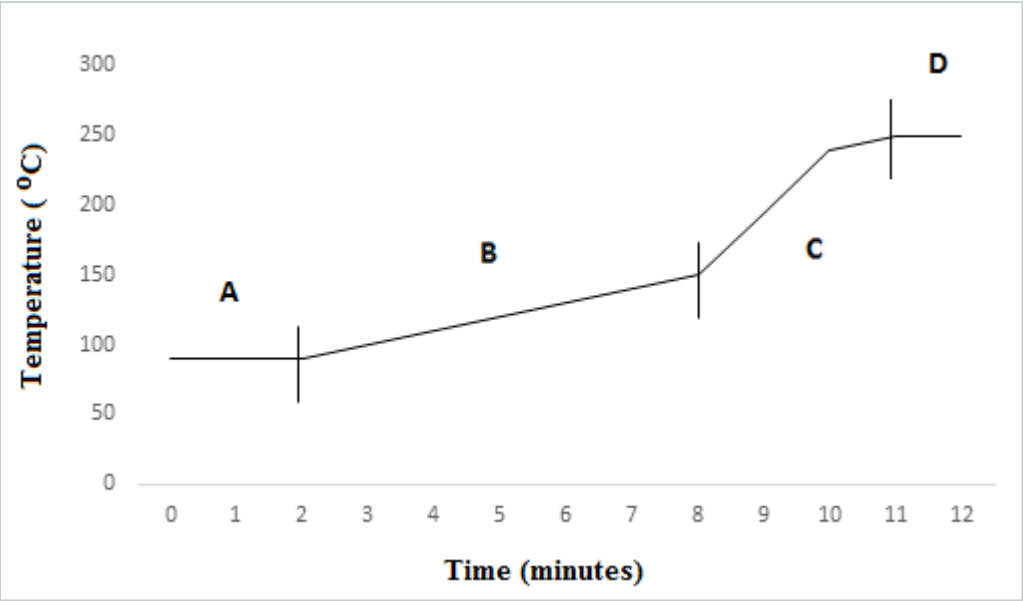

Figure 7: A: initial temp. 90ºC for 2 minutes. **B:** 10ºC increase per minute until 150ºC. **C:** 45ºC increase per minute until 250ºC. **D:** Final temperature 250ºC with 1 minute hold.

The fatty acids were separated based on length of the carbon chain and the affinity to the stationary phase of the column. Identification and quantification was based on external calibration with standard solutions of butyric acid. Material weight and dilutions of samples before quantification was taken into consideration in the quantification of butyric acid.

3.6 Data analysis

Statistical analyses were done using R studio, with R version 3.2.2 and package Vegan, version 2.3-0. All statistical testing was done at a 95% confidence level.

The 16S data was analysed using a standard workflow from a Quantitative Insights Into Microbial Ecology (QIIME) pipeline designed as a quality control of the Illumina sequences and a closed-reference OTU-picking protocol (Caporaso et al., 2010).

In the first step identification of barcode sequences were done and the forward and reverse of these reads was put together. After the joining of all paired reads; all sequences were split. The split was done to sort reads by sample. The reverse primers are unique for each sample and this were used to divide the reads. The reads were paired again and reads with low quality were removed. The quality filtering included removal of reads shorter than 200bp, reads with an average score <Q25 and reads with mismatches in the barcode region.

A chimeras search was done and these sequences were taken out before clustering. Clustering was done at 97% similarity cut off. Sequences were normalized to 2000 sequences per sample. A closed-reference search against Greengenes database was perfomred to construct an OTU table. Taxonomy was assigned using the Green Genes database at 97% similarity.

3.6.1 Diversity

Alpha diversity

To investigate the species diversity α- diversity was calculated, this was done using both Shannon and Simpson index for diversity. Alpha diversity explains the diversity of the community within one site, the number of species (how many types of bacteria in each sample) and their proportion within that one sampling site.

Beta diversity

Beta diversity in the two datasets were calculated using Bray–Curtis distances. Beta diversity describes the dissimilarity between communities of two sites (or two samples). The higher beta diversity means the two communities are more dissimilar.

Mean beta diversity for total of cecum content and tissue samples were calculated from Bray-Curti s distances. Mean beta diversity was also calculated for each age group.

A principal component analysis (PCA) was performed on weighted and unweighted UniFrac distances. PCA was performed to see if the different mouse age-groups would cluster together based on calculated UniFrac distances obtained from the sequencing data. UniFrac is an algorithm that measures similarity between microbial communities based on the degree to which their component taxa share branch length on a phylogenetic tree.

PCA is defined as a linear transformation that transforms the data to a new coordinate system. It models the variation in a set of variables into a smaller amount of independent linear combinations; this can help reduce the dimensions of the dataset. These combinations are the principal components of the variables. The greatest variance by a projection of the data lies on the first coordinate, also called the first principal component, the second greatest variance on the second coordinate and so on.

Kruskal-Wallis test was performed on the first principal component (pc1) from the PCA analysis on both unweighted and weighted UniFrac distances. The first principal component was chosen because this is the component that explains most of the variation in the dataset. Kruskal-Wallis test is used to decide whether population distributions are identical without assuming them to follow the normal distribution

3.6.2 Correlation and false discovery rate

Spearman's rank-order correlation was used to measure the strength of association between microbiota data, tumorload in both colon and small intestine and butyrate. Tumorload is the area (mm^2) of the colon or small intestine that are affected by tumor growth. Spearman's rank-order correlation is a non-parametric test that can measure the degree of association between to variables. It does not give any assumptions about the distribution of the data.

A False discovery rate (FDR) was done on the p-values obtained from Spearman's rank correlation, to minimize the number of errors in the multiple testing and to remove false positive.

4. Results

4.1 16S rRNA analyses

A total of 2495371 sequences were obtained from all samples (n = 188); on average this corresponded to 13273,250 sequences per sample with a standard deviation of 10742,196. The OTU table were “trimmed” to contain 2000 sequences per sample sequences were randomly picked to ensure even sequence information, duplicate reads were removed.

The library contained a total of 326 OTUs distributed in 7 phyla and a total of 13 bacterial classes. 9 OTUs were unclassifiable at the phylum level. The dataset was split into two tables, one for the tissue samples and one for samples with cecum content, the datasets had 76 and 93 samples respectively after trimming and removing of samples with no results. All OTUs with assigned taxonomy is presented in appendix E.

4.2 Diversity

To investigate the species diversity, the α- diversity was calculated, this was done using both Shannon and Simpson index for diversity. α- diversity was calculated for both samples from cecum content (Figure 8a and 8b) and tissue (Figure 8c and 8d).

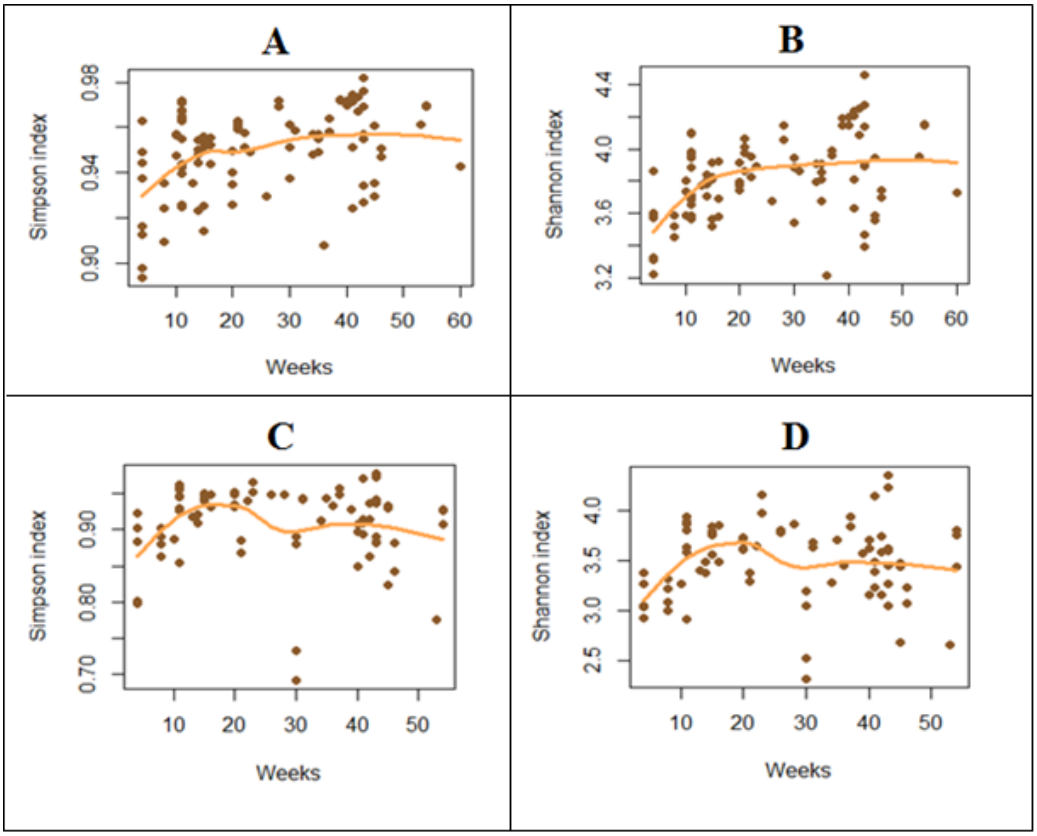

Figur 8: Calculated alpha diversity using both Shannon and Simpson index. **A)** Simpson index in cecum content, **B)** Shannon index in cecum content, **C)** Simpson index in tissue samples, **D)** Shannon index in tissue samples

Mean beta diversity in the two datasets were calculated using Bray–Curtis distances, the results for cecum content and tissue samples were 0,3325 and 0,3458 respectively. Mean beta diversity inside the different age groups in both cecum content and tissue samples were also calculated from Bray-Curtis distances. Mean beta diversity for each age group are presented in appendix F.

A PCA analysis was performed on unweighted UniFrac distances (Figure 9a and 9b). First principal component represents 29% of the variance in tissue samples and 31% in cecum content, second principal component represented 9% of the variance in both tissue samples and cecum content. There were no clear patterns or clusters of age groups in either of the PCA plots. PCA analysis was also done for the weighted UniFrac distances, plots are presented in Appendix G.

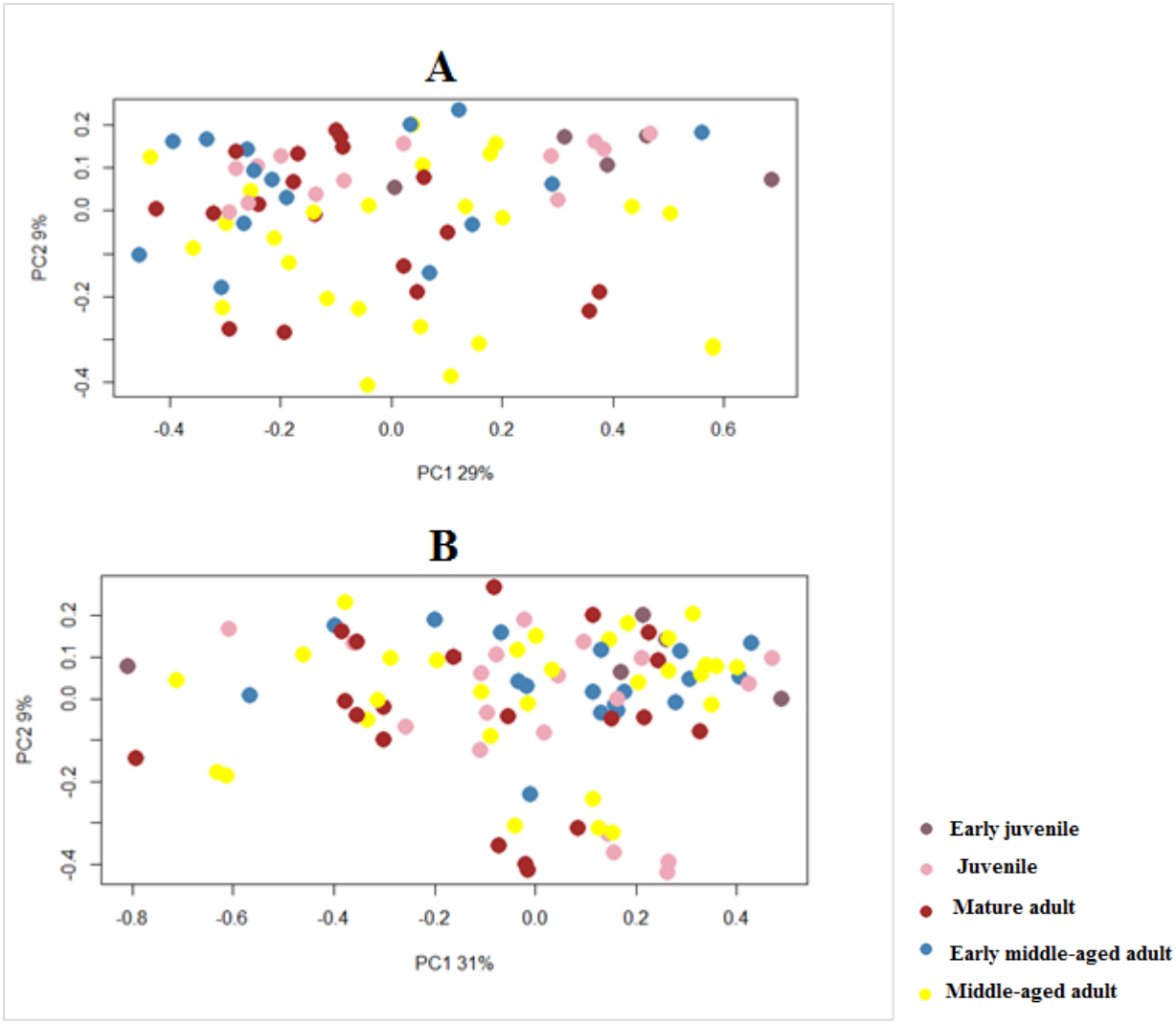

Figure 9: A) PCA plot of unweighted UniFrac distances in tissue samples **B)** PCA plot of unweighted UniFrac distances in samples from cecum content.

Kruskal-Wallis test was performed on the first principal component (pc1) from PCA on unweighted UniFrac distances, this showed significant variation between the different groups in cecum content and tissue p = 0,0217 and p = 0,0434 respectively. Indicating that at least one of the groups are different from the others at 95% significance level. No significant differences between groups were found using Kruskal-Wallis test on (pc1) for weighted UniFrac distances in either tissue (p = 0,92) or cecum content (p = 0,5).

4.3 Taxonomic analysis

The taxonomic composition in both datasets was investigated for the whole group of samples and the composition in the different age groups. The taxonomic composition at phylum level was calculated and relative abundance was used. Members of Firmicutes were the most dominant in both cecum content (61,14%) and tissue (59,47%). In samples from cecum content members of the Bacteroidetes phylum were the second most dominant (27,72%), while Deferribacteres was the second most dominant phylum (20,88%) in tissue samples. Composition in tissue samples and cecum content are presented in figure 10 and figure 11, respectively.

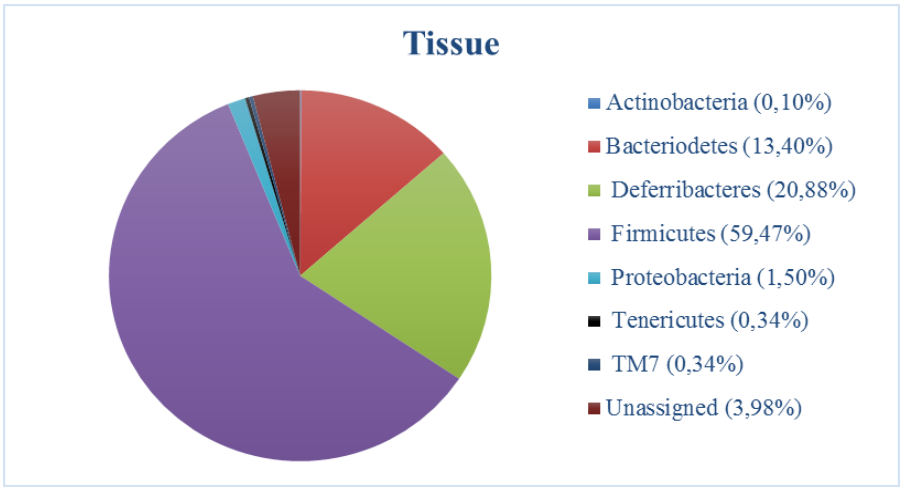

Figure 10: Taxonomic composition at phylum level in tissue samples.

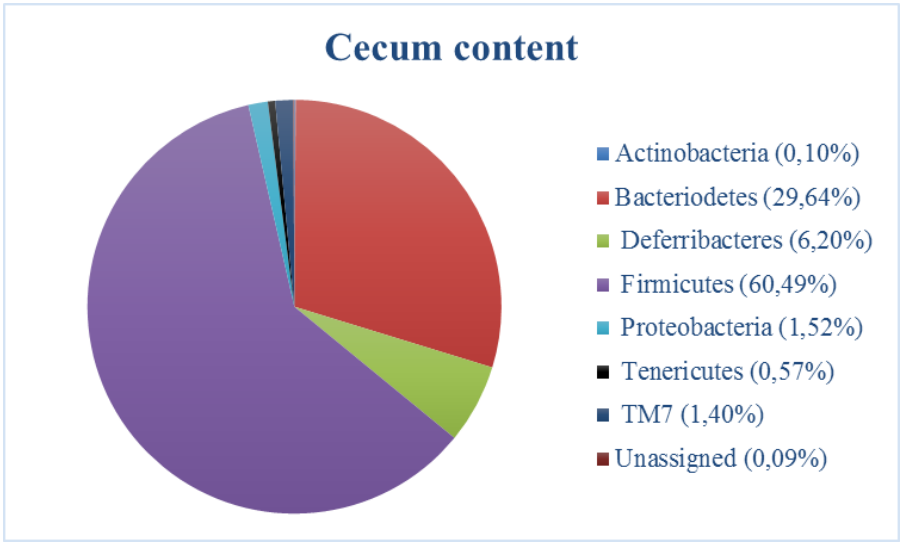

Figure 11: Taxonomic composition at phylum level in cecum content.

The most abundant classes of bacteria in phylum Firmicutes were Bacilli and had a relative abundance of 3,74% in Cecum content and 2,27% in tissue, Erysipelotrichi had a relative

abundance of 0,72% abundance in Cecum content and 0,41% in tissue samples. Clostridia was the most abundant of the classes in this phylum and had a relative abundance of 95,54% in cecum content and 97,32% in tissue samples.

In phylum Proteobacteria Alpha-, Beta-, Delta- and Gammaproteobacteria was represented. Deltaproteobacteria were the most abundant in this phylum and had a relative abundance of 46,72% in cecum content and 76,70% in tissue samples. Gammaproteobacteria were the second most abundant with a relative abundance of 38,49% in cecum content and 11,70% in tissue samples. Betaproteobacteria had a relative abundance of 12,79% in cecum content and 11,36% in tissue samples. Alphaproteobacteria was the least abundant of the classes and had a relative abundance of 1,99% in cecum content and 0,25% in tissue.

Two classes represented phylum Actinobacteria, Coriobacteriia and Actinobacteria. Coriobacteria was the most abundant class and had a relative abundance of 93,02% in cecum content and 97,83% in tissue, while class Actinobacteria had a relative abundance of 6,98% and 2,17% in cecum content and tissue respectively.

The remaining classified phyla were only represented by one class each. Bacteroidia in Bacteroidetes, Deferribacteres in phylum Deferribacteres, Mollicutes in Tenericutes and TM7-3 in phylum TM7.

Deferribacteres had a high relative abundance in both cecum content (5,26%) and tissue (20,88%). this phylum was represented by one bacterial species *Mucispirillum schaedleri*.

In phylum Bacteriodetes the relative abundance of *Rikenellaceae* (familiy) and *S24-7* (familiy) were high. For *Rikenellaceae* the relative abundance was 22,19% in cecum content and 31,4% in tissue samples. *S24-7* had a relative abundance of 53,92% in cecum content and 54,28% in tissue samples.

4.3.1 Taxonomic analyses in the different age groups

The taxonomic composition in each age group was also investigated, to see how the relative abundance of each phylum would change with age. (Figure 12 and 13)

The different age groups used in this project was: group 1: Early juvenile (4-6 weeks), group 2: Juvenile (7-12 weeks), group 3: Mature adult (13-24 weeks), group 4: Early middle-aged adult (25-39 weeks), group 5: Middle-aged adult (40-56 weeks), and group 6: Late middle-aged adult (57-71 weeks).

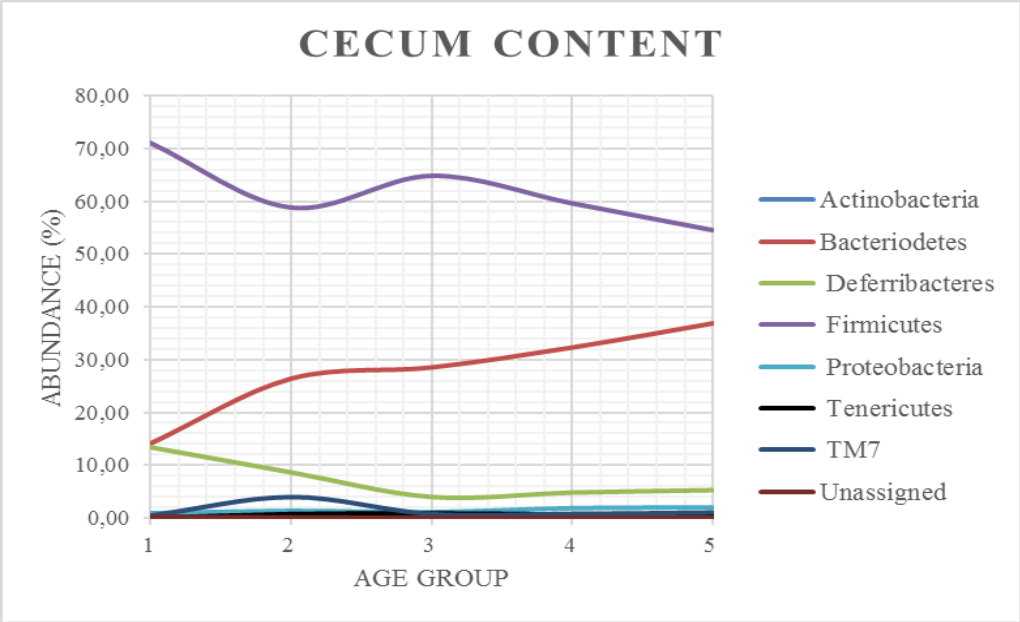

Figure 12: Relative abundance of each phylum and how the abundance varies with age in cecum content.

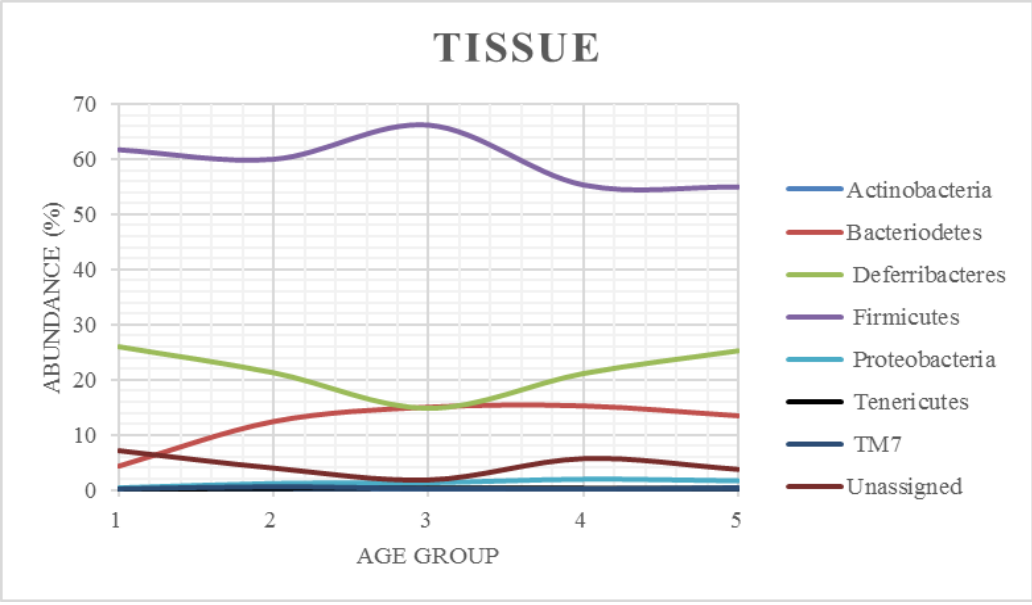

Figure 13: Relative abundance of each phylum and how the abundance varies with age in tissue samples.

4.4 Correlation between bacteria and cancer

Further analyses were done to investigate if any OTUs were significantly linked to cancer progression and age. A spearman rank correlation analysis was performed on microbiota data and tumor data to check if there was any OTUs that were significant correlated with tumor data and/or age. All p-values were corrected for multiple testing with FDR.

The spearman rank coefficient for all significant OTUs were also calculated to see if the OTU were positively or negatively correlated. In both data sets "overlapping" OTUs correlated in the same direction for age, tumorload in colon and for tumorload in small intestine. All p-values and direction of correlation is presented in appendix H.

76 OTUs were significantly linked ($p < 0,05$) to age or tumor progression in samples from cecum content and 66 OTUs were significantly linked in tissue samples. Some of these OTUs correlated with both tumor progression and age, while some correlated with only one of these parameters. Number of OTUs correlated to the different parameters are presented in Venn diagrams shown in Figure 14.

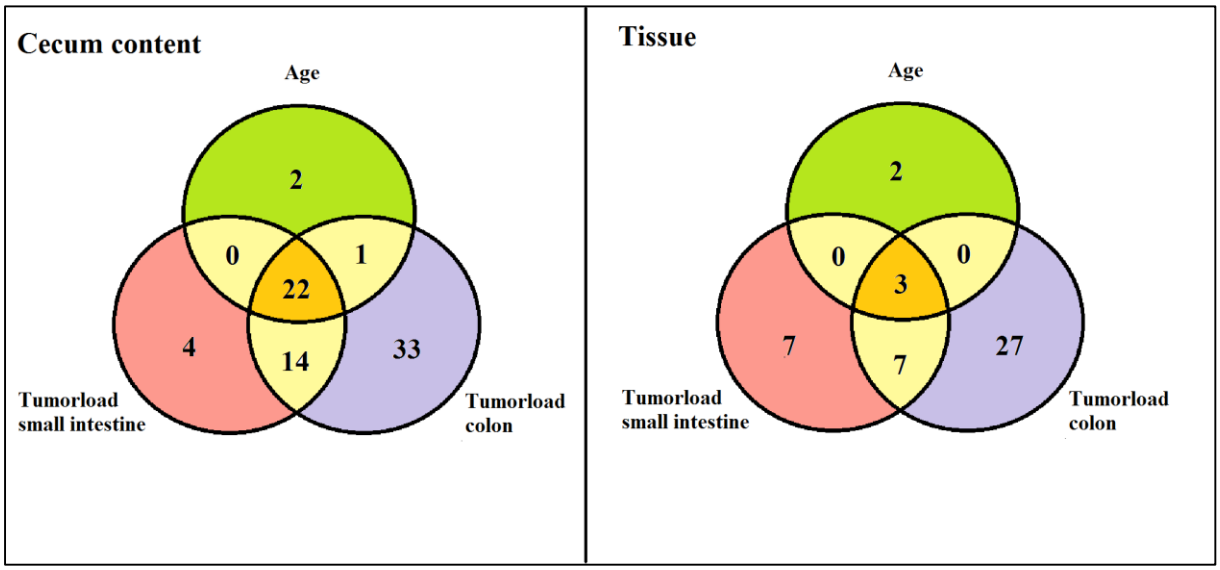

Figure 14: Number of OTUs with significant correlation to age, tumor load in colon and tumorload in small intestine. Left are samples from cecum content and right are tissue samples.

In samples from cecum content a total of 70 OTUs were significantly correlated with tumorload ($p < 0,05$) in colon, 40 OTUs were significantly correlated with tumorload in the small intestine and 25 correlated with age, 14 OTUs were significantly correlated with both tumorload small intestine and colon, 1 OTU correlated with tumorload colon and age and 22 OTUs were significantly correlated with tumorload small intestine, tumorload colon and age.

In samples from tissue a total of 37 OTUs correlated significantly with tumorload in colon, 17 correlated significantly with tumorload in the small intestine and 5 correlated significantly with age.

Only 4 OTUs in total correlated with age alone, only one of these OTUs were positively correlated and was classified as *Parabacteroides*. The three other OTUs were negatively correlated with age and classified as *Lachnospiraceae* (familiy), *Candidatur Arthromitus* and *S24-7* (familiy).

In cecum content, 22 of the OTUs found to correlate with tumor progression and age were from the phylum Bacteroidetes, 20 of these OTUs belonged to the *S24-7* family, one OTU belonged to *Rikenellaceae* and the last OTU was classified as *Prevotella* (genus). All OTUs belonging to the *S24-7* family was correlated either to age and tumor progression in both small intestine and colon or to just tumor progression at both sites, also they were all positively correlated.

For tissue samples, 17 of the OTUs were from phylum Bacteroidetes, 12 of these OTUs were from *S24-7* (family), 4 from *Rikenellaceae* (family) and the last OTU was classified as *Prevotella* (genus). Only two of these 17 OTUs were negatively correlated. One OTU classified as *Desulfovibrionaceae* was also positively correlated to tumor progression in colon in tissue samples.

From phylum Firmicutes 47 and 27 OTUs were significantly correlated to age and tumor progression in cecum content and tissue samples respectively, the correlated OTUs were classified as Clostridiales (order), *Ruminococcaceae* (family), *Lachnospiraceae* (family), *Oscillospira*, *Ruminococcus* and *Ruminococcus gnavus*.

Because of the observed increase in relative abundance of Bacteroidetes and decrease in the relative abundance of Firmicutes in cecum content, the ratio between these two were calculated.

Plots was made to investigate the correlation between tumor progression at both sites and Bacteroidetes/Firmicutes ratio, the results indicated significant correlation between tumorload in colon and Bacteroidetes/Firmicutes ratio, p = 0,0167 (Fig. 15) and significant correlation with tumorload in small intestine, p = 0,0112 (Fig. 16).

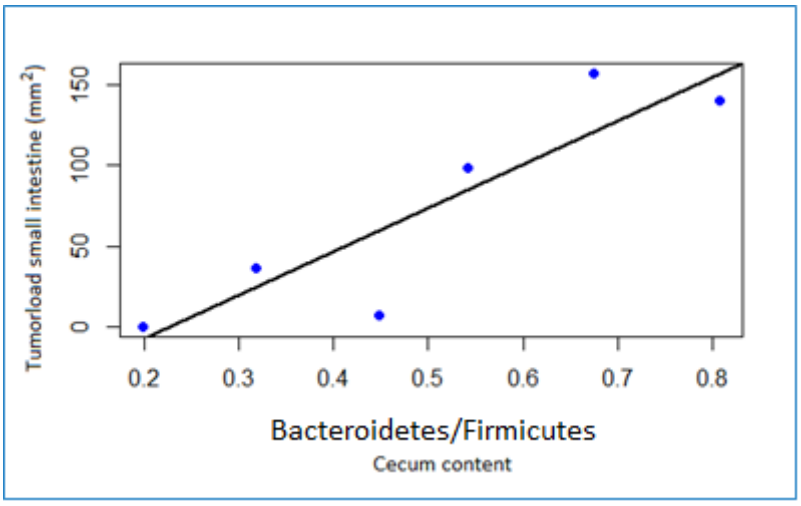

Figure 15: Correlation between Bacteroidetes/Firmicutes from cecum content and Tumorload (mm^2) in small intestine.

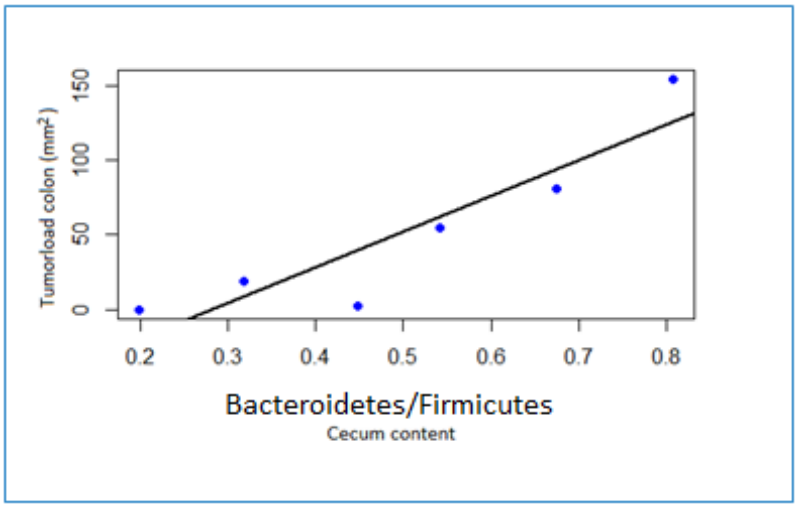

Figure 16: Correlation between Bacteroidetes/Firmicutes from cecum content and Tumorload (mm^2) in colon.

4.5 Butyrate

Detected levels of butyrate in each samples is presented in appendix I.

Plots of tumorload in both colon and small intestine against age were made in order to show the progression of tumors with age. (Figure 17a and 17b). There is a significant correlation between tumorload in both colon (p = 2.5e-08) and small intestine (p = 4.22e-10), Sødring *et al.* (Sodring et al., 2015a) have already investigated the progression of tumors with age in these samples.

The effect of age on butyrate levels in cecum content was also investigated by plotting butyrate levels (mM) against age. There was no significant correlation between age and butyrate levels (p = 0,543), the plot indicates that butyrate levels in these samples are relatively stable with age progression. (Fig. 17c)

Plots of tumorload and butyrate levels were also made to investigate if tumor progression had any effect on butyrate levels (figure 17d and figure17e). No significant correlation was seen between tumorload in colon and butyrate levels (p = 0,449) or tumorload in the small intestine and butyrate levels (p = 0,528).

Tumorload in both small intestine and colon were tested and plotted against both age and butyrate in each age group, however there were no significant correlation between these different factors inside the different age groups. All plots of the different age groups are presented in Appendix J.

The spearman rank correlation analysis with following FDR was also done to investigate if there were any correlations between any bacteria and butyrate levels. One OTU classified as *Ruminococcus* had a significant (p = 0,0450) negative correlation to butyrate in tissue samples and in cecum content one OTU classified as *Ruminococcaceae* had a significant (p = 0,0032) negative correlation with butyrate levels.

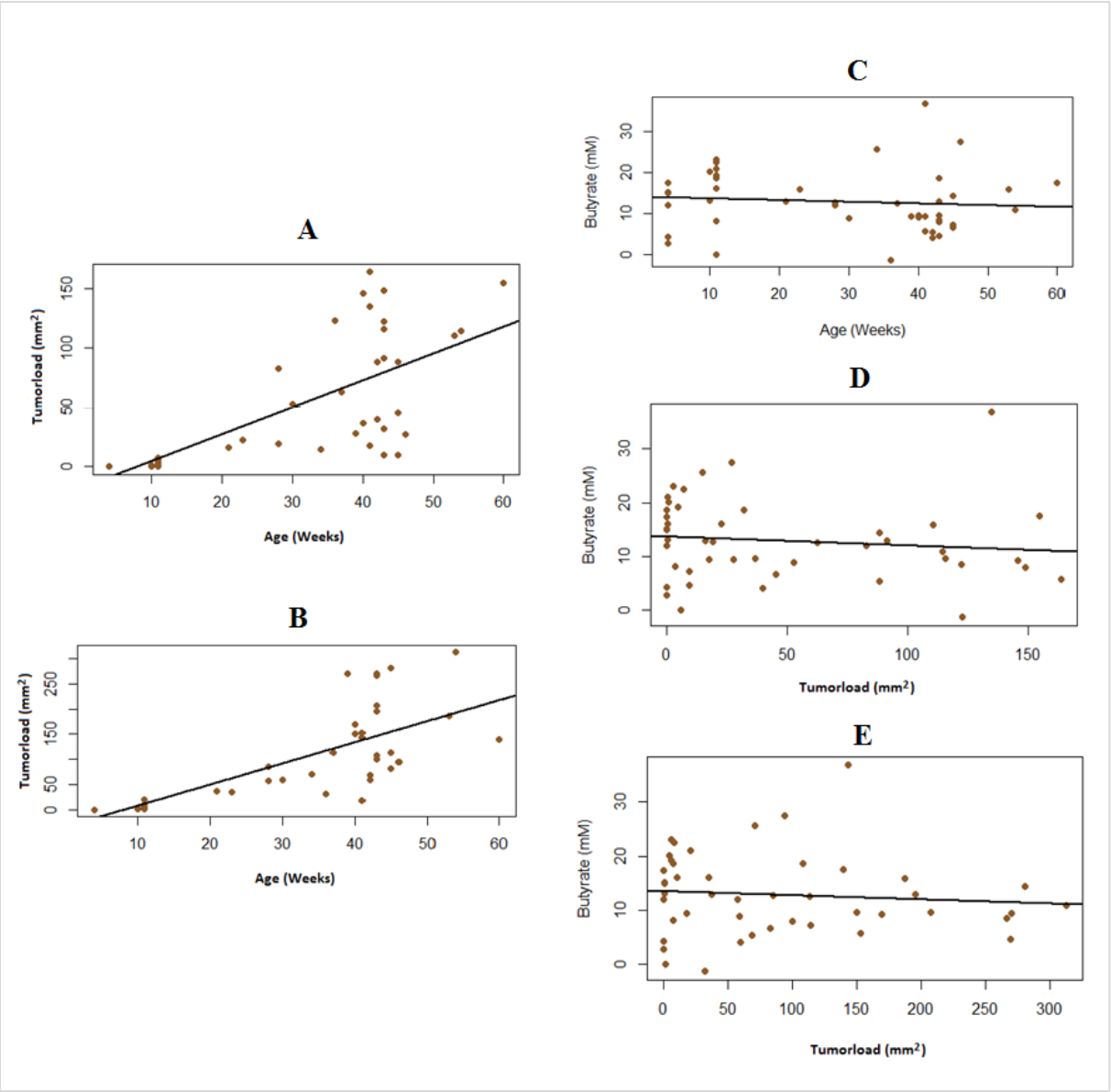

Figure 17: A) Correlation between tumorload small intestine (mm^2) and age (weeks) **B)** Correlation between tumorload colon (mm^2) and age (weeks) **C)** Correlation between butyrate (mM) and age (weeks) **D)** Correlation between butyrate (mM) and tumorload small intestine (mm^2) **E)** Correlation between butyrate (mM) and tumorload colon (mm^2)

5. Discussion

5.1 Diversity

Our data suggests that the alpha diversity reaches a relatively stable microbiota around 20 weeks. In humans the microbiota evolves to resemble a stable adult-like microbiota over the first two years of age (Palmer et al., 2007). Perhaps the stabilisation of diversity seen in microbiota from these samples resembles the evolvement towards a stable adult microbiota seen in humans, and that mouse microbiota reaches this kind of stable "adult" microbiota at around 20 weeks.

Data obtained from analysis on unweighted UniFrac distances suggests that at least one of the age groups are significantly different from the others, but it is difficult to say more without further testing. Comparing the results from weighted and unweighted UniFrac distances suggest that the presence or absence of OTUs is more important than the taxonomic relationships and abundance of the OTUs, when separating samples according to age. This is consistent with observations done by other researchers. (Langille et al., 2014)

A research done by Langlille *et al.* found significant clustering of different age groups in mice also by the use of PCA on UniFrac distances (Langille et al., 2014). Significant differences between age groups using both weighted and unweighted UniFrac distances were found in this study. Interestingly, they divided the mice into only three different age groups; young 174 ±15 days (around 25 weeks), middle 584 ±18 days (around 83 weeks), old 857 ±16 days (around 122 weeks). These groups are very different from those used in this project, where the oldest mouse is 60 weeks. Another study that sampled 4 mice multiple times for a period of over 200 days found a significant increase in UniFrac distance as time between sampling of the mouse increased (Hoy et al., 2015). Therefore, it is possible that one explanation for the little clustering of samples according to age might be due to the fact that the mice used in this project are too close in age or that the sampling interval is too short to see clear clustering and significant taxonomic differences in the microbiota due to differences in age.

5.2 Taxonomic analysis

Our data suggests that there are compositional differences between the luminal and mucosal adherent microbiota. Firmicutes were found to be the most abundant in both compartments, however our data indicated that Bacteroidetes was the second most abundant phylum in the luminal microbiota, while Deferribacteres was the second most abundant in the mucosal adherent microbiota.

This is consistent with other studies investigating mouse microbiota who also found that Firmicutes is the dominant phyla. (Ley et al., 2005, Son et al., 2015b) Deferribacteres have been identified in mouse microbiota before but at a much lower abundance (Gu et al., 2013), to our knowledge this high abundance has not been detected in the mouse microbiota before. *M. schaedleri*, which was the only classified species in this phylum, is a spiral shaped anaerobic bacteria isolated from mucus layer in cecum, colon and liver in laboratory mice (Robertson et al., 2005).

An explanation for the very distinct microbial composition could be due to environmental effects. Vendor specific variations in the microbial composition of A/J mice from the Jackson Laboratory have been suggested in a previous study (Ericsson et al., 2015). Another study that investigated different strains bought from different vendors to see how the genotype of the mouse affected the microbiota, concluded that the environmental effect on the microbial composition might be greater than the genetic background (Friswell et al., 2010).

The A/J Min/+ used in this project has been maintained for several generations at the Norwegian University of Life Sciences, Campus Adamstuen. The homogenous environments of laboratory mice are a familiar challenge and the development of "facilicty-specific" composition of microbiota in laboratory mice strains, kept in facilities for several years have been proposed in a previous study (Friswell et al., 2010). The backcrossing of these mice were done with A/J +/+ females purchased from Jackson Laboratory with resident A/J Min/+mice in order to uphold the A/J Min/+mouse line (Sødring et al., 2015). Perhaps the characteristic microbial composition seen in this study is an example of a facility-specific composition, as the colonies of these mice have been kept at the Norweigian Univeristy of Life Sciences as an inbred colony for many years.

5.4 Correlation between bacteria and cancer

The low amount of OTUs that correlated with age alone is interesting, in concurrence with the results from the diversity analysis, tumor progression seems to have a greater impact than age on the microbiota in these samples. A potential explanation for not finding as many correlations with age as with tumor progression could be the rapid tumor progression compared to the already mentioned argument of the mice being to close in age.

A higher number of OTUs from both microbial compartments correlated with tumor progression in colon rather than tumor progression in small intestine. Cecum and colon are both part of the large intestine in the mouse GI and relatively stable microbiota in the mouse large intestine (cecum, colon and feces) have been suggested before (Gu et al., 2013), similarities between cecal and rectal microbiota in wild mouse have also been indicated (Weldon et al., 2015). The similarities between microbiota in mouse cecum and colon might be an explanation for the high numbers of OTUs correlating with tumor progression in colon rather than the progression of tumorigenesis in the small intestine.

Our data also suggested a relative increase in Bacteroidetes and decrease of Firmicutes, and the ratio of these two correlated significantly to tumor progression. An overrepresentation of Bacteroidetes compared to Firmicutes in samples related to colon cancer have been shown in another research as well (Marchesi et al., 2011). Sobhani *et al.* have also investigated microbiota in CRC patients and controls, elevated levels of Bacteroidetes in CRC patients were found in this study (Sobhani et al., 2011).

These findings are consistent with our data, which indicated that the majority of OTUs from cecum content that correlated positively with tumor progression were from phylum Bacteroides. A potential explanation for the high abundance of Bacteroidetes and S24-7 (family) in our study could be the mouse genotype. A study by Son *et al.* (Son et al., 2015b) found that the APC genotype had a significant dominant effect on the relative abundance on Bacteroidetes and the *S24-7* (family) in mice harbouring the APC Min/+ genotype. They therefore suggested that mutation of the *APC* gene alters the colonic-microbial interactions prior to polyposis.

Our data also suggested a positive significant correlation between *Desulfovibrionaceae* and tumor progression in colon. Tjalsma *et al.* proposed a “driver passenger” model for microbiota associated with colorectal cancer (Tjalsma et al., 2012). The idea was that some types of bacteria can help

initiate CRC ("drivers") while other bacterial species might replace the "driver bacteria" by having a growth advantage in the tumor microenvironment ("passenger") and then stall or promote further tumorigenesis (Tjalsma et al., 2012). Another study investigating the microbial connection to colorectal cancer found evidence supporting the proposition of bacterial "driver-passenger model" for CRC (Geng et al., 2014).

Its intriguing to think that sulphate reducing bacteria and *S24-7* family of Bacteroidetes might be so called "passenger bacteria" in the progression of CRC. Its plausible that the changes in tumor microenvironment is beneficial for these types of bacteria, as they are positively correlated with the progression of tumorigenesis and perhaps they also contribute to further tumor progression.

5.5 Butyrate

We could not find any significant correlation between age and butyrate levels or tumor progression and butyrate in this study. In mice, the fermentation of indigestible food components and the production of SCFAs is compartmentalized in the cecum (Nguyen et al., 2015). It would therefore be natural to think that samples from luminal cecum would give the best representation of butyrate levels in mice samples.

Tumor development in cecum is not as usual for these mice, tumors can occur in cecum, but to our knowledge this has not yet been systematically investigated. The causative effect of butyrate in the tumor-suppressive mechanism of microbial species have been implicated before (Donohoe et al., 2014), this study also conclude that dietary fibre does in fact protect against CRC. Perhaps, the low number of tumors seen in cecum so far is due to the fact that cecum is the primary centre for production of SCFAs in mouse GI and that this protects cecum from being as heavily involved in tumor formation as the other compartments of the mouse GI.

There is also a possibility that the correlation between tumor progression and butyrate levels in samples obtained from cecum might not give an accurate picture of how the butyrate correlates with tumor progression. Mainly because our samples are obtained from cecum while the detected tumor progression is from colon and the small intestine, samples of luminal microbiota and tumor data should perhaps be collected from the same compartments of the mouse GI in order to provide a more accurate correlation of butyrate and tumor progression.

An important aspect that also must be taken into consideration when discussing the fact that this study did not reveal any strong connections between butyrate and tumor progression or age, is the possibility of errors due to technical weaknesses, sample preparations and all the challenges that we encountered with the GC analysis in this project.

5.6 Future work

Because time became a limitation in this project either gender or the so called “cage effect” were not taken into consideration during data the analysis, these are factors known to affect the microbiota and for future work this needs to be addressed.

How the microbial composition vary with age needs to be more elaborated, and it would be of great interest to investigate how this vary in wild type mouse. Then, comparison studies of microbial composition between wild type and the A/J Min mouse strain used in this project would be interesting in order to elaborate the difference in composition and the effect of tumor progression. Systematic investigation of tumor formation in cecum would be of interest in order to better correlate butyrate levels to tumor formation. Levels of butyrate in samples from luminal microbiota in small intestine and colon could also be used for this type of correlation with tumor progression in the different compartments.

It would also be of interest to know how the amount of other abundant SCFAs (propionate and acetate) varies with tumor progression and age. Both compositional variation and the functional aspect of the microbiota according to age and disease needs to be addressed. Further work with larger groups of samples, older mice will also be needed, especially when investigating the effect of age on the microbiota and levels of SCFA. Understanding of how the mouse genotype affects the microbial composition is still unclear and deserves future investigation. More information about host-microbial associations may be useful and important in cancer research using rodent models as models for human CRC.

6. Conclusion

This study investigated the co-variation between age, tumor progression and microbial composition. Levels of butyrate in the luminal microbiota of cecum samples were also investigated. The results from this project indicate that the compositional diversity of the mouse microbiota stabilizes at around 20 weeks and seems to be stable after this. This indicates that the mouse microbiota, as in humans evolves towards an “adult-microbiota”. The results from this project also show that there are bacteria associated with both age and tumor progression. The great amount of groups of bacteria found to correlate with only tumor progression indicates that tumor progression likely has a stronger impact on the microbial composition than age in these samples. We could not find any significant correlation between butyrate and microbiota, age or tumor progression in this study. So from our point of view it does not seem like butyrate have a great association with age or a great impact on tumor progression in these samples. The understanding of how the microbiota affects disease or how host genotype and disease affect microbiota is still not complete. However, this study provides some insight to consider in further analysis of host-microbial interactions.

7. References

2014. The Integrative Human Microbiome Project: dynamic analysis of microbiome-host omics profiles during periods of human health and disease. *Cell Host Microbe,* 16**,** 276-89.

ABREU, M. T. & PEEK, R. M., JR. 2014. Gastrointestinal malignancy and the microbiome. *Gastroenterology,* 146**,** 1534-1546 e3.

AKIN, H. & TOZUN, N. 2014. Diet, microbiota, and colorectal cancer. *J Clin Gastroenterol,* 48 Suppl 1**,** S67-9.

ALBERTS, D. S., MARTINEZ, M. E., ROE, D. J., GUILLEN-RODRIGUEZ, J. M., MARSHALL, J. R., VAN LEEUWEN, J. B., REID, M. E., RITENBAUGH, C., VARGAS, P. A., BHATTACHARYYA, A. B., EARNEST, D. L. & SAMPLINER, R. E. 2000. Lack of effect of a high-fiber cereal supplement on the recurrence of colorectal adenomas. Phoenix Colon Cancer Prevention Physicians' Network. *N Engl J Med,* 342**,** 1156-62.

AOYAMA, M., KOTANI, J. & USAMI, M. 2010. Butyrate and propionate induced activated or non-activated neutrophil apoptosis via HDAC inhibitor activity but without activating GPR-41/GPR-43 pathways. *Nutrition,* 26**,** 653-61.

BAXTER, N. T., ZACKULAR, J. P., CHEN, G. Y. & SCHLOSS, P. D. 2014a. Structure of the gut microbiome following colonization with human feces determines colonic tumor burden. *Microbiome,* 2**,** 20.

BAXTER, N. T., ZACKULAR, J. P., CHEN, G. Y. & SCHLOSS, P. D. 2014b. Structure of the gut microbiome following colonization with human feces determines colonic tumor burden. *Microbiome,* 2**,** 20-20.

BIENZ, M. & HAMADA, F. 2004. Adenomatous polyposis coli proteins and cell adhesion. *Curr Opin Cell Biol,* 16**,** 528-35.

BIRD, R. P. & GOOD, C. K. 2000. The significance of aberrant crypt foci in understanding the pathogenesis of colon cancer. *Toxicol Lett,* 112-113**,** 395-402.

BULTMAN, S. J. 2014. Molecular pathways: gene-environment interactions regulating dietary fiber induction of proliferation and apoptosis via butyrate for cancer prevention. *Clin Cancer Res,* 20**,** 799-803.

CADIGAN, K. M. & LIU, Y. I. 2006. Wnt signaling: complexity at the surface. *J Cell Sci,* 119**,** 395-402.

CAPORASO, J. G., KUCZYNSKI, J., STOMBAUGH, J., BITTINGER, K., BUSHMAN, F. D., COSTELLO, E. K., FIERER, N., PENA, A. G., GOODRICH, J. K., GORDON, J. I., HUTTLEY, G. A., KELLEY, S. T., KNIGHTS, D., KOENIG, J. E., LEY, R. E., LOZUPONE, C. A., MCDONALD, D., MUEGGE, B. D., PIRRUNG, M., REEDER, J., SEVINSKY, J. R., TURNBAUGH, P. J., WALTERS, W. A., WIDMANN, J., YATSUNENKO, T., ZANEVELD, J. & KNIGHT, R. 2010. QIIME allows analysis of high-throughput community sequencing data. *Nat Methods,* 7**,** 335-6.

CLEMENTE, J. C., URSELL, L. K., PARFREY, L. W. & KNIGHT, R. 2012. The impact of the gut microbiota on human health: an integrative view. *Cell,* 148**,** 1258-70.

CLEVERS, H. 2013. The intestinal crypt, a prototype stem cell compartment. *Cell,* 154**,** 274-84.

COLLINS, S. M., SURETTE, M. & BERCIK, P. 2012. The interplay between the intestinal microbiota and the brain. *Nat Rev Microbiol,* 10**,** 735-42.

CRESS, W. D. & SETO, E. 2000. Histone deacetylases, transcriptional control, and cancer. *J Cell Physiol,* 184**,** 1-16.

CUMMINGS, J. H., POMARE, E. W., BRANCH, W. J., NAYLOR, C. P. & MACFARLANE, G. T. 1987. Short chain fatty acids in human large intestine, portal, hepatic and venous blood. *Gut,* 28**,** 1221-7.

DAVE, M., HIGGINS, P. D., MIDDHA, S. & RIOUX, K. P. 2012. The human gut microbiome: current knowledge, challenges, and future directions. *Transl Res,* 160**,** 246-57.

DONOHOE, D. R., COLLINS, L. B., WALI, A., BIGLER, R., SUN, W. & BULTMAN, S. J. 2012. The Warburg effect dictates the mechanism of butyrate-mediated histone acetylation and cell proliferation. *Mol Cell,* 48**,** 612-26.

DONOHOE, D. R., HOLLEY, D., COLLINS, L. B., MONTGOMERY, S. A., WHITMORE, A. C., HILLHOUSE, A., CURRY, K. P., RENNER, S. W., GREENWALT, A., RYAN, E. P., GODFREY, V., HEISE, M. T., THREADGILL, D. S., HAN, A., SWENBERG, J. A., THREADGILL, D. W. & BULTMAN, S. J. 2014. A Gnotobiotic Mouse Model Demonstrates that Dietary Fiber Protects Against Colorectal Tumorigenesis in a Microbiota- and Butyrate–Dependent Manner. *Cancer discovery,* 4**,** 1387-1397.

ERICSSON, A. C., DAVIS, J. W., SPOLLEN, W., BIVENS, N., GIVAN, S., HAGAN, C. E., MCINTOSH, M. & FRANKLIN, C. L. 2015. Effects of Vendor and Genetic Background on the Composition of the Fecal Microbiota of Inbred Mice. *PLoS ONE,* 10**,** e0116704.

FADROSH, D. W., MA, B., GAJER, P., SENGAMALAY, N., OTT, S., BROTMAN, R. M. & RAVEL, J. 2014. An improved dual-indexing approach for multiplexed 16S rRNA gene sequencing on the Illumina MiSeq platform. *Microbiome,* 2**,** 6.

FEARNHEAD, N. S., BRITTON, M. P. & BODMER, W. F. 2001. The ABC of APC. *Hum Mol Genet,* 10**,** 721-33.

FERLAY, J., SOERJOMATARAM, I., ERVIK, M., FORMAN, D. & BRAY, F. 2013. *Cancer incidence and mortality worldwide: IARC CancerBase No. 11* [Online]. Internet: GLOBOCAN 2012 v.1.0. Available: http://http://globocan.iarc.fr/ [Accessed January 10 2016].

FRISWELL, M. K., GIKA, H., STRATFORD, I. J., THEODORIDIS, G., TELFER, B., WILSON, I. D. & MCBAIN, A. J. 2010. Site and Strain-Specific Variation in Gut Microbiota Profiles and Metabolism in Experimental Mice. *PLoS ONE,* 5**,** e8584.

FURET, J. P., KONG, L. C., TAP, J., POITOU, C., BASDEVANT, A., BOUILLOT, J. L., MARIAT, D., CORTHIER, G., DORE, J., HENEGAR, C., RIZKALLA, S. & CLEMENT, K. 2010. Differential adaptation of human gut microbiota to bariatric surgery-induced weight loss: links with metabolic and low-grade inflammation markers. *Diabetes,* 59**,** 3049-57.

GENG, J., SONG, Q., TANG, X., LIANG, X., FAN, H., PENG, H., GUO, Q. & ZHANG, Z. 2014. Co-occurrence of driver and passenger bacteria in human colorectal cancer. *Gut Pathog,* 6**,** 26.

GREGORIEFF, A. & CLEVERS, H. 2005. Wnt signaling in the intestinal epithelium: from endoderm to cancer. *Genes Dev,* 19**,** 877-90.

GU, S., CHEN, D., ZHANG, J. N., LV, X., WANG, K., DUAN, L. P., NIE, Y. & WU, X. L. 2013. Bacterial community mapping of the mouse gastrointestinal tract. *PLoS One,* 8**,** e74957.

GUARNER, F. 2006. Enteric flora in health and disease. *Digestion,* 73 Suppl 1**,** 5-12.

HALL, N. 2007. Advanced sequencing technologies and their wider impact in microbiology. *J Exp Biol,* 210**,** 1518-25.

HESTER, C. M., JALA, V. R., LANGILLE, M. G., UMAR, S., GREINER, K. A. & HARIBABU, B. 2015. Fecal microbes, short chain fatty acids, and colorectal cancer across racial/ethnic groups. *World J Gastroenterol,* 21**,** 2759-69.

HOLMBERG, J., GENANDER, M., HALFORD, M. M., ANNEREN, C., SONDELL, M., CHUMLEY, M. J., SILVANY, R. E., HENKEMEYER, M. & FRISEN, J. 2006. EphB receptors coordinate migration and proliferation in the intestinal stem cell niche. *Cell,* 125**,** 1151-63.

HOY, Y. E., BIK, E. M., LAWLEY, T. D., HOLMES, S. P., MONACK, D. M., THERIOT, J. A. & RELMAN, D. A. 2015. Variation in Taxonomic Composition of the Fecal Microbiota in an Inbred Mouse Strain across Individuals and Time. *PLoS ONE,* 10**,** e0142825.

IRRAZABAL, T., BELCHEVA, A., GIRARDIN, S. E., MARTIN, A. & PHILPOTT, D. J. 2014. The multifaceted role of the intestinal microbiota in colon cancer. *Mol Cell,* 54**,** 309-20.

KARLSSON, F. H., TREMAROLI, V., NOOKAEW, I., BERGSTROM, G., BEHRE, C. J., FAGERBERG, B., NIELSEN, J. & BACKHED, F. 2013. Gut metagenome in European women with normal, impaired and diabetic glucose control. *Nature,* 498**,** 99-103.

KIMELMAN, D. & XU, W. 2006. beta-catenin destruction complex: insights and questions from a structural perspective. *Oncogene,* 25**,** 7482-91.

KINZLER, K. W., NILBERT, M. C., SU, L. K., VOGELSTEIN, B., BRYAN, T. M., LEVY, D. B., SMITH, K. J., PREISINGER, A. C., HEDGE, P., MCKECHNIE, D. & ET AL. 1991. Identification of FAP locus genes from chromosome 5q21. *Science,* 253**,** 661-5.

KOLAR, S. S., BARHOUMI, R., CALLAWAY, E. S., FAN, Y. Y., WANG, N., LUPTON, J. R. & CHAPKIN, R. S. 2007. Synergy between docosahexaenoic acid and butyrate elicits p53-independent apoptosis via mitochondrial Ca(2+) accumulation in colonocytes. *Am J Physiol Gastrointest Liver Physiol,* 293**,** G935-43.

KORINEK, V., BARKER, N., MORIN, P. J., VAN WICHEN, D., DE WEGER, R., KINZLER, K. W., VOGELSTEIN, B. & CLEVERS, H. 1997. Constitutive transcriptional activation by a beta-catenin-Tcf complex in APC-/- colon carcinoma. *Science,* 275**,** 1784-7.

KRAUSOVA, M. & KORINEK, V. 2014. Wnt signaling in adult intestinal stem cells and cancer. *Cell Signal,* 26**,** 570-9.

LANGILLE, M. G. I., MEEHAN, C. J., KOENIG, J. E., DHANANI, A. S., ROSE, R. A., HOWLETT, S. E. & BEIKO, R. G. 2014. Microbial shifts in the aging mouse gut. *Microbiome,* 2**,** 1-12.

LEY, R. E., BACKHED, F., TURNBAUGH, P., LOZUPONE, C. A., KNIGHT, R. D. & GORDON, J. I. 2005. Obesity alters gut microbial ecology. *Proc Natl Acad Sci U S A,* 102**,** 11070-5.

LI, H., LIMENITAKIS, J. P., FUHRER, T., GEUKING, M. B., LAWSON, M. A., WYSS, M., BRUGIROUX, S., KELLER, I., MACPHERSON, J. A., RUPP, S., STOLP, B., STEIN, J. V., STECHER, B., SAUER, U., MCCOY, K. D. & MACPHERSON, A. J. 2015. The outer mucus layer hosts a distinct intestinal microbial niche. *Nat Commun,* 6.

LOZUPONE, C. A., STOMBAUGH, J. I., GORDON, J. I., JANSSON, J. K. & KNIGHT, R. 2012. Diversity, stability and resilience of the human gut microbiota. *Nature,* 489**,** 220-230.

MACDONALD, B. T., TAMAI, K. & HE, X. 2009. Wnt/β-catenin signaling: components, mechanisms, and diseases. *Developmental cell,* 17**,** 9-26.

MACHIELS, K., JOOSSENS, M., SABINO, J., DE PRETER, V., ARIJS, I., EECKHAUT, V., BALLET, V., CLAES, K., VAN IMMERSEEL, F., VERBEKE, K., FERRANTE, M., VERHAEGEN, J., RUTGEERTS, P. & VERMEIRE, S. 2014. A decrease of the butyrate-producing species Roseburia hominis and Faecalibacterium prausnitzii defines dysbiosis in patients with ulcerative colitis. *Gut,* 63**,** 1275-83.

MARCHESI, J. R., DUTILH, B. E., HALL, N., PETERS, W. H., ROELOFS, R., BOLEIJ, A. & TJALSMA, H. 2011. Towards the human colorectal cancer microbiome. *PLoS One,* 6**,** e20447.

MAXAM, A. M. & GILBERT, W. 1977. A new method for sequencing DNA. *Proc Natl Acad Sci U S A,* 74**,** 560-4.

MIYAKI, M., KONISHI, M., KIKUCHI-YANOSHITA, R., ENOMOTO, M., IGARI, T., TANAKA, K., MURAOKA, M., TAKAHASHI, H., AMADA, Y., FUKAYAMA, M. &

ET AL. 1994. Characteristics of somatic mutation of the adenomatous polyposis coli gene in colorectal tumors. *Cancer Res,* 54**,** 3011-20.

MOREY, M., FERNANDEZ-MARMIESSE, A., CASTINEIRAS, D., FRAGA, J. M., COUCE, M. L. & COCHO, J. A. 2013. A glimpse into past, present, and future DNA sequencing. *Mol Genet Metab,* 110**,** 3-24.

MORIN, P. J., SPARKS, A. B., KORINEK, V., BARKER, N., CLEVERS, H., VOGELSTEIN, B. & KINZLER, K. W. 1997. Activation of beta-catenin-Tcf signaling in colon cancer by mutations in beta-catenin or APC. *Science,* 275**,** 1787-90.

MOSER, A. R., LUONGO, C., GOULD, K. A., MCNELEY, M. K., SHOEMAKER, A. R. & DOVE, W. F. 1995. ApcMin: a mouse model for intestinal and mammary tumorigenesis. *Eur J Cancer,* 31A**,** 1061-4.

MOSER, A. R., PITOT, H. C. & DOVE, W. F. 1990. A dominant mutation that predisposes to multiple intestinal neoplasia in the mouse. *Science,* 247**,** 322-4.

NADKARNI, M. A., MARTIN, F. E., JACQUES, N. A. & HUNTER, N. 2002. Determination of bacterial load by real-time PCR using a broad-range (universal) probe and primers set. *Microbiology,* 148**,** 257-66.

NAJDI, R., HOLCOMBE, R. F. & WATERMAN, M. L. 2011. Wnt signaling and colon carcinogenesis: beyond APC. *J Carcinog,* 10**,** 5.

NGUYEN, T. L. A., VIEIRA-SILVA, S., LISTON, A. & RAES, J. 2015. How informative is the mouse for human gut microbiota research? *Disease Models and Mechanisms,* 8**,** 1-16.

NISHISHO, I., NAKAMURA, Y., MIYOSHI, Y., MIKI, Y., ANDO, H., HORII, A., KOYAMA, K., UTSUNOMIYA, J., BABA, S. & HEDGE, P. 1991. Mutations of chromosome 5q21 genes in FAP and colorectal cancer patients. *Science,* 253**,** 665-9.

NORWAY, C. R. O. 2015. *Cancer in Norway 2014* [Online]. Internet. Available: http://www.kreftregisteret.no/en/General/Publications/Cancer-in-Norway/Cancer-in-Norway-2014/ [Accessed January 10 2016].

PALMER, C., BIK, E. M., DIGIULIO, D. B., RELMAN, D. A. & BROWN, P. O. 2007. Development of the human infant intestinal microbiota. *PLoS Biol,* 5**,** e177.

PARK, Y., HUNTER, D. J., SPIEGELMAN, D., BERGKVIST, L., BERRINO, F., VAN DEN BRANDT, P. A., BURING, J. E., COLDITZ, G. A., FREUDENHEIM, J. L., FUCHS, C. S., GIOVANNUCCI, E., GOLDBOHM, R. A., GRAHAM, S., HARNACK, L., HARTMAN, A. M., JACOBS, D. R., JR., KATO, I., KROGH, V., LEITZMANN, M. F., MCCULLOUGH, M. L., MILLER, A. B., PIETINEN, P., ROHAN, T. E., SCHATZKIN, A., WILLETT, W. C., WOLK, A., ZELENIUCH-JACQUOTTE, A., ZHANG, S. M. & SMITH-WARNER, S. A. 2005. Dietary fiber intake and risk of colorectal cancer: a pooled analysis of prospective cohort studies. *JAMA,* 294**,** 2849-57.

PAULSEN, J. E. 2000. Modulation by dietary factors in murine FAP models. *Toxicol Lett,* 112-113**,** 403-9.

PAULSEN, J. E., NAMORK, E., STEFFENSEN, I. L., EIDE, T. J. & ALEXANDER, J. 2000. Identification and quantification of aberrant crypt foci in the colon of Min mice--a murine model of familial adenomatous polyposis. *Scand J Gastroenterol,* 35**,** 534-9.

PETERS, U., SINHA, R., CHATTERJEE, N., SUBAR, A. F., ZIEGLER, R. G., KULLDORFF, M., BRESALIER, R., WEISSFELD, J. L., FLOOD, A., SCHATZKIN, A. & HAYES, R. B. 2003. Dietary fibre and colorectal adenoma in a colorectal cancer early detection programme. *Lancet,* 361**,** 1491-5.

QIN, J., LI, R., RAES, J., ARUMUGAM, M., BURGDORF, K. S., MANICHANH, C., NIELSEN, T., PONS, N., LEVENEZ, F., YAMADA, T., MENDE, D. R., LI, J., XU, J., LI, S., LI, D., CAO, J., WANG, B., LIANG, H., ZHENG, H., XIE, Y., TAP, J., LEPAGE, P., BERTALAN, M., BATTO, J. M., HANSEN, T., LE PASLIER, D., LINNEBERG, A., NIELSEN, H. B., PELLETIER, E., RENAULT, P., SICHERITZ-PONTEN, T., TURNER,

K., ZHU, H., YU, C., LI, S., JIAN, M., ZHOU, Y., LI, Y., ZHANG, X., LI, S., QIN, N., YANG, H., WANG, J., BRUNAK, S., DORE, J., GUARNER, F., KRISTIANSEN, K., PEDERSEN, O., PARKHILL, J., WEISSENBACH, J., BORK, P., EHRLICH, S. D. & WANG, J. 2010. A human gut microbial gene catalogue established by metagenomic sequencing. *Nature,* 464**,** 59-65.

REMELY, M., AUMUELLER, E., MEROLD, C., DWORZAK, S., HIPPE, B., ZANNER, J., POINTNER, A., BRATH, H. & HASLBERGER, A. G. 2014. Effects of short chain fatty acid producing bacteria on epigenetic regulation of FFAR3 in type 2 diabetes and obesity. *Gene,* 537**,** 85-92.

ROBERTSON, B. R., APOS, ROURKE, J. L., NEILAN, B. A., VANDAMME, P., ON, S. L. W., FOX, J. G. & LEE, A. 2005. Mucispirillum schaedleri gen. nov., sp. nov., a spiral-shaped bacterium colonizing the mucus layer of the gastrointestinal tract of laboratory rodents. *International Journal of Systematic and Evolutionary Microbiology,* 55**,** 1199-1204.

ROY, S. & MAJUMDAR, A. P. N. 2012. Signaling in colon cancer stem cells. *J Mol Signal,* 7**,** 11.

RUSTGI, A. K. 2007. The genetics of hereditary colon cancer. *Genes Dev,* 21**,** 2525-38.

SANGER, F., NICKLEN, S. & COULSON, A. R. 1977. DNA sequencing with chain-terminating inhibitors. *Proc Natl Acad Sci U S A,* 74**,** 5463-7.

SANKAR, S. A., LAGIER, J. C., PONTAROTTI, P., RAOULT, D. & FOURNIER, P. E. 2015. The human gut microbiome, a taxonomic conundrum. *Syst Appl Microbiol,* 38**,** 276-86.

SENDA, T., IIZUKA-KOGO, A., ONOUCHI, T. & SHIMOMURA, A. 2007. Adenomatous polyposis coli (APC) plays multiple roles in the intestinal and colorectal epithelia. *Med Mol Morphol,* 40**,** 68-81.

SHEN, X. J., RAWLS, J. F., RANDALL, T., BURCAL, L., MPANDE, C. N., JENKINS, N., JOVOV, B., ABDO, Z., SANDLER, R. S. & KEKU, T. O. 2010. Molecular characterization of mucosal adherent bacteria and associations with colorectal adenomas. *Gut Microbes,* 1**,** 138-47.

SOBHANI, I., TAP, J., ROUDOT-THORAVAL, F., ROPERCH, J. P., LETULLE, S., LANGELLA, P., CORTHIER, G., TRAN VAN NHIEU, J. & FURET, J. P. 2011. Microbial dysbiosis in colorectal cancer (CRC) patients. *PLoS One,* 6**,** e16393.

SODRING, M., GUNNES, G. & PAULSEN, J. E. 2015a. Spontaneous initiation, promotion, and progression of colorectal cancer in the novel A/J Min/+ mouse. *Int J Cancer*.

SODRING, M., OOSTINDJER, M., EGELANDSDAL, B. & PAULSEN, J. E. 2015b. Effects of hemin and nitrite on intestinal tumorigenesis in the A/J Min/+ mouse model. *PLoS One,* 10**,** e0122880.

SON, J. S., KHAIR, S., PETTET, D. W., 3RD, OUYANG, N., TIAN, X., ZHANG, Y., ZHU, W., MACKENZIE, G. G., ROBERTSON, C. E., IR, D., FRANK, D. N., RIGAS, B. & LI, E. 2015a. Altered Interactions between the Gut Microbiome and Colonic Mucosa Precede Polyposis in APCMin/+ Mice. *PLoS One,* 10**,** e0127985.

SON, J. S., KHAIR, S., PETTET, D. W., III, OUYANG, N., TIAN, X., ZHANG, Y., ZHU, W., MACKENZIE, G. G., ROBERTSON, C. E., IR, D., FRANK, D. N., RIGAS, B. & LI, E. 2015b. Altered Interactions between the Gut Microbiome and Colonic Mucosa Precede Polyposis in APC^{Min/+} Mice. *PLoS ONE,* 10**,** e0127985.

SONG, J. H., HUELS, D. J., RIDGWAY, R. A., SANSOM, O. J., KHOLODENKO, B. N., KOLCH, W. & CHO, K. H. 2014. The APC network regulates the removal of mutated cells from colonic crypts. *Cell Rep,* 7**,** 94-103.

SRIVASTAVA, S., VERMA, M. & HENSON, D. E. 2001. Biomarkers for early detection of colon cancer. *Clin Cancer Res,* 7**,** 1118-26.

SU, L. K., KINZLER, K. W., VOGELSTEIN, B., PREISINGER, A. C., MOSER, A. R., LUONGO, C., GOULD, K. A. & DOVE, W. F. 1992. Multiple intestinal neoplasia caused by a mutation in the murine homolog of the APC gene. *Science,* 256**,** 668-70.

SZCZESNIAK, O., K, A. H., HANSSEN, J. F. & RUDI, K. 2015. Isovaleric acid in stool correlates with human depression. *Nutr Neurosci*.

SØDRING, M., OOSTINDJER, M., EGELANDSDAL, B. & PAULSEN, J. E. 2015. Effects of Hemin and Nitrite on Intestinal Tumorigenesis in the A/J Min/+ Mouse Model. *PLoS ONE,* 10**,** e0122880.

TJALSMA, H., BOLEIJ, A., MARCHESI, J. R. & DUTILH, B. E. 2012. A bacterial driver–passenger model for colorectal cancer: beyond the usual suspects. *Nat Rev Micro,* 10**,** 575-582.

TOJO, R., SUAREZ, A., CLEMENTE, M. G., DE LOS REYES-GAVILAN, C. G., MARGOLLES, A., GUEIMONDE, M. & RUAS-MADIEDO, P. 2014. Intestinal microbiota in health and disease: role of bifidobacteria in gut homeostasis. *World J Gastroenterol,* 20**,** 15163-76.

VAN DIJK, E. L., AUGER, H., JASZCZYSZYN, Y. & THERMES, C. 2014. Ten years of next-generation sequencing technology. *Trends Genet,* 30**,** 418-26.

VINOLO, M. A., RODRIGUES, H. G., HATANAKA, E., SATO, F. T., SAMPAIO, S. C. & CURI, R. 2011. Suppressive effect of short-chain fatty acids on production of proinflammatory mediators by neutrophils. *J Nutr Biochem,* 22**,** 849-55.

WALDECKER, M., KAUTENBURGER, T., DAUMANN, H., VEERIAH, S., WILL, F., DIETRICH, H., POOL-ZOBEL, B. L. & SCHRENK, D. 2008. Histone-deacetylase inhibition and butyrate formation: Fecal slurry incubations with apple pectin and apple juice extracts. *Nutrition,* 24**,** 366-74.

WELDON, L., ABOLINS, S., LENZI, L., BOURNE, C., RILEY, E. M. & VINEY, M. 2015. The Gut Microbiota of Wild Mice. *PLoS One,* 10**,** e0134643.

WILLEY, J. M., SHERWOOD, L. M. & WOOLVERTON, C. J. 2012. *Prescott's Principles of MICROBIOLOGY*, McGraw-Hill.

YARZA, P., YILMAZ, P., PRUESSE, E., GLOCKNER, F. O., LUDWIG, W., SCHLEIFER, K. H., WHITMAN, W. B., EUZEBY, J., AMANN, R. & ROSSELLO-MORA, R. 2014. Uniting the classification of cultured and uncultured bacteria and archaea using 16S rRNA gene sequences. *Nat Rev Microbiol,* 12**,** 635-45.

YU, Y., LEE, C., KIM, J. & HWANG, S. 2005. Group-specific primer and probe sets to detect methanogenic communities using quantitative real-time polymerase chain reaction. *Biotechnol Bioeng,* 89**,** 670-9.

ZENG, B., LI, G., YUAN, J., LI, W., TANG, H. & WEI, H. 2013. Effects of age and strain on the microbiota colonization in an infant human flora-associated mouse model. *Curr Microbiol,* 67**,** 313-21.

ZHU, Y., MICHELLE LUO, T., JOBIN, C. & YOUNG, H. A. 2011. Gut microbiota and probiotics in colon tumorigenesis. *Cancer Lett,* 309**,** 119-27.

8. Appendix

Appendix A: Weight of material extracted from mouse cecum

Table 1: Sample ID and material weight (g). Sample ID "I" as are cecum samples and sample ID "E" is tissue samples.

Sample ID	Material weight (g)	Sample ID	Material weight (g)
I1	0,158	E1	0,166
I2	0,029	E2	0,217
I3	0,106	E3	0,087
I4	0,119	E4	0,154
I5	0,234	E5	0,264
I6	0,158	E6	0,154
I7	0,09	E7	0,146
I8	0,123	E8	0,191
I9	0,162	E9	0,374
I10	0,194	E10	0,423
I11	0,206	E11	0,18
I12	0,241	E12	0,207
I13	0,108	E13	0,313
I14	0,174	E14	0,208
I15	0,096	E15	0,281
I16	0,148	E16	0,213
I17	0,15	E17	0,206
I18	0,229	E18	0,224
I19	0,165	E19	0,186
I20	0,063	E20	0,216
I21	0,144	E21	0,154
I22	0,139	E22	0,143
I23	0,166	E23	0,126
I24	0,097	E24	0,125
I25	0,182	E25	0,219
I26	0,157	E26	0,189
I27	0,098	E27	0,145
I28	0,207	E28	0,342
I29	0,083	E29	0,072
I30	0,094	E30	0,13
I31	0,181	E31	0,187
I32	0,156	E32	0,167
I33	0,164	E33	0,154
I34	0,183	E34	0,227
I35	0,087	E35	0,147
I36	0,175	E36	0,209
I37	0,202	E37	0,291
I38	0,134	E38	0,127
I39	0,069	E39	0,081
I40	0,09	E40	0,059
I41	0,164	E41	0,11
I42	0,114	E42	0,106
I43	0,218	E43	0,112
I44	0,13	E44	0,161
I45	0,114	E45	0,073
I46	0,148	E46	0,198
I47	0,2	E47	0,142
I48	0,228	E48	0,191
I49	0,143	E49	0,141
I50	0,212	E50	0,161
I51	0,112	E51	0,162
I52	0,248	E52	0,117
I53	0,185	E53	0,126
I54	0,239	E54	0,133
I55	0,173	E55	0,137
I56	0,162	E56	0,156
I57	0,221	E57	0,145
I58	0,202	E58	0,13
I59	0,096	E59	0,188
I60	0,089	E60	0,091
I61	0,176	E61	0,126
I62	0,235	E62	0,213
I63	0,141	E63	0,155
I64	0,145	E64	0,11
I65	0,133	E65	0,134
I66	0,251	E66	0,188
I67	0,202	E67	0,15
I75w	0,174	E75W	0,104

Appendix B: Primer sequences

Table 2: Primers, sequence (5'→ 3'), direction, target region/gene, bacteria target and reference.

Primer name	Sequence, 5' -> 3'	Target region	Target bacteria	Direction	Reference
Univ_F	TCCTACGGGAGGCAGCAGT	16S rRNA	Total bacteria (universalMangala)	forward	(Nadkarni et al., 2002)
Univ_R	GGACTACCAGGGTATCTAATCCTGTT	16S rRNA	Total bacteria (universalMangala)	reverse	(Nadkarni et al., 2002)
PRK341F	CCTACGGGRBGCASCAG	16S rRNA	Prokaryotes	forward	(Yu et al., 2005)
PRK806R	GGACTACYVGGGTATCTAAT	16S rRNA	Prokaryotes	reverse	(Yu et al., 2005)
IlluminaColoniR	CCAGCAGAAGACGGCATACGAGAT	Colony site Illumina	All tagged DNA fragments- After Illumina PCR	reverse	Illumina
IlluminaColoniF	AATGATACGGCGACCACCGAGATCT	Colony site Illumina	All tagged DNA fragments- After Illumina PCR	Forward	Illumina

Primer sequences for Illumina Index PCR:

PRK Illumina forward primers (5' - 3'):

1. aatgatacggcgaccaccgagatctacactctttccctacacgacgctcttccgatctagtcaaCCTACGGGRBGCASCAG
2. aatgatacggcgaccaccgagatctacactctttccctacacgacgctcttccgatctagttccCCTACGGGRBGCASCAG
3. aatgatacggcgaccaccgagatctacactctttccctacacgacgctcttccgatctatgtcaCCTACGGGRBGCASCAG
4. aatgatacggcgaccaccgagatctacactctttccctacacgacgctcttccgatctccgtccCCTACGGGRBGCASCAG
5. aatgatacggcgaccaccgagatctacactctttccctacacgacgctcttccgatctgtagagCCTACGGGRBGCASCAG
6. aatgatacggcgaccaccgagatctacactctttccctacacgacgctcttccgatctgtccgcCCTACGGGRBGCASCAG
7. aatgatacggcgaccaccgagatctacactctttccctacacgacgctcttccgatctgtgaaaCCTACGGGRBGCASCAG
8. aatgatacggcgaccaccgagatctacactctttccctacacgacgctcttccgatctgtggccCCTACGGGRBGCASCAG

PRK Illumina reverse primers (5' - 3'):

1. caagcagaagacggcatacgagatcgtgatgtgactggagttcagacgtgtgctcttccgatctGGACTACYVGGGTATCTAAT
2. caagcagaagacggcatacgagatacatcggtgactggagttcagacgtgtgctcttccgatctGGACTACYVGGGTATCTAAT
3. caagcagaagacggcatacgagatgcctaagtgactggagttcagacgtgtgctcttccgatctGGACTACYVGGGTATCTAAT
4. caagcagaagacggcatacgagattggtcagtgactggagttcagacgtgtgctcttccgatctGGACTACYVGGGTATCTAAT
5. caagcagaagacggcatacgagatcactctgtgactggagttcagacgtgtgctcttccgatctGGACTACYVGGGTATCTAAT
6. caagcagaagacggcatacgagatattggcgtgactggagttcagacgtgtgctcttccgatctGGACTACYVGGGTATCTAAT
7. caagcagaagacggcatacgagatgatctggtgactggagttcagacgtgtgctcttccgatctGGACTACYVGGGTATCTAAT
8. caagcagaagacggcatacgagattcaagtgtgactggagttcagacgtgtgctcttccgatctGGACTACYVGGGTATCTAAT
9. caagcagaagacggcatacgagatctgatcgtgactggagttcagacgtgtgctcttccgatctGGACTACYVGGGTATCTAAT
10. caagcagaagacggcatacgagataagctagtgactggagttcagacgtgtgctcttccgatctGGACTACYVGGGTATCTAAT
11. caagcagaagacggcatacgagatgtagccgtgactggagttcagacgtgtgctcttccgatctGGACTACYVGGGTATCTAAT

12. caagcagaagacggcatacgagattacaaggtgactggagttcagacgtgtgctcttccgatctGGACTACYVGGGTATCTAAT
13. caagcagaagacggcatacgagatttgactgtgactggagttcagacgtgtgctcttccgatctGGACTACYVGGGTATCTAAT
14. caagcagaagacggcatacgagatggaactgtgactggagttcagacgtgtgctcttccgatctGGACTACYVGGGTATCTAAT
15. caagcagaagacggcatacgagattgacatgtgactggagttcagacgtgtgctcttccgatctGGACTACYVGGGTATCTAAT
16. caagcagaagacggcatacgagatggacgggtgactggagttcagacgtgtgctcttccgatctGGACTACYVGGGTATCTAAT
17. caagcagaagacggcatacgagatctctacgtgactggagttcagacgtgtgctcttccgatctGGACTACYVGGGTATCTAAT
18. caagcagaagacggcatacgagatgcggacgtgactggagttcagacgtgtgctcttccgatctGGACTACYVGGGTATCTAAT
19. caagcagaagacggcatacgagatttcacgtgactggagttcagacgtgtgctcttccgatctGGACTACYVGGGTATCTAAT
20. caagcagaagacggcatacgagatggccacgtgactggagttcagacgtgtgctcttccgatctGGACTACYVGGGTATCTAAT
21. caagcagaagacggcatacgagatcgaaacgtgactggagttcagacgtgtgctcttccgatctGGACTACYVGGGTATCTAAT
22. caagcagaagacggcatacgagatcgtacggtgactggagttcagacgtgtgctcttccgatctGGACTACYVGGGTATCTAAT
23. caagcagaagacggcatacgagatccactcgtgactggagttcagacgtgtgctcttccgatctGGACTACYVGGGTATCTAAT
24. caagcagaagacggcatacgagatgctaccgtgactggagttcagacgtgtgctcttccgatctGGACTACYVGGGTATCTAAT

Appendix C: Control of PCR quality

Gel pictures to control PCR quality after 16S amplification (figure 1), PCR with PRK primers (figure 2) and after PCR with Illumina-indexing PRK primers (figure 3).

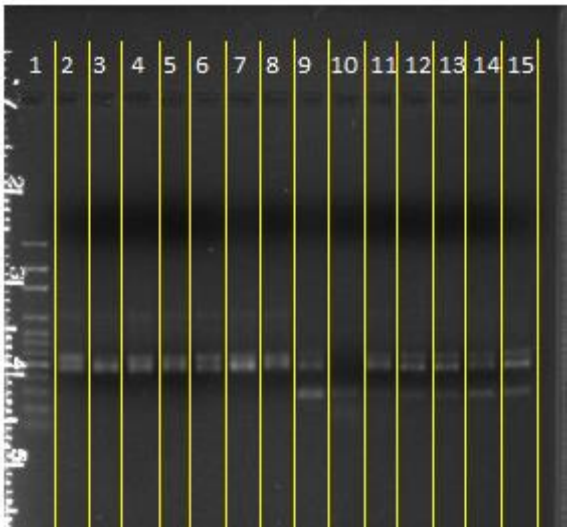

Figure 1: Control of 16S amplification, ladder in well 1, samples from cecum content are in well 2-8 and tissue samples in well 9-15.

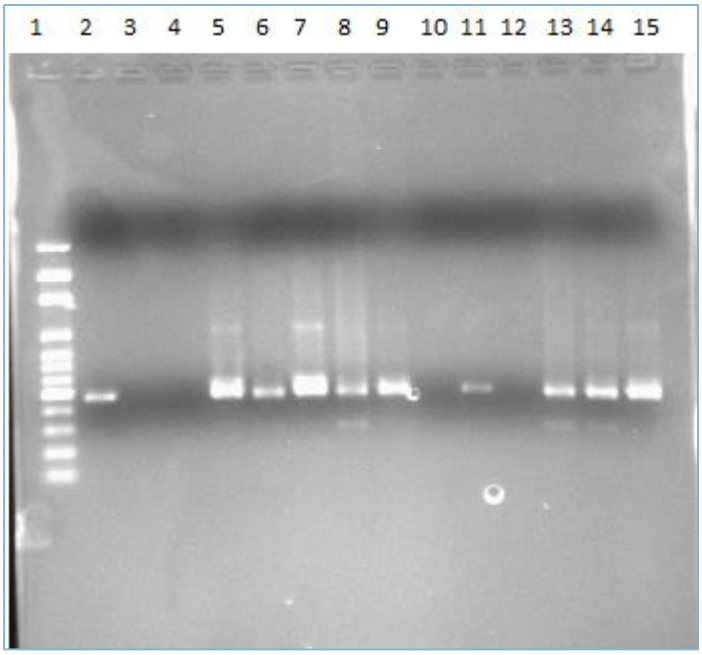

Figure 2: Control of PCR quality after PCR with PRK primers. Well 1: ladder, positive controls were in well 2 and 11, negative controls were in 3,4,11 and 12, samples from cecum content were in well 5,7,9 and 15, tissue samples were in well 6, 8, 13 and 14.

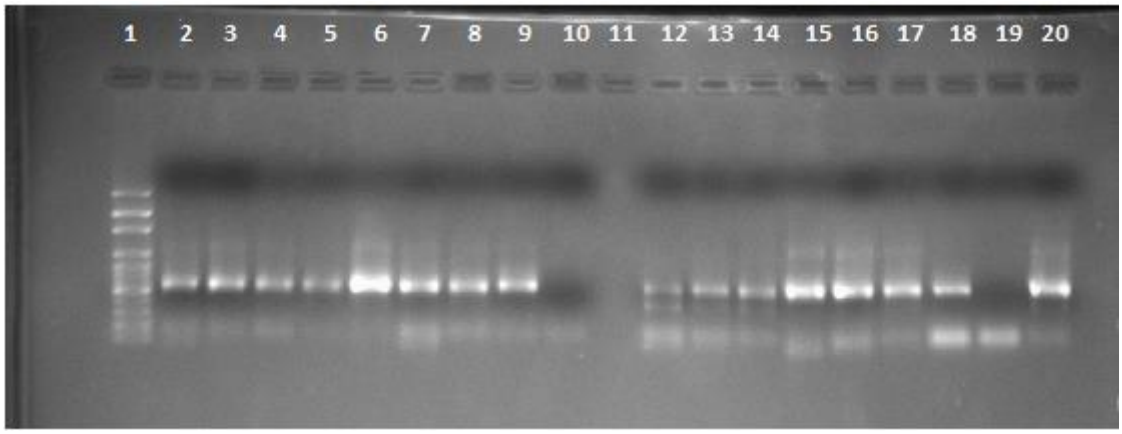

Figure 3: Control of PCR quality after indexing PCR. Well 1: ladder, positive control: 9 and 18, negative control: 10 and 19, samples from cecum content: 2-4,7 and 15-17, tissue samples: 5,6,8 and 12-14, 20. Well 11 was empty

Appendix D: Standard curves

Detected ct values (table 3) and standard curve (figure 4) used in calculation of copy number from TaqMan qPCR. Equation 1 was used to calculate copy number in our samples.

Table 3: Concentration of standards, measured ct values and mean ct value of standards.

Standard	Conc. (10^)	Ct1	Ct2	Ct3	Mean Ct
1	8	17,91	18,27	17,89	18,0233
2	7	21,91	22,55	22,01	22,1567
3	6	26,06	26,18	26,18	26,1400
4	5	30,13	30,53	30,33	30,3300
5	4	33,39	34,39	34,39	34,0567

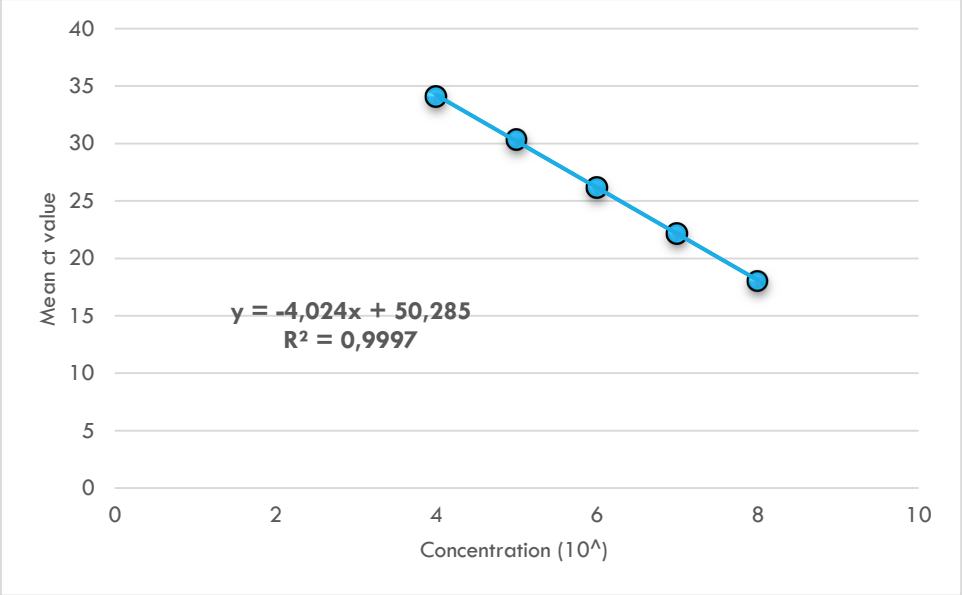

Figure 4: Standard curve used in calculation of copy number after TaqMan qPCR.

$$Y = -4{,}024x + 50{,}285 \quad (1)$$

Where:
y = measured Ct value
x = unknown copy number

An approximately median for copy numbers in the samples was determined to be 6,45e10, and volumes needed for pooling of samples was calculated using equation 2.

$$\text{Volume} = \frac{6{,}45e10}{X} \quad (2)$$

Where:
X = Calculated copy number from equation 1

Detected ct values (table 4) and standard curve (figure 5) used in calculation of concentration after Perfecta quantification. Equation 2 was used to calculate concentration in our samples.

Table 4: Concentration of standards, measured ct values and mean ct value of standards.

Standard	Conc. DNA (pM)	Ct1	Ct2	Ct3	Mean ct value
1	0,0005	26,42	26,3	26,42	26,38
2	0,005	22,71	22,68	22,52	22,64
3	0,05	19,46	19,33	19,17	19,32
4	0,5	16,89	16,48	16,85	16,74
5	5	-	-	12,21	12,21

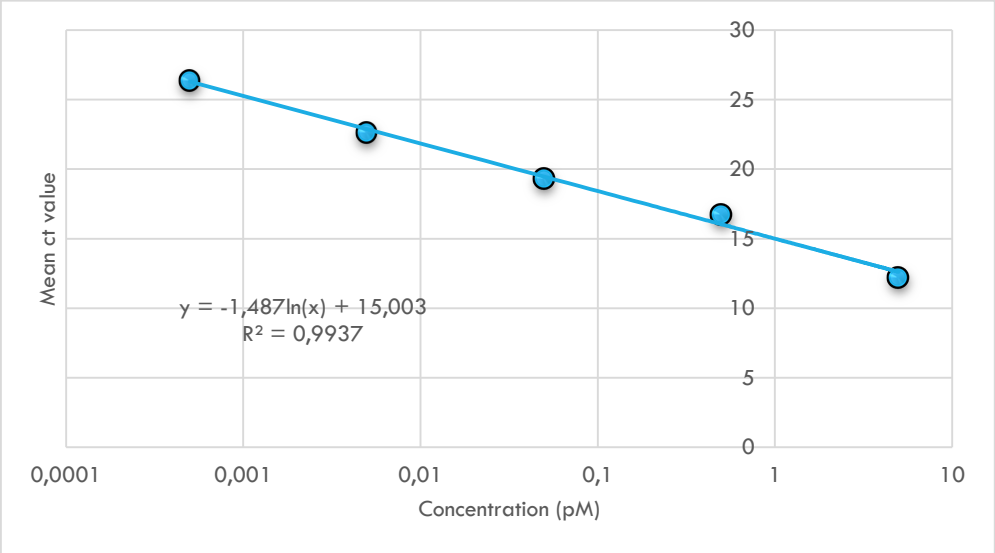

Figure 5: Standard curve used in calculation of concentration after perfecta quantification.

$$Y = -1{,}487 \ln(x) + 15{,}003 \quad (2)$$

Where:
Y = Measured ct value
X = unknown concentration

Appendix E: Taxonomy

Table 12: All OTUs detected in 16S rRNA analysis with assigned taxonomy.

Phylum	Class	Order	Family	Genus	Species	OTU
Actinobacteria	Coriobacteriia	Coriobacteriales	Coriobacteriaceae	Adlercreutzia		217
Actinobacteria	Coriobacteriia	Coriobacteriales	Coriobacteriaceae	Adlercreutzia		243
Actinobacteria	Coriobacteriia	Coriobacteriales	Coriobacteriaceae	Adlercreutzia		251
Actinobacteria	Coriobacteriia	Coriobacteriales	Coriobacteriaceae	Adlercreutzia		252
Actinobacteria	Coriobacteriia	Coriobacteriales	Coriobacteriaceae	Adlercreutzia		256
Actinobacteria	Coriobacteriia	Coriobacteriales	Coriobacteriaceae	Adlercreutzia		270
Actinobacteria	Actinobacteria	Bifidobacteriales	Bifidobacteriaceae	Bifidobacterium	pseudolongum	292
Actinobacteria	Coriobacteriia	Coriobacteriales	Coriobacteriaceae	Adlercreutzia		301
Actinobacteria	Coriobacteriia	Coriobacteriales	Coriobacteriaceae	Adlercreutzia		310
Actinobacteria	Coriobacteriia	Coriobacteriales	Coriobacteriaceae	Adlercreutzia		317
Bacteroidetes	Bacteroidia	Bacteroidales	Bacteroidaceae	Bacteroides		6
Bacteroidetes	Bacteroidia	Bacteroidales	Rikenellaceae			7
Bacteroidetes	Bacteroidia	Bacteroidales	S24-7			9
Bacteroidetes	Bacteroidia	Bacteroidales	S24-7			12
Bacteroidetes	Bacteroidia	Bacteroidales	Rikenellaceae			13
Bacteroidetes	Bacteroidia	Bacteroidales	S24-7			17
Bacteroidetes	Bacteroidia	Bacteroidales	Rikenellaceae			19
Bacteroidetes	Bacteroidia	Bacteroidales	Bacteroidaceae	Bacteroides		22
Bacteroidetes	Bacteroidia	Bacteroidales	S24-7			29
Bacteroidetes	Bacteroidia	Bacteroidales	S24-7			30
Bacteroidetes	Bacteroidia	Bacteroidales	S24-7			41
Bacteroidetes	Bacteroidia	Bacteroidales	S24-7			47
Bacteroidetes	Bacteroidia	Bacteroidales	S24-7			49
Bacteroidetes	Bacteroidia	Bacteroidales	S24-7			51
Bacteroidetes	Bacteroidia	Bacteroidales	Rikenellaceae			52
Bacteroidetes	Bacteroidia	Bacteroidales	Rikenellaceae	AF12		57
Bacteroidetes	Bacteroidia	Bacteroidales	[Paraprevotellaceae]	[Prevotella]		59
Bacteroidetes	Bacteroidia	Bacteroidales	Porphyromonadaceae	Parabacteroides	distasonis	64
Bacteroidetes	Bacteroidia	Bacteroidales	Rikenellaceae			65
Bacteroidetes	Bacteroidia	Bacteroidales	[Odoribacteraceae]	Odoribacter		75
Bacteroidetes	Bacteroidia	Bacteroidales				77
Bacteroidetes	Bacteroidia	Bacteroidales	S24-7			80
Bacteroidetes	Bacteroidia	Bacteroidales	S24-7			82
Bacteroidetes	Bacteroidia	Bacteroidales	Bacteroidaceae	Bacteroides	acidifaciens	87
Bacteroidetes	Bacteroidia	Bacteroidales	S24-7			88
Bacteroidetes	Bacteroidia	Bacteroidales	S24-7			90
Bacteroidetes	Bacteroidia	Bacteroidales	S24-7			94

Bacteroidetes	Bacteroidia	Bacteroidales	S24-7			98
Bacteroidetes	Bacteroidia	Bacteroidales	S24-7			100
Bacteroidetes	Bacteroidia	Bacteroidales	S24-7			105
Bacteroidetes	Bacteroidia	Bacteroidales	S24-7			107
Bacteroidetes	Bacteroidia	Bacteroidales	Rikenellaceae			110
Bacteroidetes	Bacteroidia	Bacteroidales	Rikenellaceae			119
Bacteroidetes	Bacteroidia	Bacteroidales	S24-7			121
Bacteroidetes	Bacteroidia	Bacteroidales	Bacteroidaceae	Bacteroides		123
Bacteroidetes	Bacteroidia	Bacteroidales	S24-7			124
Bacteroidetes	Bacteroidia	Bacteroidales	Porphyromonadaceae	Parabacteroides		125
Bacteroidetes	Bacteroidia	Bacteroidales	S24-7			127
Bacteroidetes	Bacteroidia	Bacteroidales	S24-7			140
Bacteroidetes	Bacteroidia	Bacteroidales	S24-7			148
Bacteroidetes	Bacteroidia	Bacteroidales	S24-7			151
Bacteroidetes	Bacteroidia	Bacteroidales	S24-7			154
Bacteroidetes	Bacteroidia	Bacteroidales	S24-7			157
Bacteroidetes	Bacteroidia	Bacteroidales	S24-7			164
Bacteroidetes	Bacteroidia	Bacteroidales	Rikenellaceae			173
Bacteroidetes	Bacteroidia	Bacteroidales	Bacteroidaceae	Bacteroides		175
Bacteroidetes	Bacteroidia	Bacteroidales	S24-7			193
Bacteroidetes	Bacteroidia	Bacteroidales	S24-7			194
Bacteroidetes	Bacteroidia	Bacteroidales	Prevotellaceae	Prevotella		206
Bacteroidetes	Bacteroidia	Bacteroidales	S24-7			207
Bacteroidetes	Bacteroidia	Bacteroidales				211
Bacteroidetes	Bacteroidia	Bacteroidales	S24-7			226
Bacteroidetes	Bacteroidia	Bacteroidales	S24-7			228
Bacteroidetes	Bacteroidia	Bacteroidales	Porphyromonadaceae	Parabacteroides		229
Bacteroidetes	Bacteroidia	Bacteroidales	Rikenellaceae			250
Bacteroidetes	Bacteroidia	Bacteroidales				263
Bacteroidetes	Bacteroidia	Bacteroidales	S24-7			268
Bacteroidetes	Bacteroidia	Bacteroidales	S24-7			275
Bacteroidetes	Bacteroidia	Bacteroidales	Porphyromonadaceae	Parabacteroides	distasonis	285
Bacteroidetes	Bacteroidia	Bacteroidales	[Odoribacteraceae]	Odoribacter		307
Deferribacteres	Deferribacteres	Deferribacterales	Deferribacteraceae	Mucispirillum	schaedleri	1
Deferribacteres	Deferribacteres	Deferribacterales	Deferribacteraceae	Mucispirillum	schaedleri	199
Firmicutes	Clostridia	Clostridiales				3
Firmicutes	Clostridia	Clostridiales				4
Firmicutes	Clostridia	Clostridiales				8
Firmicutes	Clostridia	Clostridiales	Lachnospiraceae			10
Firmicutes	Clostridia	Clostridiales				11
Firmicutes	Bacilli	Lactobacillales	Lactobacillaceae	Lactobacillus		14
Firmicutes	Clostridia	Clostridiales	Lachnospiraceae			15
Firmicutes	Clostridia	Clostridiales				16

Firmicutes	Clostridia	Clostridiales	Lachnospiraceae			18
Firmicutes	Clostridia	Clostridiales	Lachnospiraceae			20
Firmicutes	Clostridia	Clostridiales				21
Firmicutes	Clostridia	Clostridiales	Lachnospiraceae			24
Firmicutes	Clostridia	Clostridiales	Lachnospiraceae			25
Firmicutes	Clostridia	Clostridiales	Ruminococcaceae	Oscillospira		26
Firmicutes	Clostridia	Clostridiales				27
Firmicutes	Clostridia	Clostridiales	Lachnospiraceae	[Ruminococcus]	gnavus	28
Firmicutes	Clostridia	Clostridiales				31
Firmicutes	Clostridia	Clostridiales				32
Firmicutes	Clostridia	Clostridiales	Ruminococcaceae			33
Firmicutes	Clostridia	Clostridiales				34
Firmicutes	Clostridia	Clostridiales				35
Firmicutes	Clostridia	Clostridiales	Lachnospiraceae			36
Firmicutes	Clostridia	Clostridiales				37
Firmicutes	Clostridia	Clostridiales				39
Firmicutes	Clostridia	Clostridiales	Lachnospiraceae			40
Firmicutes	Clostridia	Clostridiales				42
Firmicutes	Clostridia	Clostridiales	Ruminococcaceae	Oscillospira		43
Firmicutes	Clostridia	Clostridiales				46
Firmicutes	Clostridia	Clostridiales	Clostridiaceae	Candidatus Arthromitus		48
Firmicutes	Clostridia	Clostridiales	Ruminococcaceae			50
Firmicutes	Clostridia	Clostridiales				53
Firmicutes	Clostridia	Clostridiales	Ruminococcaceae			54
Firmicutes	Clostridia	Clostridiales	Ruminococcaceae	Ruminococcus		55
Firmicutes	Clostridia	Clostridiales				56
Firmicutes	Clostridia	Clostridiales	Lachnospiraceae			60
Firmicutes	Clostridia	Clostridiales				61
Firmicutes	Clostridia	Clostridiales	Lachnospiraceae			62
Firmicutes	Clostridia	Clostridiales	Ruminococcaceae	Ruminococcus		66
Firmicutes	Clostridia	Clostridiales	Lachnospiraceae			67
Firmicutes	Clostridia	Clostridiales				68
Firmicutes	Clostridia	Clostridiales	Ruminococcaceae			69
Firmicutes	Clostridia	Clostridiales				70
Firmicutes	Clostridia	Clostridiales	Ruminococcaceae	Oscillospira		71
Firmicutes	Bacilli	Lactobacillales	Lactobacillaceae	Lactobacillus		72
Firmicutes	Clostridia	Clostridiales				74
Firmicutes	Clostridia	Clostridiales				76
Firmicutes	Clostridia	Clostridiales	Ruminococcaceae	Oscillospira		78
Firmicutes	Clostridia	Clostridiales	Lachnospiraceae			79
Firmicutes	Erysipelotrichi	Erysipelotrichales	Erysipelotrichaceae			83
Firmicutes	Clostridia	Clostridiales				84
Firmicutes	Clostridia	Clostridiales				85

Firmicutes	Clostridia	Clostridiales	Ruminococcaceae	Oscillospira		86
Firmicutes	Clostridia	Clostridiales	Lachnospiraceae			89
Firmicutes	Clostridia	Clostridiales	Lachnospiraceae	Coprococcus		91
Firmicutes	Clostridia	Clostridiales				92
Firmicutes	Clostridia	Clostridiales				93
Firmicutes	Clostridia	Clostridiales	Lachnospiraceae			95
Firmicutes	Clostridia	Clostridiales				96
Firmicutes	Clostridia	Clostridiales				97
Firmicutes	Clostridia	Clostridiales				99
Firmicutes	Clostridia	Clostridiales				101
Firmicutes	Clostridia	Clostridiales				102
Firmicutes	Clostridia	Clostridiales				103
Firmicutes	Clostridia	Clostridiales				104
Firmicutes	Clostridia	Clostridiales	Lachnospiraceae			106
Firmicutes	Clostridia	Clostridiales				108
Firmicutes	Clostridia	Clostridiales	Lachnospiraceae			109
Firmicutes	Clostridia	Clostridiales	Ruminococcaceae	Ruminococcus		111
Firmicutes	Clostridia	Clostridiales				112
Firmicutes	Clostridia	Clostridiales	Ruminococcaceae	Oscillospira		113
Firmicutes	Clostridia	Clostridiales				114
Firmicutes	Bacilli	Lactobacillales	Lactobacillaceae	Lactobacillus	reuteri	115
Firmicutes	Clostridia	Clostridiales	Lachnospiraceae	[Ruminococcus]	gnavus	116
Firmicutes	Clostridia	Clostridiales				117
Firmicutes	Clostridia	Clostridiales				118
Firmicutes	Clostridia	Clostridiales	Ruminococcaceae	Ruminococcus		120
Firmicutes	Clostridia	Clostridiales				122
Firmicutes	Clostridia	Clostridiales				126
Firmicutes	Clostridia	Clostridiales				128
Firmicutes	Clostridia	Clostridiales				129
Firmicutes	Clostridia	Clostridiales				130
Firmicutes	Clostridia	Clostridiales	Lachnospiraceae			131
Firmicutes	Clostridia	Clostridiales				132
Firmicutes	Clostridia	Clostridiales	Lachnospiraceae			133
Firmicutes	Clostridia	Clostridiales	Lachnospiraceae			134
Firmicutes	Clostridia	Clostridiales	Lachnospiraceae			135
Firmicutes	Clostridia	Clostridiales	Ruminococcaceae	Oscillospira		136
Firmicutes	Clostridia	Clostridiales	Lachnospiraceae			137
Firmicutes	Clostridia	Clostridiales				138
Firmicutes	Clostridia	Clostridiales	Lachnospiraceae			139
Firmicutes	Clostridia	Clostridiales	Ruminococcaceae	Oscillospira		141
Firmicutes	Clostridia	Clostridiales				142
Firmicutes	Clostridia	Clostridiales	Ruminococcaceae			143
Firmicutes	Clostridia	Clostridiales				144

Firmicutes	Clostridia	Clostridiales	Ruminococcaceae	Ruminococcus		145
Firmicutes	Clostridia	Clostridiales				146
Firmicutes	Clostridia	Clostridiales				147
Firmicutes	Bacilli	Lactobacillales	Enterococcaceae	Enterococcus		149
Firmicutes	Clostridia	Clostridiales	Lachnospiraceae			150
Firmicutes	Clostridia	Clostridiales				152
Firmicutes	Clostridia	Clostridiales				153
Firmicutes	Clostridia	Clostridiales	Ruminococcaceae	Ruminococcus		155
Firmicutes	Clostridia	Clostridiales	Ruminococcaceae			156
Firmicutes	Clostridia	Clostridiales	Ruminococcaceae	Oscillospira		158
Firmicutes	Clostridia	Clostridiales	Ruminococcaceae			159
Firmicutes	Bacilli	Lactobacillales	Streptococcaceae	Streptococcus		160
Firmicutes	Clostridia	Clostridiales	Ruminococcaceae			161
Firmicutes	Erysipelotrichi	Erysipelotrichales	Erysipelotrichaceae			163
Firmicutes	Clostridia	Clostridiales	Ruminococcaceae	Oscillospira		165
Firmicutes	Clostridia	Clostridiales	Ruminococcaceae	Oscillospira		166
Firmicutes	Clostridia	Clostridiales	Ruminococcaceae	Oscillospira		167
Firmicutes	Clostridia	Clostridiales	Ruminococcaceae			168
Firmicutes	Clostridia	Clostridiales	Lachnospiraceae	Dorea		169
Firmicutes	Clostridia	Clostridiales				170
Firmicutes	Clostridia	Clostridiales				171
Firmicutes	Clostridia	Clostridiales				172
Firmicutes	Clostridia	Clostridiales				174
Firmicutes	Clostridia	Clostridiales	Dehalobacteriaceae	Dehalobacterium		176
Firmicutes	Erysipelotrichi	Erysipelotrichales	Erysipelotrichaceae	Coprobacillus		177
Firmicutes	Clostridia	Clostridiales				178
Firmicutes	Clostridia	Clostridiales	Ruminococcaceae	Ruminococcus		179
Firmicutes	Clostridia	Clostridiales				181
Firmicutes	Clostridia	Clostridiales				182
Firmicutes	Clostridia	Clostridiales				183
Firmicutes	Clostridia	Clostridiales	Ruminococcaceae	Ruminococcus		184
Firmicutes	Clostridia	Clostridiales				185
Firmicutes	Clostridia	Clostridiales	[Mogibacteriaceae]			186
Firmicutes	Clostridia	Clostridiales	Dehalobacteriaceae	Dehalobacterium		187
Firmicutes	Clostridia	Clostridiales	Lachnospiraceae			188
Firmicutes	Clostridia	Clostridiales	Lachnospiraceae			189
Firmicutes	Clostridia	Clostridiales	Ruminococcaceae			190
Firmicutes	Clostridia	Clostridiales	Lachnospiraceae			191
Firmicutes	Clostridia	Clostridiales	Ruminococcaceae			192
Firmicutes	Clostridia	Clostridiales				195
Firmicutes	Clostridia	Clostridiales				196
Firmicutes	Clostridia	Clostridiales	Lachnospiraceae			197
Firmicutes	Clostridia	Clostridiales	Lachnospiraceae			198

Firmicutes	Clostridia	Clostridiales				200
Firmicutes	Clostridia	Clostridiales	[Mogibacteriaceae]			201
Firmicutes	Clostridia	Clostridiales				202
Firmicutes	Clostridia	Clostridiales	Ruminococcaceae	Ruminococcus		203
Firmicutes	Clostridia	Clostridiales	Ruminococcaceae	Oscillospira		204
Firmicutes	Clostridia	Clostridiales				205
Firmicutes	Clostridia	Clostridiales	Ruminococcaceae	Oscillospira		208
Firmicutes	Clostridia	Clostridiales				209
Firmicutes	Clostridia	Clostridiales	Lachnospiraceae			210
Firmicutes	Erysipelotrichi	Erysipelotrichales	Erysipelotrichaceae			212
Firmicutes	Clostridia	Clostridiales	Lachnospiraceae			214
Firmicutes	Clostridia	Clostridiales				215
Firmicutes	Clostridia	Clostridiales				216
Firmicutes	Erysipelotrichi	Erysipelotrichales	Erysipelotrichaceae			218
Firmicutes	Clostridia	Clostridiales	Lachnospiraceae	Coprococcus		219
Firmicutes	Clostridia	Clostridiales	Ruminococcaceae	Ruminococcus		220
Firmicutes	Clostridia	Clostridiales	Ruminococcaceae			221
Firmicutes	Erysipelotrichi	Erysipelotrichales	Erysipelotrichaceae	Coprobacillus		222
Firmicutes	Clostridia	Clostridiales				223
Firmicutes	Clostridia	Clostridiales	Ruminococcaceae			225
Firmicutes	Clostridia	Clostridiales	Ruminococcaceae			227
Firmicutes	Clostridia	Clostridiales	Lachnospiraceae	Dorea		230
Firmicutes	Clostridia	Clostridiales	Peptococcaceae			231
Firmicutes	Erysipelotrichi	Erysipelotrichales	Erysipelotrichaceae			232
Firmicutes	Clostridia	Clostridiales				233
Firmicutes	Clostridia	Clostridiales				234
Firmicutes	Clostridia	Clostridiales				235
Firmicutes	Clostridia	Clostridiales	Ruminococcaceae	Oscillospira		236
Firmicutes	Clostridia	Clostridiales				237
Firmicutes	Clostridia	Clostridiales				238
Firmicutes	Clostridia	Clostridiales	[Mogibacteriaceae]			239
Firmicutes	Clostridia	Clostridiales				240
Firmicutes	Clostridia	Clostridiales	Lachnospiraceae			241
Firmicutes	Erysipelotrichi	Erysipelotrichales	Erysipelotrichaceae			242
Firmicutes	Clostridia	Clostridiales	Lachnospiraceae	Coprococcus		244
Firmicutes	Clostridia	Clostridiales	Ruminococcaceae			247
Firmicutes	Clostridia	Clostridiales				248
Firmicutes	Clostridia	Clostridiales	Lachnospiraceae			249
Firmicutes	Clostridia	Clostridiales				253
Firmicutes	Clostridia	Clostridiales				254
Firmicutes	Clostridia	Clostridiales				257
Firmicutes	Clostridia	Clostridiales	Lachnospiraceae			258
Firmicutes	Clostridia	Clostridiales	Ruminococcaceae	Ruminococcus		259

Firmicutes	Clostridia	Clostridiales	Lachnospiraceae			260
Firmicutes	Clostridia	Clostridiales				262
Firmicutes	Clostridia	Clostridiales	Lachnospiraceae	Coprococcus		264
Firmicutes	Erysipelotrichi	Erysipelotrichales	Erysipelotrichaceae			265
Firmicutes	Clostridia	Clostridiales	Ruminococcaceae			266
Firmicutes	Clostridia	Clostridiales	Ruminococcaceae	Oscillospira		267
Firmicutes	Clostridia	Clostridiales	[Mogibacteriaceae]			269
Firmicutes	Clostridia	Clostridiales				271
Firmicutes	Clostridia	Clostridiales	Ruminococcaceae			272
Firmicutes	Clostridia	Clostridiales				273
Firmicutes	Clostridia	Clostridiales	Ruminococcaceae	Ruminococcus		274
Firmicutes	Clostridia	Clostridiales				276
Firmicutes	Clostridia	Clostridiales	Ruminococcaceae	Oscillospira		277
Firmicutes	Clostridia	Clostridiales				278
Firmicutes	Clostridia	Clostridiales	Christensenellaceae			279
Firmicutes	Clostridia	Clostridiales				280
Firmicutes	Clostridia	Clostridiales	Clostridiaceae	Clostridium		281
Firmicutes	Clostridia	Clostridiales				283
Firmicutes	Clostridia	Clostridiales	Ruminococcaceae			284
Firmicutes	Clostridia	Clostridiales				286
Firmicutes	Clostridia	Clostridiales				287
Firmicutes	Clostridia	Clostridiales				289
Firmicutes	Clostridia	Clostridiales				290
Firmicutes	Clostridia	Clostridiales	Clostridiaceae			291
Firmicutes	Clostridia	Clostridiales	Lachnospiraceae			293
Firmicutes	Clostridia	Clostridiales				294
Firmicutes	Clostridia	Clostridiales	Lachnospiraceae			295
Firmicutes	Clostridia	Clostridiales	Ruminococcaceae	Oscillospira		296
Firmicutes	Clostridia	Clostridiales	Ruminococcaceae	Oscillospira		297
Firmicutes	Clostridia	Clostridiales	Lachnospiraceae	Anaerostipes		298
Firmicutes	Clostridia	Clostridiales	Ruminococcaceae			299
Firmicutes	Clostridia	Clostridiales	Ruminococcaceae			300
Firmicutes	Clostridia	Clostridiales				302
Firmicutes	Erysipelotrichi	Erysipelotrichales	Erysipelotrichaceae			303
Firmicutes	Clostridia	Clostridiales	Ruminococcaceae	Ruminococcus		304
Firmicutes	Clostridia	Clostridiales	Ruminococcaceae			305
Firmicutes	Clostridia	Clostridiales	Ruminococcaceae	Ruminococcus		308
Firmicutes	Clostridia	Clostridiales	Ruminococcaceae			309
Firmicutes	Clostridia	Clostridiales				311
Firmicutes	Clostridia	Clostridiales				312
Firmicutes	Clostridia	Clostridiales				313
Firmicutes	Clostridia	Clostridiales	[Mogibacteriaceae]			314
Firmicutes	Erysipelotrichi	Erysipelotrichales	Erysipelotrichaceae			315

Firmicutes	Clostridia	Clostridiales	Lachnospiraceae			316
Firmicutes	Clostridia	Clostridiales				318
Firmicutes	Clostridia	Clostridiales				320
Firmicutes	Clostridia	Clostridiales	Ruminococcaceae			321
Firmicutes	Clostridia	Clostridiales	Lachnospiraceae	Coprococcus		322
Firmicutes	Clostridia	Clostridiales	Ruminococcaceae			323
Firmicutes	Clostridia	Clostridiales	Lachnospiraceae	[Ruminococcus]	gnavus	324
Firmicutes	Clostridia	Clostridiales	Peptostreptococcaceae			325
Firmicutes	Clostridia	Clostridiales				326
Proteobacteria	Gammaproteobacteria	Enterobacteriales	Enterobacteriaceae			2
Proteobacteria	Deltaproteobacteria	Desulfovibrionales	Desulfovibrionaceae	Desulfovibrio		44
Proteobacteria	Deltaproteobacteria	Desulfovibrionales	Desulfovibrionaceae			58
Proteobacteria	Betaproteobacteria	Burkholderiales	Alcaligenaceae	Sutterella		73
Proteobacteria	Deltaproteobacteria	Desulfovibrionales	Desulfovibrionaceae	Desulfovibrio		81
Proteobacteria	Alphaproteobacteria					213
Tenericutes	Mollicutes	RF39				38
Tenericutes	Mollicutes	Anaeroplasmatales	Anaeroplasmataceae	Anaeroplasma		63
Tenericutes	Mollicutes	RF39				162
Tenericutes	Mollicutes	Anaeroplasmatales	Anaeroplasmataceae	Anaeroplasma		180
Tenericutes	Mollicutes	RF39				224
TM7	TM7-3	CW040	F16			23
TM7	TM7-3	CW040	F16			261
Unassigned	Unassigned	Unassigned	Unassigned	Unassigned	Unassigned	5
Unassigned	Unassigned	Unassigned	Unassigned	Unassigned	Unassigned	45
Unassigned	Unassigned	Unassigned	Unassigned	Unassigned	Unassigned	245
Unassigned	Unassigned	Unassigned	Unassigned	Unassigned	Unassigned	246
Unassigned	Unassigned	Unassigned	Unassigned	Unassigned	Unassigned	255
Unassigned	Unassigned	Unassigned	Unassigned	Unassigned	Unassigned	282
Unassigned	Unassigned	Unassigned	Unassigned	Unassigned	Unassigned	288
Unassigned	Unassigned	Unassigned	Unassigned	Unassigned	Unassigned	306
Unassigned	Unassigned	Unassigned	Unassigned	Unassigned	Unassigned	319

Appendix F: Mean beta diversity in age groups

Mean beta diversity for each age group was calculated from Bray-Curtis distances, the mean beta diversity is presented in table 5.

Table 5: Mean beta diversity for cecum content and tissue samples in each age group.

Age groups	Cecum content	Tissue
Early juvenile	0,3459	0,3492
Juvenile	0,3047	0,3274
Mature adult	0,3205	0,3461
Early middle-aged adult	0,3096	0,3182
Middle-aged adult	0,3020	0,3221
Late middle-aged adult	One sample	-

Appendix G: PCA weighted Unifrac distances

PCA analysis were performed on weighted UniFrac distances. Plot of PC1 and PC2 for both tissue samples and samples from cecum content are presented in figure 6 and figure 7, respectively.

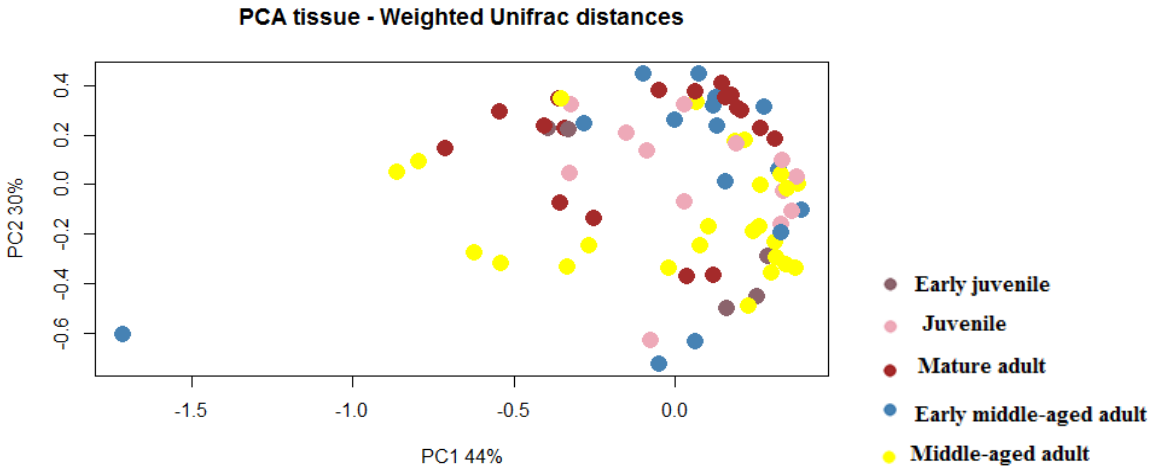

Figur 6: PCA results of weighted UniFrac distances in tissue samples**.**

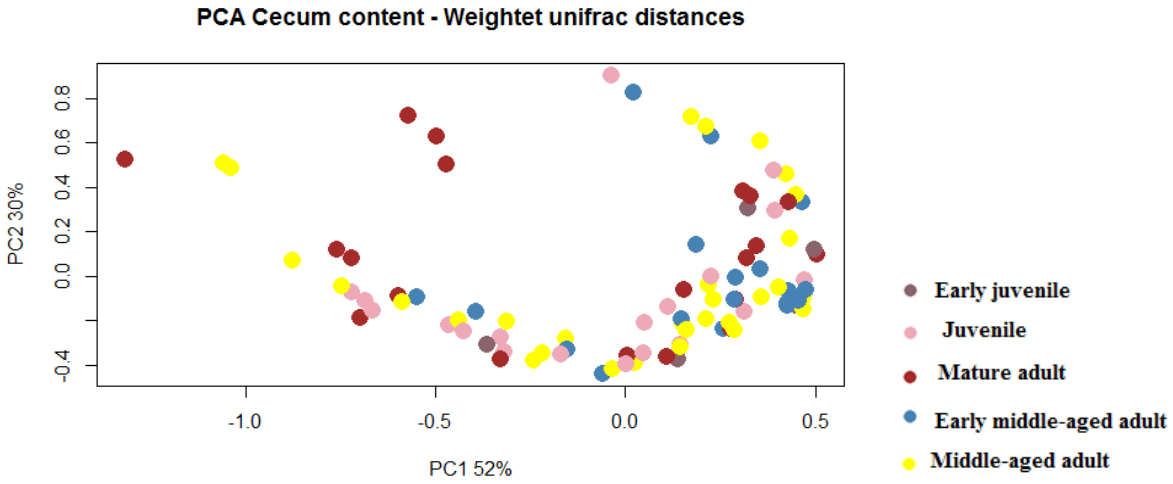

Figur 7: PCA results of weighted UniFrac distances in samples from cecum content.

Appendix H: Spearman correlation

Correlation coefficients and p-values calculated from spearman correlation. All P-values were corrected for multiple testing with FDR, correlations for cecum content samples are in table 6-8 and tissue samples are in table 9-11.

Table 6: OUTs with significant correlation to age in cecum content, p-value and rank coefficient.

OTU number	P-value	Coeff.
9	0,0000	0,6738
13	0,0057	0,4873
29	0,0364	0,3977
36	0,0149	-0,4477
41	0,0092	0,4675
47	0,0013	0,5282
48	0,0113	-0,4586
49	0,0278	0,4161
51	0,0002	0,5783
62	0,0005	-0,5563
72	0,0167	-0,4394
73	0,0362	0,4004
84	0,0190	0,4330
108	0,0008	-0,5450
125	0,0340	0,4053
126	0,0000	0,6311
130	0,0260	0,4204
131	0,0092	-0,4691
139	0,0482	-0,3840
142	0,0000	-0,6296
157	0,0362	0,3996
216	0,0442	0,3889
254	0,0331	0,4081
257	0,0001	-0,6069
271	0,0167	0,4413

Table 7: OUTs with significant correlation to tumorload in the small intestine, p-value and rank coefficient.

OTU number	p-value	Coeff
9	0,0000	0,7651
13	0,0113	0,4400
29	0,0085	0,4551
30	0,0143	0,4238
32	0,0174	0,4134
36	0,0028	-0,4989
41	0,0001	0,6038
47	0,0000	0,6279
48	0,0393	-0,3746
49	0,0141	0,4258
51	0,0002	0,5809
62	0,0002	-0,5691
72	0,0083	-0,4595
73	0,0137	0,4291
84	0,0007	0,5420
85	0,0054	0,4763
89	0,0318	-0,3859
90	0,0097	0,4491
108	0,0002	-0,5736
120	0,0084	0,4570
121	0,0141	0,4255
126	0,0016	0,5181
127	0,0113	0,4397
130	0,0434	0,3697
131	0,0028	-0,5014
135	0,0116	-0,4374
142	0,0000	-0,6319
143	0,0274	0,3937
148	0,0362	0,3789
154	0,0137	0,4306
157	0,0055	0,4736
170	0,0110	0,4435
179	0,0041	0,4859
184	0,0154	0,4192
185	0,0274	0,3940

190	0,0242	0,4006
216	0,0154	0,4188
220	0,0318	0,3863
257	0,0001	-0,6083
271	0,0362	0,3790

Table 8: OUTs with significant correlation to tumorload colon, p-value and rank coefficient.

OTU number	P-value	Coeff
9	0,0000	0,7069
13	0,0001	0,5909
15	0,0347	-0,3623
21	0,0058	0,4452
29	0,0000	0,6059
30	0,0078	0,4328
32	0,0115	0,4173
36	0,0458	-0,3440
39	0,0394	-0,3549
41	0,0005	0,5307
47	0,0001	0,5702
48	0,0042	-0,4569
49	0,0001	0,5806
51	0,0003	0,5465
56	0,0069	0,4377
59	0,0455	-0,3450
62	0,0001	-0,5706
72	0,0037	-0,4619
73	0,0010	0,5095
79	0,0428	0,3495
84	0,0005	0,5323
88	0,0012	0,5006
89	0,0133	-0,4114
90	0,0005	0,5364
98	0,0322	0,3660
101	0,0291	-0,3722
105	0,0279	0,3753
107	0,0011	0,5049
108	0,0012	-0,4993
113	0,0069	0,4386
116	0,0269	0,3797
118	0,0233	-0,3876
120	0,0009	0,5125
121	0,0000	0,6234
126	0,0000	0,6830
127	0,0009	0,5151
130	0,0001	0,5782
131	0,0000	-0,6168
132	0,0271	0,3781
141	0,0237	0,3862
142	0,0000	-0,6307
143	0,0008	0,5188
146	0,0311	0,3681
148	0,0093	0,4263
154	0,0005	0,5331
156	0,0378	0,3574
157	0,0000	0,6172
170	0,0250	0,3833
172	0,0279	0,3746
179	0,0052	0,4497
184	0,0001	0,5743
191	0,0428	0,3500
194	0,0023	0,4775
195	0,0271	0,3779
211	0,0144	0,4079
216	0,0011	0,5050
220	0,0164	0,4024
223	0,0279	-0,3748
225	0,0036	0,4637
226	0,0020	0,4823
230	0,0354	0,3608
252	0,0308	-0,3691
254	0,0100	0,4230
257	0,0000	-0,6019
262	0,0011	0,5020
267	0,0186	0,3970
271	0,0428	0,3504
292	0,0429	0,3488
318	0,0455	0,3449
324	0,0016	0,4907

Table 9: OUTs with significant correlation to age in tissue samples, p-value and rank coefficient.

OTU number	P-value	Coeff
13	0,0246	0,5185
48	0,0444	-0,4916
62	0,0048	-0,5851
94	0,0166	-0,5394
108	0,0000	-0,7079

Table 10: OUTs with significant correlation to tumor progression in the small intestine in tissue samples, p-value and rank coefficient.

OTU number	P-value	Coeff
9	0,0176	0,5112
13	0,0092	0,5484
36	0,0310	-0,4676
41	0,0092	0,5520
51	0,0222	0,4951
52	0,0152	0,5266
62	0,0024	-0,6190
84	0,0176	0,5133
108	0,0070	-0,5751
171	0,0238	-0,4859
179	0,0275	0,4746
185	0,0222	0,4953
190	0,0483	0,4430
198	0,0316	0,4643
237	0,0483	0,4435
262	0,0234	0,4898
306	0,0264	-0,4790

Table 11: OUTs with significant correlation to tumor progression in colon in tissue samples, p-value and rank coefficient.

OTU number	P-value	Coeff
7	0,0355	0,4324
9	0,0465	0,4121
13	0,0047	0,5854
29	0,0113	0,5144
32	0,0317	0,4715
39	0,0050	-0,5731
41	0,0321	0,4611
47	0,0453	0,4157
49	0,0317	0,4695
58	0,0321	0,4508
59	0,0376	-0,4261
62	0,0321	-0,4609
84	0,0321	0,4520
86	0,0321	-0,4632
97	0,0355	0,4334
105	0,0355	0,4413
108	0,0057	-0,5621
110	0,0113	0,5214
113	0,0395	0,4227
120	0,0460	0,4138
126	0,0321	0,4548
127	0,0113	0,5141
130	0,0355	0,4384
133	0,0321	0,4490
142	0,0112	-0,5305
147	0,0139	0,5042
148	0,0093	0,5415
157	0,0047	0,5931
170	0,0355	0,4362
171	0,0364	-0,4287
172	0,0355	0,4346
179	0,0364	0,4294
216	0,0355	0,4342
226	0,0321	0,4559
262	0,0113	0,5184
298	0,0321	0,4541
306	0,0355	-0,4425

Appendix I: Levels of butyrate

Levels of butyrate in each sample from cecum content are presented in table 12.

Table 12: Sample number and detected levels of butyrate in each sample, after quantification using GC.

Sample nr.	Butyrate (mM)
2	4,591
5	9,368
8	9,200
10	8,434
12	15,982
13	27,408
14	14,218
15	7,448
16	11,350
17	12,578
18	10,964
19	4,059
20	9,616
23	20,135
24	16,017
25	6,604
26	8,851
27	14,918
28	7,920
29	12,064
34	36,742
36	14,374
37	17,560
38	12,072
39	2,846
40	17,424
41	18,692
42	25,656
43	23,068
45	15,121
46	12,772
48	13,075
49	9,408
50	0,000
51	7,182
52	19,185
53	20,978
54	12,868
55	9,595
58	8,085

59	5,749
60	4,275
62	13,001
64	22,550
65	5,444
66	18,591
67	15,873

Appendix J: Plots of each age group

Plots of tumorload in colon and age (figure 8), none of these had a significant correlation and p-values for the different groups were: group 1 no p-value, group 2 p = 0,249, group 3 no p-value, group 4 p = 0,875, group 5 p = 0,886, group 6 only one sample.

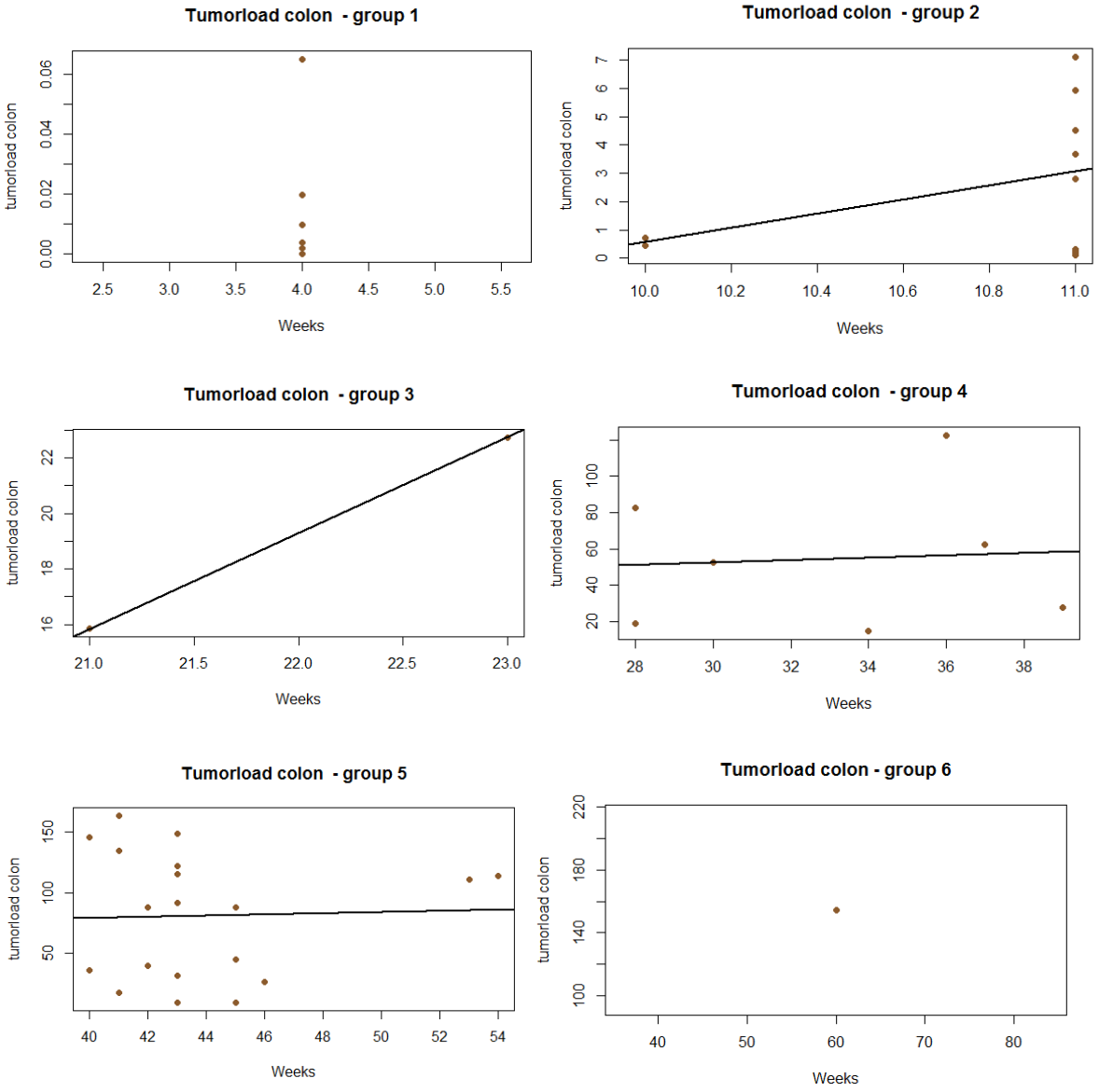

Figure 8: Plots of age against the detected tumorload (mm^2) in colon in the different age groups**.**

Plots of tumorload in small intestine and age (figure 9), none of these had a significant correlation and p-values for the different groups were: group 1 no significant p-value, group 2 p = 0,194, group 3 only two samples, no p-value, group 4 p = 0,168, group 5 p = 0,0811, group 6 only one sample.

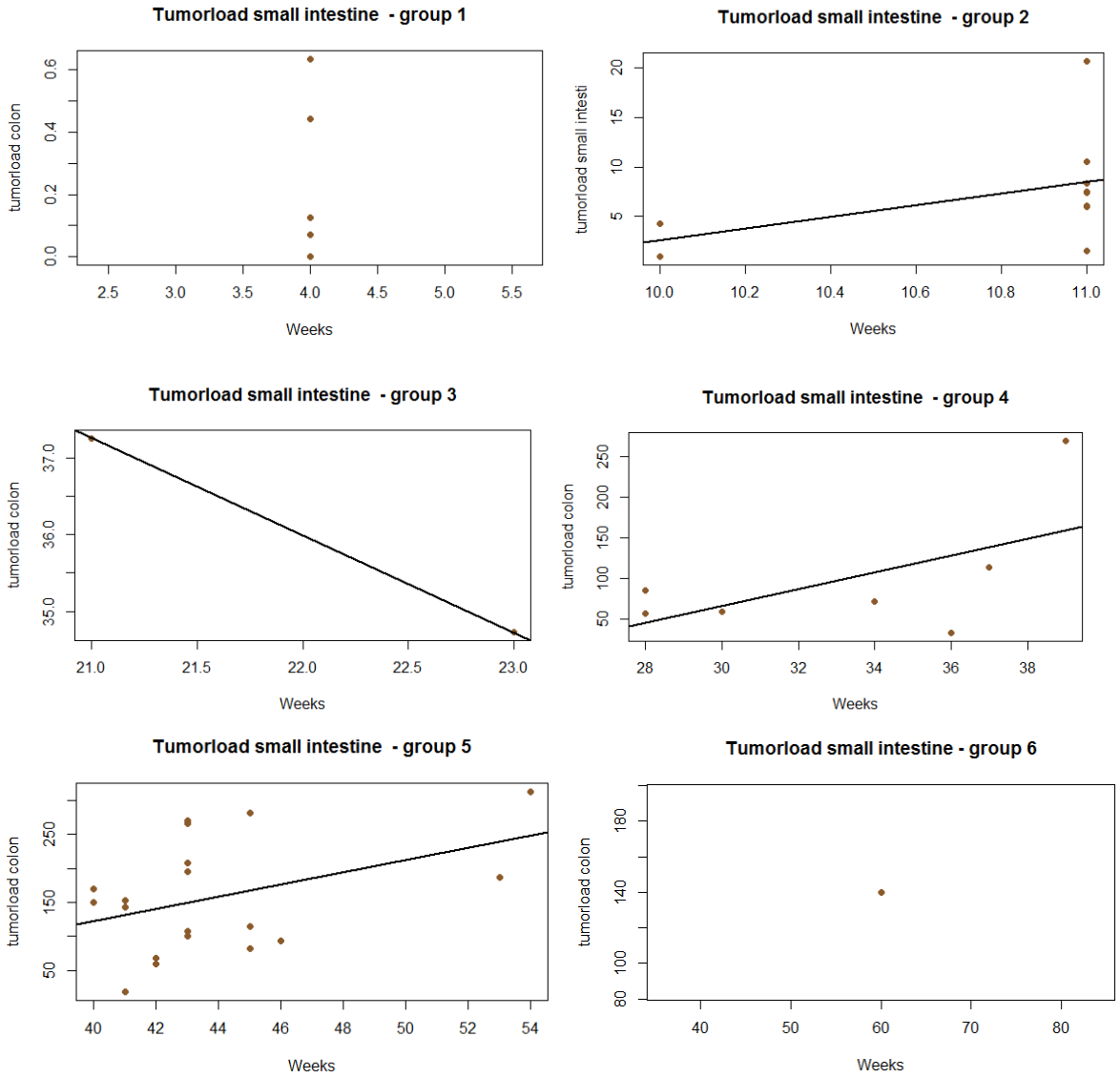

Figure 9: Plots of age against the detected tumorload (mm^2) in small intestine in the different age groups.

Plots of tumorload colon and butyrate (mM) (figure 10), none of these had a significant correlation and p-values for the different groups were: group 1 p = 0,1286, group 2 p = 0,4746, group 3 no p-value, group 4 p = 0,05088, group 5 p = 0,711, group 6 only one sample.

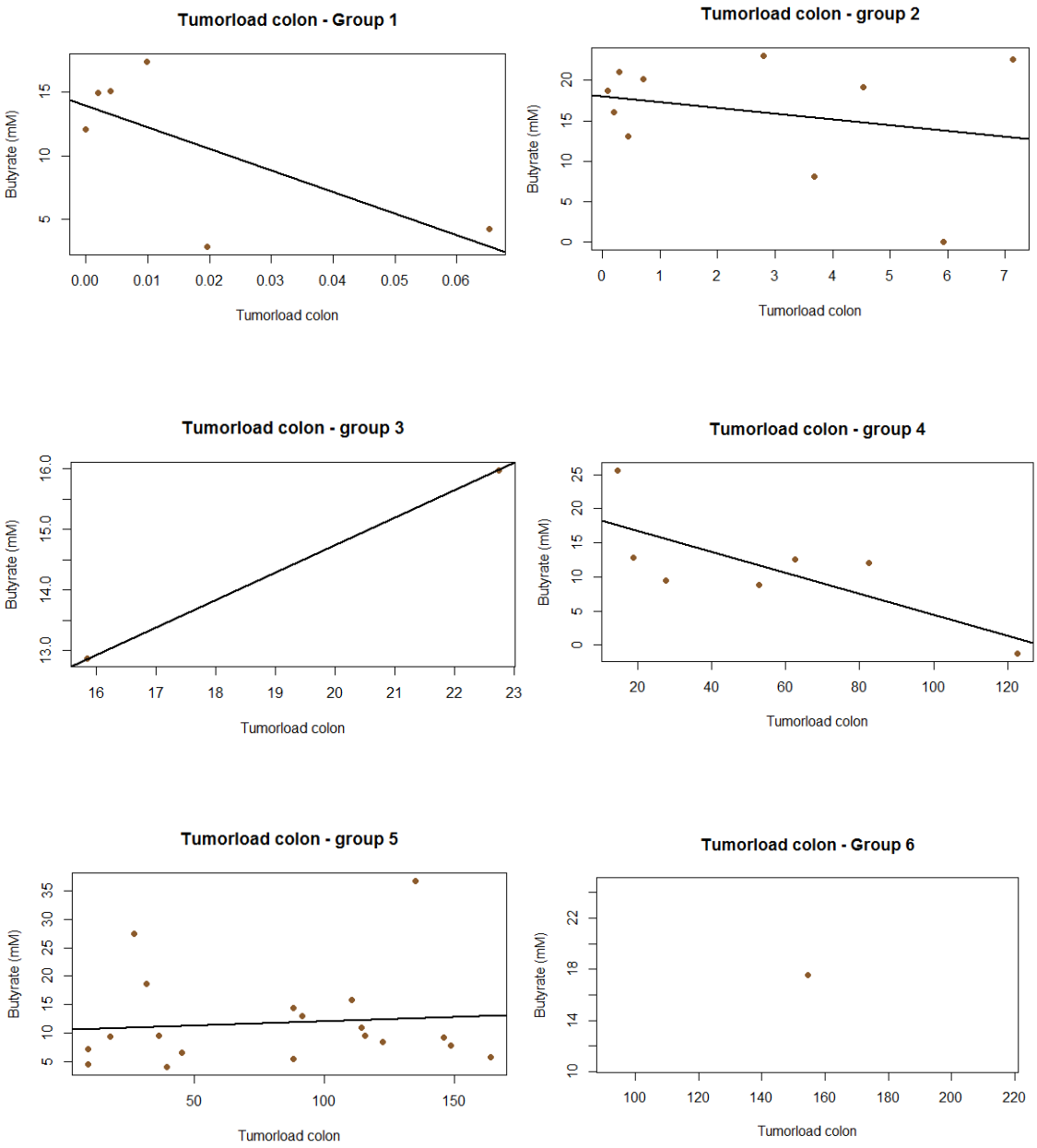

Figure 10: Plots of the detected tumorload (mm^2) in colon against butyrate (mM) in the different age groups.

Plots of tumorload in small intestine and butyrate (mM) (figure 11), none of these had a significant correlation and p-values for the different groups were: Group 1 p = 0,2522, Group 2 p = 0,2138, Group 3 no p-value, Group 4 p = 0,921, Group 5 p = 0,967, Group 6: only one sample.

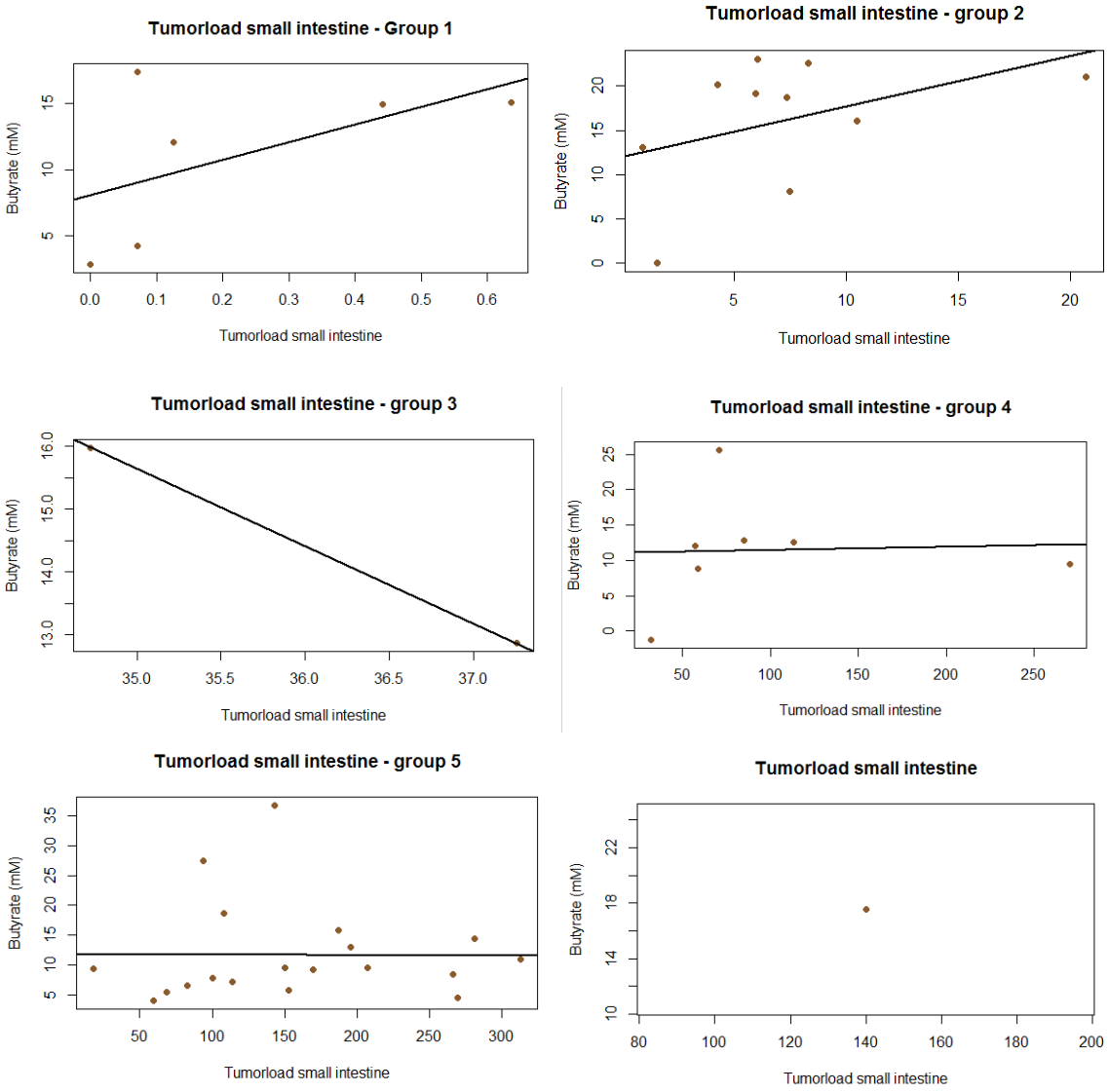

Figure 11: Plots of the detected tumorload (mm^2) in small intestine against butyrate (mM) in the different age groups.

Plots of butyrate (mM) and age (figure 12), none of these had a significant correlation and p-values for the different groups were: Group 1 no p-value, Group 2 p = 0,993, Group 3 no p-value, Group 4 p = 0,736, Group 5 p = 0,670, Group 6: only one sample.

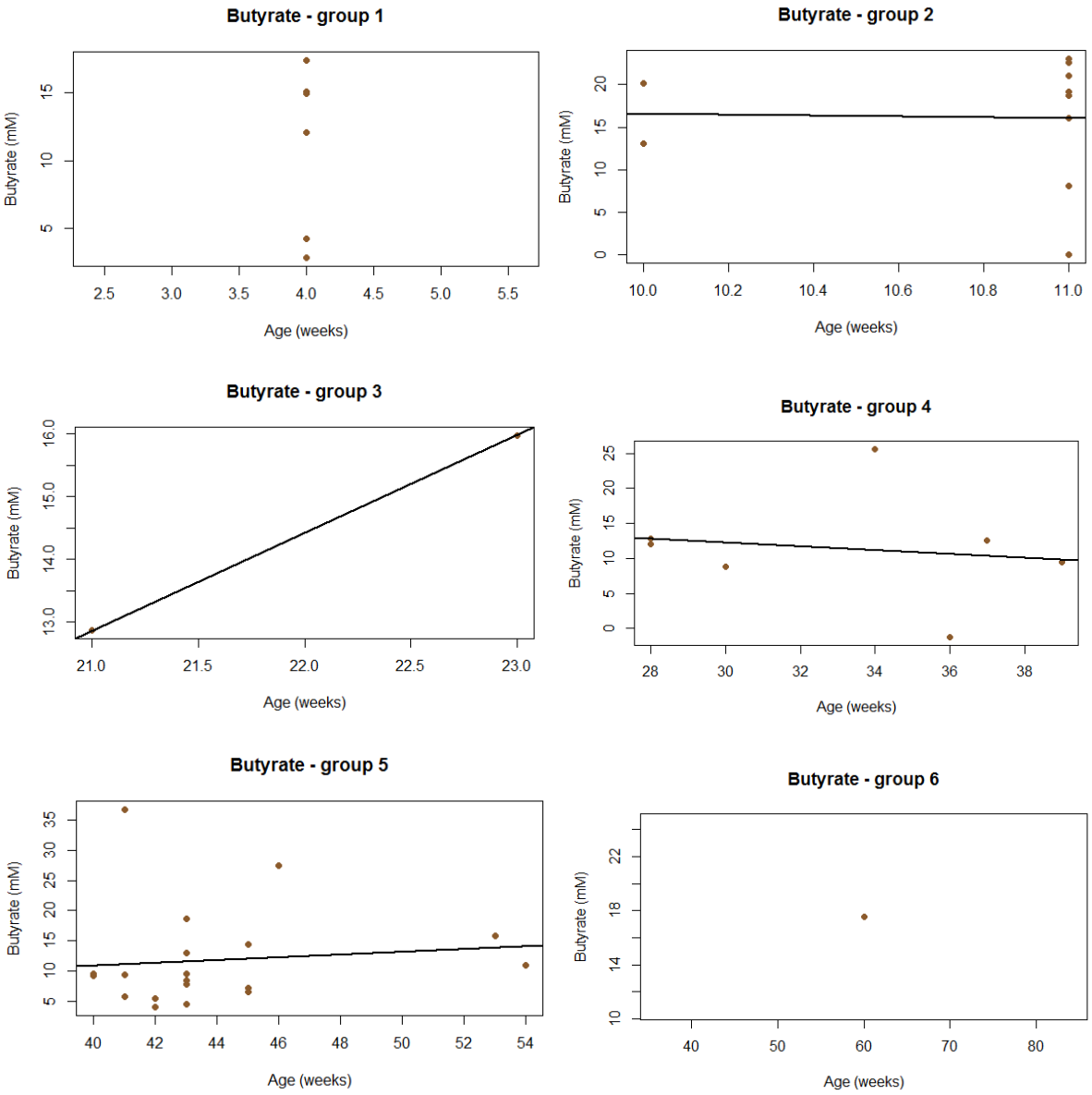

Figure 12: Plots of age against butyrate (mM) in the different age groups

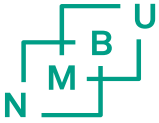

Norwegian University
of Life Sciences

Postboks 5003
NO-1432 Ås, Norway
+47 67 23 00 00
www.nmbu.no